Response RAI-NF-12

Waste inventories assumed within the annulus are not expected to contribute significantly to risk. When modeling the annulus and sand pads, no special effort was made to prevent material in these regions from becoming held up within the annular grout or contamination zone of the waste tanks (i.e., adding to the in-tank inventories) because this modeling assumption is expected to maximize the overall HTF peak doses.

As discussed in the response to RAI-NF-8, diffusion of contaminants from the annulus and sand pads inventories into annular or waste tank grout is an unintended consequence of a modeling simplification. The response to RAI-NF-8 described that this modeling approach is believed to be conservative and not inappropriate in the context of the HTF PA and its associated purposes.

For further insight, and to address more quantitatively this RAI the GoldSim model was used in deterministic mode to develop a set of additional figures showing the radionuclide-specific dose contributions from the assumed annular inventories. These figures show the peak radionuclide doses, regardless of sector. Figure RAI-NF-12.1 shows the radionuclide contributions to the MOP dose from only the annular inventories, using Base Case (Case A) modeling assumptions.

Figure RAI-NF-12.1: MOP Radionuclide Dose Contributions Using Base Case Modeling Assumptions (Annular Inventories)

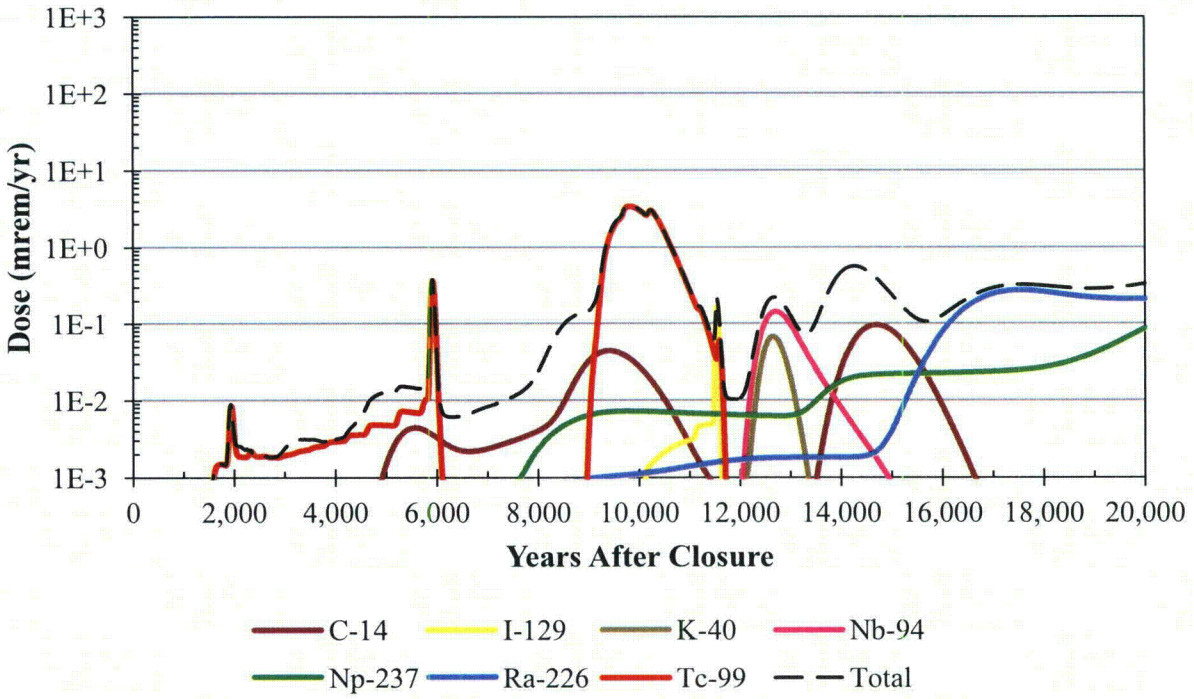

The peak dose in Figure RAI-NF-12.1, near 9,800 years after final facility closure, occurs due to the oxidation of the annular grout for the Type I tanks with intact liners (Tanks 9, 10, and 11). Note that in the GoldSim model, this transition occurs around 8,700 years. Prior to this transition, less than 1 % of the Tc-99 within the annulus inventories of Tanks 9, 10, and 11 is released. The combined annulus inventory doses from these three waste tanks peaks at approximately 3.5 mrem/yr.

In comparison, the primary and secondary waste tank liners are assumed initially failed in Tank 12, allowing more groundwater to flow through the waste tank such that the annular grout transitions earlier (around 6,000 years after final facility closure). The Tc-99 in the Tank 12 annulus inventory provides a peak dose of approximately 0.4 mrem/yr.

Figure RAI-NF-12.2 shows the radionuclide contributions to the MOP dose, regardless of sector, from only the annular inventories, using pessimistic modeling assumptions. These assumptions are defined in the response to RAI-NF-8 (for the model identified as "Flow Run 65, No Holdup"). This pessimistic model releases the majority of the contaminants at the start of the simulation and includes assumptions that accelerate flow.

Figure RAI-NF-12.2: MOP Radionuclide Dose Contributions Using Pessimistic Modeling Assumptions (Annular Inventories)

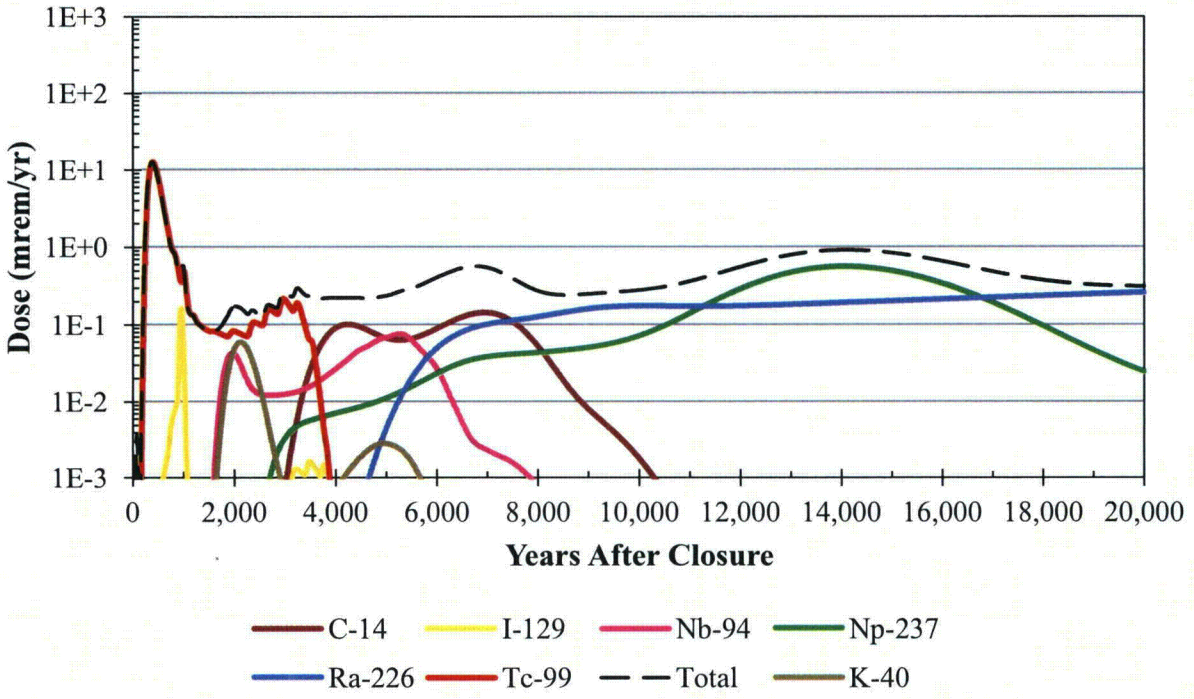

In this pessimistic modeling case, 50 % of the Tc-99 inventories associated with the annular contributions are released within the first 500 years and more than 99 % are released in the first 3,000 years. In this extremely pessimistic modeling scenario, the total dose from the annular contributions within all the HTF waste tank annulus inventories peaks at approximately 13 mrem/yr (around 400 years after final facility closure). This compares to the Base Case modeling approach, which peaked at less than 4 mrem/yr (around 9,800 years after final facility closure). These results indicate that earlier release of the annulus inventories is not likely to alter the risk significance.

Future PA Revisions and the Role of SAs

As required by DOE Manual 435.1-1, maintenance of the HTF PA will include future updates to incorporate new information, update model codes, consider actual residual inventories, etc., as appropriate. Section 8.2 of the HTF PA states that as "additional data becomes available …additional modeling may be required." Each time additional modeling is performed, DOE will

evaluate whether or not an update to the Base Case or a revision of the PA is needed. PA maintenance and the potential impact of new information is evaluated using established site practices and procedures including preparation of an SA, as appropriate, consistent with DOE Manual 435.1-1 and DOE Guide 435.1-1. New fate and transport modeling will be performed, as required, through the SA process, replacing PA assigned inventories with the final residual characterization data. If other new information has been identified (e.g., updated K_d values developed through research or experimentation), this new data would also be evaluated through inclusion in the SA. The results of the waste tank-specific SAs are then evaluated to determine if new information impacts PA-based conclusions. While it typically would not be necessary to replicate all of sensitivity and uncertainty analyses from the PA as part of a SA, it may be appropriate to include additional analyses to evaluate the new or unique waste tank-specific information.

As waste tank-specific SAs are prepared it is anticipated that sensitivity analyses will be performed to address explicitly both individual waste tank inventories and unique waste tank conditions, such as potential preferential pathways (e.g., degraded liners or in-leakage pathways). Because different as-modeled waste tank conditions may prove to be conservative or non-conservative (with respect to timing and/or magnitude of peak doses) depending on other corresponding waste tank conditions, these analyses are more suited to waste tank-specific sensitivity analyses than to changes to the overarching Base Case assumptions. For example, modeling assumptions that cause the annulus inventories to be released relatively slowly (thereby adding to releases from the in-tank inventories) versus relatively rapidly would impact peak doses differently depending on the quantity (total curies) and nature of the inventory remaining in a waste tank annulus (e.g., short-lived versus long-lived radionuclides). In a similar manner, preferential pathways such as failed liners can have very radionuclide-specific dose impacts, with earlier liner failures not necessarily corresponding to greater peak doses, as demonstrated in HTF PA Section 5.6.7.6 (Liner Failure Times Analysis using the PORFLOW Deterministic Model). Additionally, if the closure inventory for a specific radionuclide is determined to be significantly different than previously projected, the impact of the modeling simplification discussed in the RAI would need to be further evaluated.

RAI-NF-13

In Tanks 14H and 16H (Type II), it is not clear to what extent the preferential pathway interacts with the waste located in the primary and secondary sand pads.

Basis

The potential release of radionuclides from the sand pads in Tanks 14H and 16H could be limited by the amount of water flowing through the preferential pathway and/or diffusion of the radionuclides out of the sand pads (See RAI-NF-8). The sand pads in Tanks 14H (primary sand pad only) and 16H (primary and secondary sand pads) contain a significant amount of activity. In the HTF Performance Assessment, DOE assumes that the steel liners in between the sand pads in these tanks are not barriers to flow. However, the preferential pathway is modeled as occurring above the sand pads in the contaminated zone (see Figure 2). The extent to which the sand pad inventories are contacted by flow in the preferential pathway is not clear. In addition, the HTF Performance Assessment does not discuss the extent of diffusion out of the sand pads and into the adjacent cementitious materials.

It appears that a potentially significant fraction of the highly radioactive radionuclide inventory is diffusing into the basemat and/or contaminated zone prior to release. Diffusion of radionuclides out of the primary and secondary sand pads is facilitated in the model by a high diffusion coefficient, large concentration gradient, small diffusion length, assumption of no steel liners, and a delay in the flow through the fast pathway due to closure cap. Although the steel liners are not assumed to not be intact for Tanks 14H and 16H due to the large number of leak sites, the steel liner could still act as a partial barrier to diffusion. Also, the delay in flow through the preferential pathway, due to the assumption of flow being limited to infiltration through the closure cap, may overestimate the amount of time radionuclides can diffuse out of the sand pads if groundwater in-leakage were to occur.

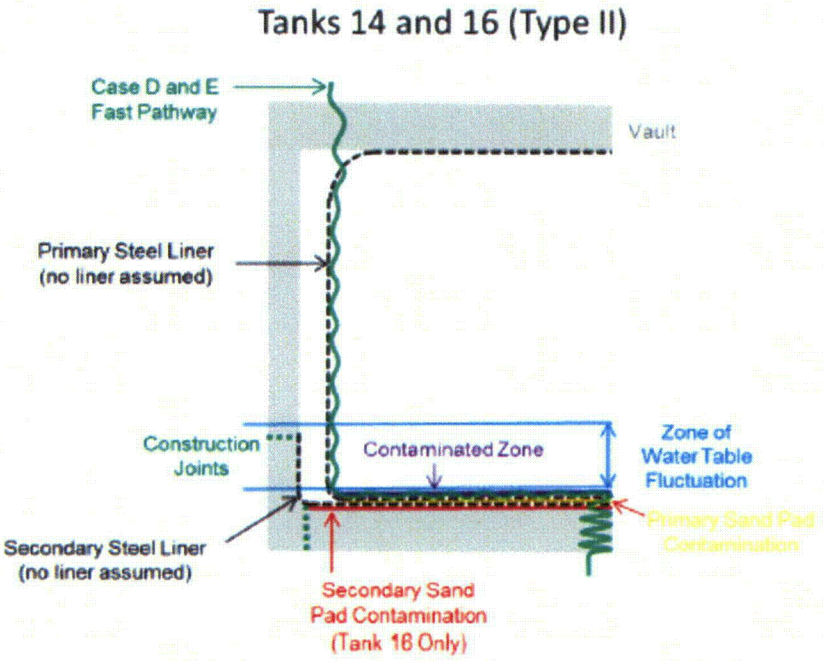

Figure 2. Illustration of the as-modeled sand pad waste and fast pathway in Tanks 14H and 16H

Path Forward

DOE should discuss the extent to which the preferential flow path affects the waste located in the sand pads and its risk significance. This should include the fraction of the inventory of the short-lived radionuclides (e.g., cesium-137 and strontium-90) that decay prior to significant flow occurring in the fast flow path. DOE should also provide discussion regarding the fraction of the highly radioactive radionuclides (e.g., technetium, plutonium, and neptunium) that diffuse out of the sand pads and into the grout or basemat.

Response RAI-NF-13

Waste inventories assumed within the sand pads are not expected to contribute significantly to risk despite assuming what is believed to be bounding values relative to the assigned inventories within these sand pads. When modeling the annulus and sand pads, no special effort was made to prevent material in these regions from migrating into the contamination zone within the waste tanks (i.e., adding to the in-tank inventories) because this modeling assumption is expected to maximize the overall HTF peak doses.

As discussed in the response to RAI-NF-8, diffusion of contaminants from the annulus and sand pads inventories into annular or waste tank grout is an unintended consequence of a modeling simplification. As discussed in the response to RAI-NF-8, the simplified approach taken facilitates modeling of solubility controls that are appropriate under most conditions.

For greater insight, the GoldSim model was used in deterministic mode to develop a set of additional figures showing the radionuclide-specific dose contributions from the assumed sand pads inventories. These figures show the peak radionuclide doses, regardless of sector. Figure RAI-NF-13.1 shows the radionuclide contributions to the MOP dose from only the sand pads inventories (i.e., Tanks 13-16 sand pads) using Base Case (Case A) modeling assumptions.

Figure RAI-NF-13.1: MOP Radionuclide Dose Contributions (from the Sand Pads) Using Base Case Modeling Assumptions

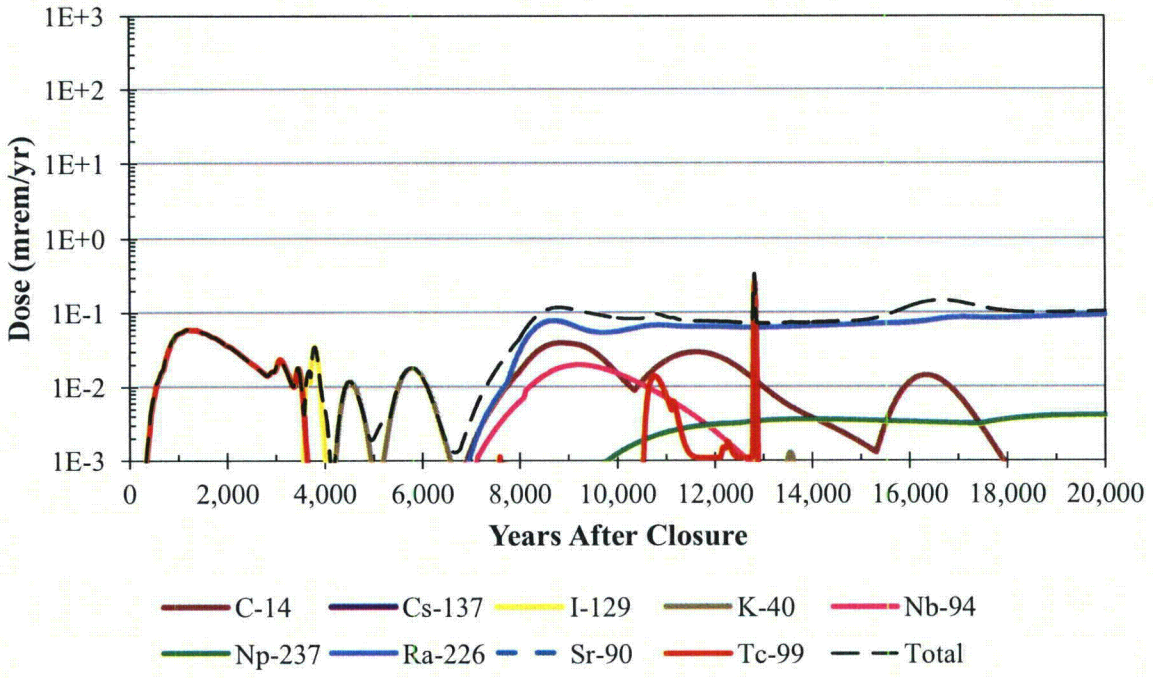

The peak dose in this figure occurs once the primary liner for Tank 13 fails (around 12,700 years after closure). As an artifact of the modeling approach, more than half (approximately 55 %) of the Tc-99 artificially migrates (via diffusion) from the sand pads, through the primary and secondary liners, and into the contamination zone and remains there until liner failure.

Alternatively, this diffusion effect is minimized for Tanks 14, 15, and 16 because the majority of the available inventory is advectively transported out of the contamination zone (due to assumed liner failure at the start of the simulation). Figure RAI-NF-13.1 shows a low magnitude Tc-99 dose occurring in the first 4,000 years. This dose comes from the sand pads inventories from Tanks 14, 15, and 16, of which 99 % of the Tc-99 is released within the first 4,000 years.

The peak Tc-99 dose from the Tank 13 sand pads is approximately 0.26 mrem/yr; whereas the peak Tc-99 dose from the Tank 16 sand pads is one order of magnitude smaller (0.024 mrem/yr), despite a much earlier release and a Tank 16 Tc-99 sand pads inventory that is approximately one order of magnitude higher than in Tank 13. Therefore, the holdup of Tc-99 that has migrated into the contamination zone is conservative.

Also note that Cs-137 and Sr-90 are included in the legend for Figure RAI-NF-13.1; however, these radionuclides have no dose significance as they decay before they are able to contribute to the peak dose.

Figure RAI-NF-13.2 shows the radionuclide contributions to the MOP dose, regardless of sector, from only the sand pads inventories, using pessimistic modeling assumptions. These assumptions are defined in the response to RAI-NF-8 (for the model identified as "Flow Run 65, No Holdup"). This pessimistic model releases the majority of the contaminants at the start of the simulation and includes assumptions that accelerate flow.

Figure RAI-NF-13.2: MOP Radionuclide Dose Contributions (from the Sand Pads) Using Pessimistic Modeling Assumptions

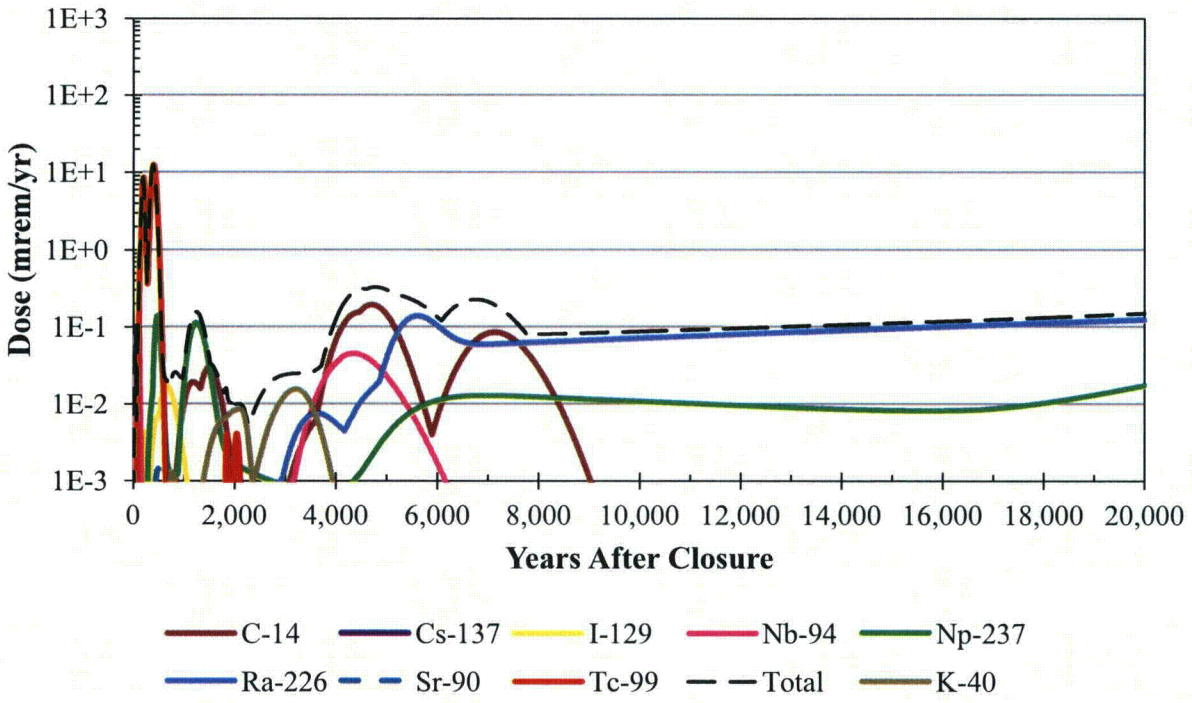

In this pessimistic modeling case, more than 99 % of the Tc-99 inventories associated with the sand pads are released within the first 300 years. Tank 16 contributes a higher Tc-99 peak dose (approximately 8.2 mrem/yr) than Tank 13 (approximately 0.42 mrem/yr), which is consistent with the higher initial inventory.

Again, note that Cs-137 and Sr-90 are included in the legend for Figure RAI-NF-13.2. A small amount of Sr-90 is visible in the figure (0.0014 mrem/yr at about 500 years after final facility closure). The Cs-137 dose never exceeds 3E-07 mrem/yr. Even under these pessimistic modeling conditions, Cs-137 and Sr-90 significantly decay before these radionuclides can contribute to the MOP peak dose. A review of the inadvertent intruder results confirmed that Cs-137 and Sr-90 also had no significant contribution to the inadvertent intruder peak-dose results. Therefore, Cs-137 and Sr-90 from the sand pads inventories have no dose significance.

Future PA Revisions and the Role of SAs

As required by DOE Manual 435.1-1, maintenance of the HTF PA will include future updates to incorporate new information, update model codes, consider actual residual inventories, etc., as appropriate. Section 8.2 of the HTF PA states that as "additional data becomes available ...additional modeling may be required." Each time additional modeling is performed, DOE will evaluate whether or not an update to the Base Case (Case A) or a revision of the PA is needed. PA maintenance and the potential impact of new information is evaluated using established site practices and procedures including preparation of an SA, as appropriate, consistent with DOE Manual 435.1-1 and DOE Guide 435.1-1. New fate and transport modeling will be performed, as required, through the SA process, replacing PA assigned inventories with the final residual characterization data. If other new information has been identified (e.g., updated K_d values developed through research or experimentation), this new data would also be evaluated through inclusion in the SA. The results of the waste tank-specific SA are then evaluated to determine if new information impacts PA-based conclusions. While it typically would not be necessary to replicate all of sensitivity and uncertainty analyses from the PA as part of a SA, it may be appropriate to include additional analyses to evaluate the new or unique waste tank-specific information.

As waste tank-specific SAs are prepared it is anticipated that sensitivity analyses will be performed to address both individual waste tank inventories and unique waste tank conditions explicitly, such as potential preferential pathways (e.g., degraded liners or in-leakage pathways). Because different as-modeled waste tank conditions may prove to be conservative or non-conservative (with respect to timing and/or magnitude of peak doses) depending on other corresponding waste tank conditions, these analyses are more suited to waste tank-specific sensitivity analyses than to changes to the overarching Base Case assumptions. For example, modeling assumptions that cause the annulus inventories to be released relatively slowly (thereby adding to releases from the in-tank inventories) versus relatively rapidly would impact peak doses differently depending on the quantity (total curies) and nature of the inventory remaining in a waste tank annulus (e.g., short-lived versus long-lived radionuclides). In a similar manner, preferential pathways such as failed liners can have very radionuclide-specific dose impacts, with earlier liner failures not necessarily corresponding to greater peak doses, as demonstrated in HTF PA Section 5.6.7.6 (Liner Failure Times Analysis using the PORFLOW Deterministic Model). Additionally, if the closure inventory for a specific radionuclide is determined to be significantly different than previously projected, the impact of the modeling simplification discussed in the RAI would need to be further evaluated.

RAI-NF-14

Although several HTF sources are expected to be located below the water table, tank releases are modeled under unsaturated conditions in the Performance Assessment. DOE should provide additional support for modeling HTF source releases under unsaturated conditions.

Basis

DOE simulates releases from HTF sources that are expected to be located below the water table through use of unsaturated, near-field flow and contaminant transport models. Radionuclide fluxes extracted from the unsaturated zone models are then used to load radioactivity into the HTF/PORFLOW® model that is used to simulate saturated zone transport at HTF.

For submerged and partially submerged tanks (i.e., Type I and II tanks), no vadose zone is expected to be present but inclusion of a vadose zone in the near-field model domain may increase travel times to a potential receptor if the contaminant flux is calculated based on flux out of the near-field model domain (versus flux out of the tank/vault system). Predicted doses may also be sensitive to the manner in which contaminant flux is loaded in the saturated zone model (e.g., number of source cells or source location). Finally, release rates from HTF sources may be higher in the saturated zone compared to the vadose zone in certain cases. Therefore, DOE should provide additional clarification or support for model simplifications to provide assurance that doses are not significantly underestimated in the HTF Performance Assessment.

Path Forward

DOE should clarify if the near-field model fluxes are calculated at the bottom of the HTF tank basemats or at the bottom of the near-field model domain.

DOE should clarify the location of source loading (elevation of source release relative to the water table) and the number of source cells used to represent the source. DOE should provide an estimate of the range in potential dose based on dilution or concentration of the contaminant flux given source loading selections.

DOE should evaluate the impact of simulation of HTF source releases in an unsaturated zone model for submerged and partially submerged tanks. DOE should consider all relevant flow/transport regimes in evaluating whether radionuclide release rates could be potentially underestimated. For example, DOE should consider cases where flow rates through the engineered system may be low and releases limited by diffusion. For example, relatively high flow around the tank/vaults in the saturated zone at early times could lead to higher release rates, if flow rates in the saturated zone maintain a higher concentration gradient. DOE should also consider cases where flow occurs predominately through preferential pathways through the tank/vaults in alternative configurations (i.e., could releases be underestimated at early times in the near-field model if flow were to occur primarily through preferential pathways in the saturated zone prior to significant cementitious material degradation). Finally, DOE should consider the period of time when flow through the grout monolith increases significantly and releases are dominated by advection through the cementitious materials. Details regarding hydraulic head gradients and the magnitude of flow through the engineered system in a saturated system should be provided. Note that additional detail from Portage modeling (PORTAGE-08-022) may be helpful in responding to a portion of this request for additional information.

Response RAI-NF-14

The HTF PA near-field models encompass both unsaturated and saturated conditions depending on the structure being simulated. For near-field model domains extending down to the water table, the aquifer modeling cells are set to the solute flux leaving the model domain (crossing the water table). For near-field model domains that extend into the water table, the aquifer modeling cells are defined to be the solute flux leaving the engineered system (entering surrounding soil) rather than the model domain. Near-field sources that are submerged fully or partially are treated in this manner. That is, near-field models all of the Type I and Type II tanks, and the transfer lines and ancillary structures within the vicinity of the Type I and Type II tanks include a portion of the saturated zone, but the flux leaving the waste tank concrete vault is modeled as aquifer modeling cells.

Aquifer modeling cells for waste tanks are defined in the horizontal plane as those computational cells with centers residing within the physical footprint of the waste tanks. For smaller sources, the nearest cell center is selected. The number of source cells varies between four and six for waste tanks. Vertically, the aquifer modeling cells are placed at the lower of the highest fully saturated cell and the cell coinciding with the basemat elevation. Figures RAI-NF-14.1 and RAI-NF-14.2 show the horizontal and vertical positions, respectively; of the HTF source nodes (note that the vertical height is exaggerated). Among waste tanks, only sources for the fully submerged waste tanks are significantly below the water table. Computational cells at the water table beneath H Area are roughly 20 feet deep and become thinner with depth (e.g., on the order of 7 feet deep in the UTRA-LZ). DOE has not investigated the specific impact of grid resolution in the source zone on solute transport, but has studied general numerical dispersion/dilution within the HTF modeling sectors (see the *Comment Response Matrix for United States Nuclear Regulatory Commission Staff Comments on the Draft Basis for Section 3116 Determination and Associated Performance Assessment for the F-Tank Farm at the Savannah River Site*, SRR-CWDA-2011-00054, RAI-FF-3).

Although the near-field models consider saturated conditions for fully and partially submerged waste tanks, the 2-D grids can only accommodate axisymmetric flow past waste tanks. Any lateral flow in the saturated zone (crossflow) is not explicitly represented in the near-field models, and would require a 3-D near-field model. DOE earlier developed a 3-D Cartesian near-field waste tank model but observed significant drawbacks with using the model to investigate 3-D flow effects. [PORTAGE-08-022] First, the Cartesian grid, although refined within the waste tank, could not accurately resolve thin features of a cylindrical waste tank (e.g., steel liner), limiting its usefulness to failed-liner scenarios. Second, large computational times required to complete simulations significantly constrained the number of baseline and sensitivity cases that could be considered. DOE considered the trade-offs between 2-D and 3-D near-field models and concluded that various effects of aquifer crossflow could be neglected. [SRNL-L6200-2010-00026]

The possibility of a "dead-zone" of contamination build-up under the basemat that would hinder diffusive release from a waste tank was acknowledged in the HTF modeling. This effect was neglected in general because diffusional release from the waste tank contamination zone is not significant compared to advection. For waste tanks assumed to have a failed liner at time zero, diffusion-dominated release may occur for a short time. Several factors tend to offset this potential non-conservatism:

- Advection in soil surrounding a waste tank, relatively high diffusion coefficients for soil, and the proximity of the lower boundary limit contamination build-up beneath the basemat;
- The modeling assumption of early liner failure encompassing the entire surface area significantly over-predicts diffusive release; and
- Early releases that are biased low tend to reduce the peak dose (that occurs at a later time), as demonstrated in the liner sensitivity analysis provided in HTF PA Section 5.6.7.6 (Liner Failure Times Analysis using the PORFLOW Deterministic Model).

As discussed in HTF PA Section 4.4.4.1.2 (General Vadose Zone Waste Tank Modeling in PORFLOW), the effect of aquifer crossflow on advective release from the waste layer following liner failure was quantitatively investigated. Contaminant release was found to be relatively insensitive to crossflow. For the range of crossflow rates expected beneath the HTF, the effect was considered small compared to other biases and uncertainties in the overall analysis.

As required by DOE Manual 435.1-1, maintenance of the HTF PA will include future updates to incorporate new information, update model codes, consider actual residual inventories, etc., as appropriate. Section 8.2 of the HTF PA states that as "additional data becomes available ...additional modeling may be required." Each time additional modeling is performed, DOE will evaluate whether or not an update to the Base Case (Case A) or a revision of the PA is needed. Maintenance of the PA and the potential impact of new information is evaluated using established site practices and procedures including preparation of an SA, as appropriate, consistent with DOE Manual 435.1-1 and DOE Guide 435.1-1. New fate and transport modeling will be performed, as required, through the SA process, replacing PA assigned inventories with the final residual characterization data. If other new information has been identified (e.g., updated K_d values developed through research or experimentation), it would also be evaluated through inclusion in the SA. The waste tank-specific SA results are then evaluated to determine if new information impacts PA-based conclusions. While it typically would not be necessary to replicate all of sensitivity and uncertainty analyses from the PA as part of a SA, it may be appropriate to include additional analyses to evaluate the new or unique waste tank-specific information.

As waste tank-specific SAs are prepared it is anticipated that sensitivity analyses will be performed to address explicitly both individual waste tank inventories and unique waste tank conditions, such as potential preferential pathways (e.g., degraded liners or in-leakage pathways). Because different as-modeled waste tank conditions may prove to be conservative or non-conservative (with respect to timing and/or magnitude of peak doses) depending on other corresponding waste tank conditions, these analyses are more suited to waste tank-specific sensitivity analyses than to changes to the overarching Base Case assumptions. For example, modeling assumptions that cause the annulus inventories to be released relatively slowly (thereby adding to releases from the in-tank inventories) versus relatively rapidly would impact peak doses differently depending on the quantity (total curies) and nature of the inventory remaining in a waste tank annulus (e.g., short-lived versus long-lived radionuclides). In a similar manner, preferential pathways such as failed liners can have very radionuclide-specific dose impacts, with earlier liner failures not necessarily corresponding to greater peak doses, as demonstrated in HTF PA Section 5.6.7.6 (Liner Failure Times Analysis using the PORFLOW Deterministic Model). Additionally, if the closure inventory for a specific radionuclide is determined to be significantly different than previously projected, the impact of the modeling simplification discussed in the RAI would need to be further evaluated.

Figure RAI-NF-14.1: Horizontal Location of Source Cells for Waste Tanks and Ancillary Structures

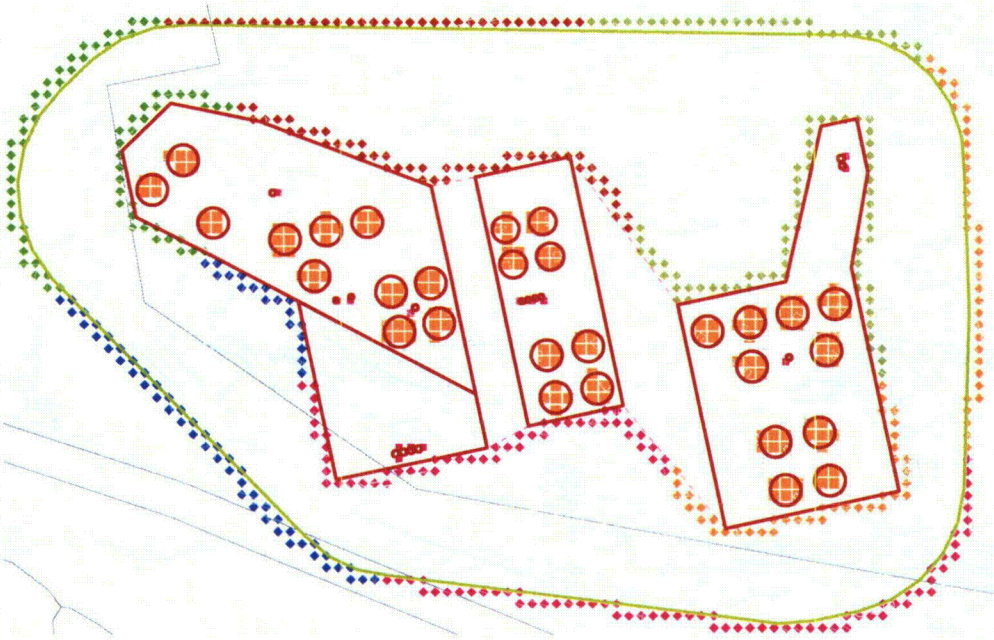

Note: Modeled source locations are shown as orange squares for waste tanks and smaller, magenta squares for ancillary structures.

Figure RAI-NF-14.2: Vertical Location of Source Cells for Waste Tanks and Ancillary Structures

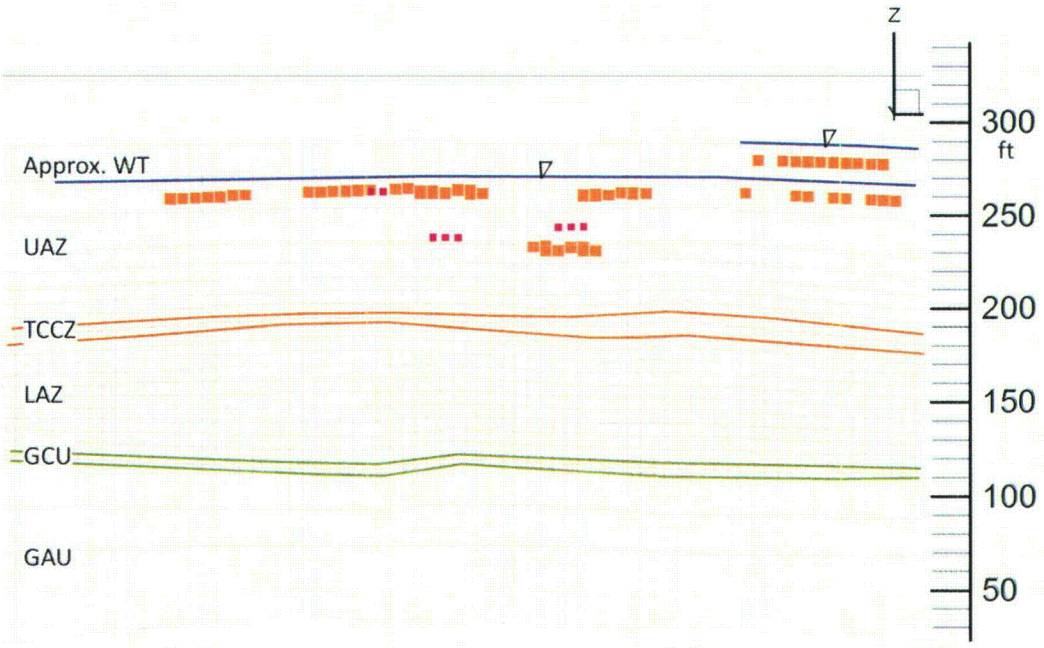

Note: Modeled source locations are shown as orange squares for waste tanks and smaller, magenta squares for ancillary structures. Vertical height is exaggerated. Triangles denote the approximate ground level and water table (i.e., Approx. WT) relative to mean sea level.

CC-NF-1

Provide documentation of groundwater in-leakage into the submerged and partially submerged tanks.

Response CC-NF-1

No specific documentation identifying waste tanks with groundwater in-leakage has been created, however, a review of waste tank-specific history reports and anecdotal evidence suggests that groundwater has intruded into the annulus of Tanks 9, 10, 11, and 12. These waste tanks are Type I tanks, the first four waste tanks constructed in HTF. All four of these waste tanks are currently submerged in the water table. In the case of Tank 9, past waste tank annulus visual inspections have indicated the presence of water in the annulus, although liquid has not been seen in the annulus during recent inspections. No visual evidence indicating a potential location of groundwater in-leakage in to the annulus has been identified for Tank 9 so it is not clear if this was groundwater intrusion through the concrete vault wall or surface rain water that ponded on the surface above the waste tank and made its way into the annulus around the riser openings. With respect to Tanks 10, 11, and 12, there has been recent events where groundwater has intruded into the annulus of each of these three waste tanks. In the case of Tank 11, there is visual evidence of the water entering the annulus at the top of the annulus liner.

Identifying groundwater intrusion is complicated by the operation of the annulus ventilation systems. In the recent events of Tanks 10, 11, and 12, the ventilation systems were not operating in normal mode. Such normal operation results in introducing heated air to the annulus that in turn heats the metal surfaces (i.e., liner) of the annulus. Operation of the ventilation system has the demonstrated effect of evaporating the water that enters the annulus before any significant quantity collects. For example, earlier in 2013, the Tank 11 ventilation system became inoperable. In time, over 20 inches of groundwater collected in the annulus. Once the majority of this liquid was removed from the Tank 11 annulus and the ventilation was restored, the annulus was once again dry.

In addition, waste tank-specific history reports indicate the possible intrusion of water into the annulus of Tanks 14 and 16 in the late 1950's but this water intrusion may have been attributable to rainwater ponding on the top of the waste tanks and entering through risers, as discussed above for the Type I tanks. Tanks 14 and 16 are both Type II tanks that are partially submerged in the water table.

CC-NF-2

DOE should provide additional support for the assumption that the chemical transition from Oxidized Region II to Oxidized Region III is not risk significant. The assumed solubilities for the highly radioactive radionuclides in the HTF do not appear to be sensitive to the pH transition. However, future revisions to the HTF Performance Assessment and updated geochemical modeling may indicate that certain radionuclide solubilities are sensitivity to pH.

The normative mineralogy of the hydrated grout assumed for the Geochemist's Workbench modeling of grout degradation is based on a mass balance calculation using the chemical composition of unhydrated cement. DOE used select phases that were taken from published cement simulations (i.e., Höglund, 2001; Lothenbach and Winnefeld, 2006; Kulik, 2011) to represent the normative mineralogy in the grout degradation modeling. However, the minerals that DOE selected to represent the hydrated grout are inconsistent with the minerals from Höglund (2001) and Lothenbach and Winnefeld (2006). Because the mineralogy used in modeling grout degradation determines the pH evolution of grout pore water, which in turn affects the calculated solubility, using an incorrect mineralogy in the model could lead to non-conservative solubilities and releases of radionuclides from the contaminated zone.

Response CC-NF-2

It should be noted that the conclusion that the chemical transition from Oxidized Region II to Oxidized Region III was not risk significant was not an inherent assumption. While it is true that there are numerous underlying assumptions made that can affect the solubility difference between Oxidized Regions II and III, the fact that the final derived Oxidized Region II and Oxidized Region III solubilities were often very similar was the result of calculations using widely accepted thermodynamic data, and was not an *a priori* assumption.

Normative mineralogy of grout assumed in most modeling efforts, including the HTF PA, was calculated from the chemical composition of the cementitious materials. The chemical composition of the cementitious materials for HTF reducing grout was different from that used in *Project SAFE: Modeling of Long-term Concrete Degradation Processes in the Swedish SFR Repository,* SKB Report R-01-08 and *Thermodynamic Modeling of the Hydration of Portland Cement,* DOI: 10.106/J, studies. Table CC-NF-2.1 lists the composition of the cementitious material used in each modeling study.

Table CC-NF-2.1: Chemical Compositions of Cementitious Materials used in Modeling Studies

	Project SAFE Study	Thermodynamic Modeling Study	SRS Waste Tank Reducing Grout
CaO (wt %)	64.0	63.2	23.6
SiO_2	21.0	19.7	44.3
Al_2O_3	3.5	4.7	19.2
Fe_2O_3	4.6	2.7	5.0
MgO	0.7	1.9	4.6
K_2O	0.6	1.1	1.7
Na_2O	0.1	0.1	0.3
SO_3	2.2	3.4	1.2

The cementitious materials used in the Project SAFE study and the Thermodynamic Modeling study are simple Portland cements, whereas the composition of the reducing grout used in the waste tanks at SRS contains large fractions of fly ash and blast furnace slag. These components are much richer in silica, alumina, and magnesia than Portland cement and this is reflected in the chemical composition of the reducing grout used in the waste tanks at SRS.

The differences in chemical composition translate into differences in normative mineralogy. The mineralogy used by the *Project SAFE: Modeling of Long-term Concrete Degradation Processes in the Swedish SFR Repository,* SKB Report R-01-08, study is dominated by the calcium silicate hydrate (CSH) phase with a high calcium / silicon ratio and Portlandite. In this study, sulfate was represented as a monosulfate phase and magnesium as brucite. Portlandite is not stable at complete hydration of SRS reducing grout because the abundant silica reacts with it to form CSH. The low calcium / silicon ratio in the chemical composition of the cementitious materials of SRS reducing grout means that the dominant CSH phase has a low calcium / silicon ratio relative to the CSH phase in the Project SAFE study. Initially, gypsum was used to represent sulfate in the SRS reducing grout, but starting mineralogy recalculated by the Geochemist's Workbench placed the sulfate in the more thermodynamically stable phase ettringite (see Table 3 from the *Evolution of Chemical Conditions and Estimated Solubility Controls on Radionuclides in the Residual Waste Layer During Post-Closure Aging of High-Level Waste Tanks,* SRNL-STI-2012-00404). The abundant alumina in SRS reducing grout makes hydrotalcite a more stable phase for magnesium than brucite. The difference in the initial mineralogy of these two modeling studies illustrates how chemical composition of cementitious materials affects normative mineralogy. Therefore, the initial normative mineralogy used to model degradation of SRS reducing grout is not in error, but rather is consistent with the chemical composition of the cementitious materials.

The initial normative mineralogy used in the *Thermodynamic Modeling of the Hydration of Portland Cement,* DOI: 10.106/J, study is not comparable to the initial normative mineralogy of the SRS waste tank reducing grout. The Thermodynamic Modeling study modeled hydration of Portland cement and their initial normative mineralogy is unhydrated. A basic assumption in the modeling of degradation of SRS waste tank reducing grout in the *Evolution of Chemical Conditions and Estimated Solubility Controls on Radionuclides in the Residual Waste Layer During Post-Closure Aging of High-Level Waste Tanks,* SRNL-STI-2012-00404, report is that the starting point of the model is a fully hydrated grout. Therefore, different initial normative mineralogy between the two studies is expected. Interestingly, the mineralogy at the end of the hydration period (10,000 hours) modeled in the Thermodynamic Modeling study is similar to the initial normative mineralogy used in the Evolution of Chemical Conditions report. They are both dominated by CSH, ettringite, and hydrotalcite. At the end-point for the model of the Thermodynamic Modeling study, the cement also contains Portlandite and a calcium monocarboaluminate phase. Again, Portlandite does not exist in the normative mineralogy of the SRS waste tank reducing grout because of the abundance of silica. Hence, the only difference is the presence of the calcium monocarboaluminate phase in the final mineralogy of the Thermodynamic Modeling study.

CC-NF-3

DOE should provide a basis that the use of Hanford sediments to develop the cement-leachate impacted K_ds (Table 4.2-25 of the HTF Performance Assessment) for HTF vadose zone soil is appropriate. Further, DOE should clarify why the Hanford derived cement leachate factor for plutonium (a factor of two) was not applied to derive the cement-leachate impacted from the non-impacted K_d in the HTF Performance Assessment. In its clarification, DOE should also more clearly describe how the factor of two was derived from PNNL-16663, which resulted in a factor of 0.25.

Response CC-NF-3

The cement-leachate impact factors were taken from the *Geochemical Data Package for Performance Assessment Calculations Related to the Savannah River Site,* SRNL-STI-2009-00473. As explained in this document, these factors represent literature values, which were used in the PA because site-specific values are not available. The Hanford Site cementitious radionuclide K_d value data set recorded in *Geochemical Processes Data Package for the Vadose Zone in the Single-Shell Tank Waste Management Areas at the Hanford Site,* PNNL-13421, was one of the few extensive studies identified in the literature, and as such, were used to determine impact factors on the Hanford Site sediment. These impact factors were then used (taking into consideration SRS soil conditions) to adjust the expected K_d values in a cement-leachate SRS sediment.

Regarding the question about the selection of the plutonium impact factor, all the plutonium impact factors are based on the Hanford Site PA database, which in turn are based on experimental data specific to the *Geochemical Processes Data Package for the Vadose Zone in the Single-Shell Tank Waste Management Areas at the Hanford Site,* PNNL-13421, data set. This report includes "best values" for plutonium sorption in groundwater (PNNL-13421, Page B.3, Table B1; for intermediate impacted sand) of 600 mL/g and for cementitious waste impacted K_d values of 150 mL/g (PNNL-13421, Page B.4, Table B1). The impact factor is the ratio of these two values, or 0.25. The experimental data to support this value of 150 mL/g was not noted in the Hanford Site data set. The reported Hanford Site cement-impacted K_d value was inconsistent with thermodynamic considerations of plutonium. Plutonium solubility has been measured to decrease sharply as the pH increases from 7 ($K_{solubility}$ = 1E-05 mol) to pH > 9 ($K_{solubility}$ = 1E-10 mol), as documented in *The Solubility of Actinides in a Cementitious Near-Field Environment*, 0956-053X(92)90051-J. To capture this geochemical phenomenon of reduced aqueous plutonium concentrations as the pH increases, it was elected in the *Geochemical Data Package for Performance Assessment Calculations Related to the Savannah River Site,* SRNL-STI-2009-00473, to depart from the best estimates used at Hanford Site and to rely on known thermodynamic trends. Furthermore, under SRS site-specific conditions, it has been recently shown in *Iodine, Neptunium, Plutonium, and Technetium Sorption to Saltstone and Cement Formulations under Oxidizing and Reducing Conditions*, SRNL-STI-2009-00636 (Table 9.1 and 9.2), that in cement leachate simulants at pH values between 11 and 12, that plutonium rapidly precipitates out of solution in the absence of any solids, resulting in solubility values in the order of 1E-09 to 1E-10 mol. The Hanford Site K_d data suggest that the plutonium aqueous concentrations increase at higher pH values, contrary to thermodynamic considerations and experimental results. [0956-053X(92)90051-J, SRNL-STI-2009-00636] To capture the pH-Pu_{aq} trend, DOE elected to employ a cement impact factor of two, to capture the expected trend of Pu_{aq} concentrations decreasing in the presence of the cementitious leachate compared to pH 5.5 groundwater. The factor of two was based on expert judgment considering the available data and the other impact factors.

CC-NF-4

DOE should clarify whether the piping that enters the tanks will be grouted.

Response CC-NF-4

As each waste tank is filled with grout, grout material will flow into the open end of transfer line piping that penetrates either the waste tank risers or walls, thereby sealing and effectively isolating the transfer line piping. Though the waste tank fill-grout will seal the transfer line piping at the waste tank penetrations, there are no current plans to specifically grout or fill the HTF transfer lines.

CC-NF-5

The analytic solution to the diffusion equation to compute the chloride concentration on page 32 in SRNL-STI-2010-00047 appears to be incorrect to use at long times. It appears to only be valid to use at short times, when the depth of the chloride penetration is small compared to the vault thickness. The analytical solution assumes a fixed concentration at x=0, zero concentration at x=∞, and zero initial concentration. Instead, a correct solution for long times should consider zero flux at the concrete/liner interface, to keep all of the chloride within the vault thickness. Because of the incorrect use of the analytic equation, chloride concentrations at the concrete/steel interface in Figures 18 and 19 may be underestimated. Such figures are only provided to derive a notion of times for chloride to diffuse. These results do not appear relevant to time estimates in the stochastic methodology. Confirm that these results are not relevant to estimates of liner failure.

Response CC-NF-5

DOE acknowledges that the diffusion equation used may not be appropriate at long times, but the comment is correct that the results of the diffusion equation were not used in the stochastic methodology. The equations in Sections 3.3.2 and 6.2 of *Life Estimation of High Level Waste Tank Steel for H-Tank Farm Closure Performance Assessment,* SRNL-STI-2010-00047, were used to determine the time of corrosion initiation due to chlorides.

Hydrology and Far-Field Transport (FF)

RAI-FF-1

The HTF/PORFLOW® model may not be well calibrated. DOE should provide more detail regarding model calibration at HTF.

Basis

GSA/PORFLOW® (and GSA/FACT2) documentation suggests that the GSA model is not well calibrated local to HTF. For example, WSRC-TR-96-00399, Rev. 1, Volume 2 indicates that:

- there are unexpected high residuals east of HTF (Page 23);
- relatively larger residuals are found in and east of HTF (Page 24);
- additional work is needed to better define the artificial recharge and hydraulic conductivity field at HTF, and that artificial recharge may be excessive suggesting the hydraulic conductivity field may require additional adjustment (Page 25); and
- additional work is needed to better define uncertainty in model predictions (Page 25).

Further, WSRC-TR-2004-00106, Rev. 0 indicates on page 23 that GSA/PORFLOW head residuals are generally relatively large compared to GSA/FACT and that the artificial recharge zone in the GSA/FACT model was more effective at reducing head residuals at HTF but was considered less realistic. Page 24 of WSRC-TR-2004-00106, Rev. 0 goes on to state that more extensive model calibration would improve the GSA/PORFLOW® model.

The HTF/PORFLOW® model uses the flow field output from the GSA/PORFLOW® model to simulate contaminant fate and transport for the purpose of making dose predictions in the HTF Performance Assessment. If the HTF/PORFLOW® model is not well-calibrated, the dose predictions may be over- or under-estimated depending on such factors as source location and radionuclide.

Path Forward

DOE should provide additional information regarding the goodness of fit of the model to calibration targets (e.g., water levels) local to the area of interest at HTF. This information should include residuals and calibration statistics for calibration targets available at the time of GSA/PORFLOW® modeling. More recent information could also be used to evaluate model agreement to measured values, if calibration targets used at the time of modeling are not thought to be representative of post-closure conditions (see RAI-FF-2). Environmental monitoring data could also be used to help validate the HTF/PORFLOW® model and demonstrate the sufficiency of the model in predicting contaminant fate and transport at HTF. For example, DOE could perform backwards particle tracking to identify the source of observed Gordon aquifer contamination. If corroborating source release information is available, validation exercises may provide additional support for the predictive capability of the HTF/PORFLOW® model.

[2] The GSA/FACT model is the predecessor to the GSA/PORFLOW® model. Similar data sets were used to construct both models. A similar conceptual model of the GSA is implemented in the models.

Response RAI-FF-1

Use of HTF Environmental Monitoring Data to Validate the Model

A preliminary review of HTF environmental monitoring data was performed to identify any areas in which the data might be used to help validate the HTF PORFLOW modeling. An informal review of the HTF monitoring well sampling results contained within the ERDMS database was conducted to see if any trends or occurrences of interest were noted. The review concentrated on non-volatile beta sample events at wells close to the HTF Tank 16 (i.e., wells HTF-5 through HTF-8), based on the reasonable assumption that radionuclides of primary interest for this exercise (e.g., Tc-99) would show up in the non-volatile beta data at these wells. While this review did identify some non-volatile beta detection results of interest (e.g., high with respect to other results around the same time frame), no obvious trends with respect to location, timing, or magnitude of the events was apparent. While it is possible that a more in depth review of the ERDMS data might result in data tendencies that might be used to help validate the HTF PORFLOW modeling, this possibility was not apparent from the preliminary review.

The following complications muddle the use of HTF well sampling data in HTF PORFLOW Model validation:

1. Well sampling data for HTF before the late 1970s is not available in ERDMS.
2. The HTF well sampling locations with data available vary over time. For example, wells HTF-1 through HTF-17 were drilled in June through September of 1973, while wells HTF-18 through HTF-34 were not drilled until December 1984 through August 1985. In addition, many of the older wells (such as HTF-5 through HTF-9) that had supplied data of interest have been abandoned over the years for various reasons.
3. There are no precisely quantified releases of record against which sampling data could be associated since the few historical releases of note in HTF (e.g., the Tank 16 leak) have material release ranges (versus precise characterization) associated with them and no source-term quantities useful for contaminant tracking.
4. The factors with the most impact on infiltration rates (e.g., rainfall, waste tank asphalting) will have a corresponding impact on travel time, and these factors have varied greatly over time in degrees not easily quantified.

Calibration Target Study

In order to investigate "the goodness of fit of the GSA model to calibration targets (e.g., water levels) local to the area of interest at HTF," a review of the wells utilized in the GSA model calibration was first performed. First, the original set of GSA model well calibration targets was replaced with a more recent, existing set (comprising data from 2002 through 2003) for GSA water table wells (see *An Updated Regional Water Table of the Savannah River Site and Related Coverages*, WSRC-TR-2003-00250). Second, calibration statistics were recomputed. Further study was then concentrated on 52 of the wells across the GSA that were identified to have a > 6-foot residual when compared to the GSA steady-state flow field heads. This threshold was adopted to reflect what is thought to be approximately double, what the water level fluctuation is in most SRS wells, from year to year, due to differences in local and regional precipitation and subsequent deep recharge to the aquifers. Additional data associated with these 52 wells were extracted from the ERDMS database to evaluate each well further as part of this study. Many of the SRS "water table" wells have additional measurements recorded since the 2002 to 2003 period when the Median or Adjusted Median was computed; however, some of the 52 wells have had no additional measurements since that time.

The findings of the present well study are documented in Table RAI-FF-1.1. This Table RAI-FF-1.1 contains a listing of the 52 wells evaluated and a status disposition for each well (each well is generally indicated as "Not Credible" or "Dependable water level estimate"). In most "Not Credible" cases, a reason for the "Not Credible" designation is provided in the comments. Overall, 21 of the 52 wells studied were designated as "Not Credible" while 31 were found to be wells with a dependable estimate of the water level.

Table RAI-FF-1.1: Summary List of High Residual Wells with Status

Well	Median WT	Model Head	Residual	Absolute Residual	Comments
FC4D	**151**	**178.05**	**27.05**	**27.05**	Not credible - screen or borehole likely penetrates into Gordon Aquifer.
HCA1 (a)	269.1	253.95	-15.15	15.15	Dependable water level estimate - No obvious reason to remove this well from target list, 37 measurements.
BGO12CX	**218.5**	**232.66**	**14.16**	**14.16**	Not credible - surrounded by wells whose water levels are 11-13 ft higher, screen zone is situated ~ 10 ft lower in aquifer unit.
HCA2 (a)	269.8	256.3	-13.5	13.5	Dependable water level estimate.
HTF30	**270**	**283.37**	**13.37**	**13.37**	Not credible - limited record, only 3 measurements, last sampled in 1986, surrounded by wells that conform more closely to model.
HAA3D (b)	263.9	250.93	-12.97	12.97	Dependable water level estimate.
HAA5D	**275.3**	**288.22**	**12.92**	**12.92**	Not credible - There are discrepancies in ERDMS database, suggesting the screen zones and water levels of HAA-5D and -5C are mixed.
HCA4 (a)	269	256.14	-12.86	12.86	Dependable water level estimate.
BRR6D	**207.3**	**219.9**	**12.6**	**12.6**	Not credible - ambiguous information in database. Unexplained 11-13 foot drop in water levels after the first 4 measurements.
FBP46D	**166.2**	**178.67**	**12.47**	**12.47**	Not credible - only 2 measurements, possible borehole penetration into Gordon Aquifer
HSL4D (b)	260.9	249.55	-11.35	11.35	Dependable water level estimate
NWP1D	**210.9**	**222.16**	**11.26**	**11.26**	Not credible - anomalous readings. Nearby well has more reasonable water level elevation.
HAA15D (a)	269.8	258.68	-11.12	11.12	Dependable water level estimate
HET1D (b)	268.8	257.77	-11.03	11.03	Dependable water level estimate
HAA2D (b)	276.4	265.73	-10.67	10.67	Dependable water level estimate
FBP44D	**167.5**	**178.15**	**10.65**	**10.65**	Not credible - only 2 measurements, possible borehole into Gordon Aquifer.
HET4D (b)	259.6	249.5	-10.1	10.1	Dependable water level estimate
HET2D (b)	258.7	248.75	-9.95	9.95	Dependable water level estimate
ZW7 (b)	266.7	256.8	-9.9	9.9	Dependable water level estimate
FAL2	**217.3**	**227.16**	**9.86**	**9.86**	Not credible - very close to another well that has much more credible water levels. Possible preferential recharge paths might be influencing well levels.
FCA19D	**217.1**	**226.92**	**9.82**	**9.82**	Not credible - anomalous readings. Nearby well has more reasonable water level elevation.
HHP1D (b)	271.3	261.48	-9.82	9.82	Dependable water level estimate
FNB4	213.9	204.14	-9.76	9.76	Probably dependable - but no new measurements since 1999, after which water levels declined. Other wells nearby have lower water levels since then. Modeled water levels are generally a little low in this area.
HET3D (b)	259.1	249.36	-9.74	9.74	Dependable water level estimate
HSL5D (b)	266.3	256.59	-9.71	9.71	Dependable water level estimate
HC8C	**198**	**207.47**	**9.47**	**9.47**	Not credible - only 1 measurement (in 1988) other suitable calibration targets nearby.

Table RAI-FF-1.1: Summary List of High Residual Wells with Status (Continued)

Well	Median WT	Model Head	Residual	Absolute Residual	Comments
MGC32	**245.2**	**235.95**	**-9.25**	**9.25**	Not credible - anomalous water levels. Surrounded by wells that all have lower median water levels.
BGX8DR	204.9	213.95	9.05	9.05	Dependable water level estimate. New measurements, now 99 total, new median = 203.2 ft; new residual = 10.75 ft, model may be too high here.
FAL1	**218.4**	**227.2**	**8.8**	**8.8**	Not credible - very close to another well that has much more credible water levels. Possible preferential recharge paths might be influencing well levels.
H19	**228.5**	**219.72**	**-8.78**	**8.78**	Not credible - surrounded by wells with more credible water levels. Screen zone reported to be 1.5 ft. in length.
HSB141D	237.9	229.4	-8.5	8.5	Dependable water level estimate
FBP47D	**170.4**	**178.78**	**8.38**	**8.38**	Not credible - only 2 measurements, possible borehole into Gordon Aquifer.
BG29	**244**	**235.87**	**-8.13**	**8.13**	Not credible
HAA8D	266.5	258.9	-7.6	7.6	Dependable water level estimate
NWP3D	225	232.52	7.52	7.52	Dependable water level estimate - conforms to neighbors BGO-13DR and -14DR closely.
HR811	246.8	239.38	-7.42	7.42	Dependable water level estimate
HHP2D	274.5	267.11	-7.39	7.39	Dependable water level estimate
NEP4D	191.6	198.9	7.3	7.3	Dependable water level estimate - about 10 ft higher than nearby flowing stream. Model needs to honor flowing stream elevations as = to the water table.
FSL4D	216.8	224.01	7.21	7.21	Dependable water level estimate - new median water table for full record is 214.7 ft, so new residual is ~ 9.3 ft.
BGX3D	214.5	221.49	6.99	6.99	Dependable water level estimate - many new measurements, general drop in water levels since 2003; new full record median = 212.4 ft.
BG115	**215.8**	**222.76**	**6.96**	**6.96**	Not credible; only 1 measurements in 1988; other suitable calibration targets nearby.
Z1	**218.7**	**225.59**	**6.89**	**6.89**	Not credible; only 1 measurements in 1986; other suitable calibration targets nearby.
NWP2D	200.2	207.02	6.82	6.82	Dependable water level estimate. very similar to HMD-2D and HMD-1D during the period of record overlap.
BGX5D	208.2	215	6.8	6.8	Dependable water level estimate. Now 115 measurements. Median water table = 202.6 ft, new residual = 8.8 ft, no obvious reason to eliminate.
ZW2	**207.5**	**200.77**	**-6.73**	**6.73**	Not credible. No new measurements since 1995. Nearby well FNB-5 has same screen interval, longer record of measurements - complete overlap. Its residual is -1.2 ft.
FAC2	**235.9**	**229.31**	**-6.59**	**6.59**	Not credible -- older construction, screen too high, may partially reflect perching. More reliable sources close-by.
NBG3	217.5	223.99	6.49	6.49	Dependable WL estimate.
FNB3	208.7	202.31	-6.39	6.39	Dependable water level estimate. New median computed - 208.0 ft, new Residual = -5.69 ft; < 6 ft residual now.
FAC6	220.7	227.01	6.31	6.31	Dependable water level estimate. Even though slightly out of acceptable range, several other similar wells near, with median water levels less than the 6-ft threshold.
BG30	**241.1**	**234.86**	**-6.24**	**6.24**	Not credible.
BG94	191.9	185.69	-6.21	6.21	Dependable water level estimate. Water levels have dropped since the last measurement in this well and probably the residual is < 6 ft, now.
NWP101D	225.5	231.56	6.06	6.06	Dependable water level estimate. Conforms to neighbors BGO-13DR and -14DR closely.

Wells shown in **Bold** were designated "Not Credible"
a: Wells in zone near H-Canyon in H Area where model seems to be low in computing water table elevations
b: Wells southwest of HTF where model seems to be low in computing water table elevations

Two relatively small areas were identified over which the GSA model could be improved to make the computed water levels conform somewhat better to well measurements. Both areas are near HTF and they both have the model predicting water level a little low. The wells associated with these two areas are noted in Table RAI-FF-1.1. Specifically, the two areas where the GSA model seems to be low in computing heads (residuals > 6 foot) are a zone just southwest of HTF and a zone near H-Canyon. An image of each area (shaded blue in the figures) is provided in Figures RAI-FF-1.1 and RAI-FF-1.2. Model refinements in these areas would produce modest perturbations to hydraulic gradients and groundwater velocities. Based on the location of these two relatively small areas, any potential model improvements would not be expected to significantly impact near field (i.e., 100 meter) releases from the HTF. The risk significance of groundwater velocity variability is investigated in the response to RAI-FF-3 through two aquifer flow field sensitivity cases.

In general, the GSA model "goodness-of-fit" improved with consideration of the updated and screened calibration targets from 2002 to 2003. Additional information regarding the Goodness of Fit of the Model to Calibration Targets is provided in the response to RAI-FF-2, including calibration statistics local to H Area.

Figure RAI-FF-1.1: Low Zone Outside H Area Southwest of HTF (Wells with Residuals > 6 foot)

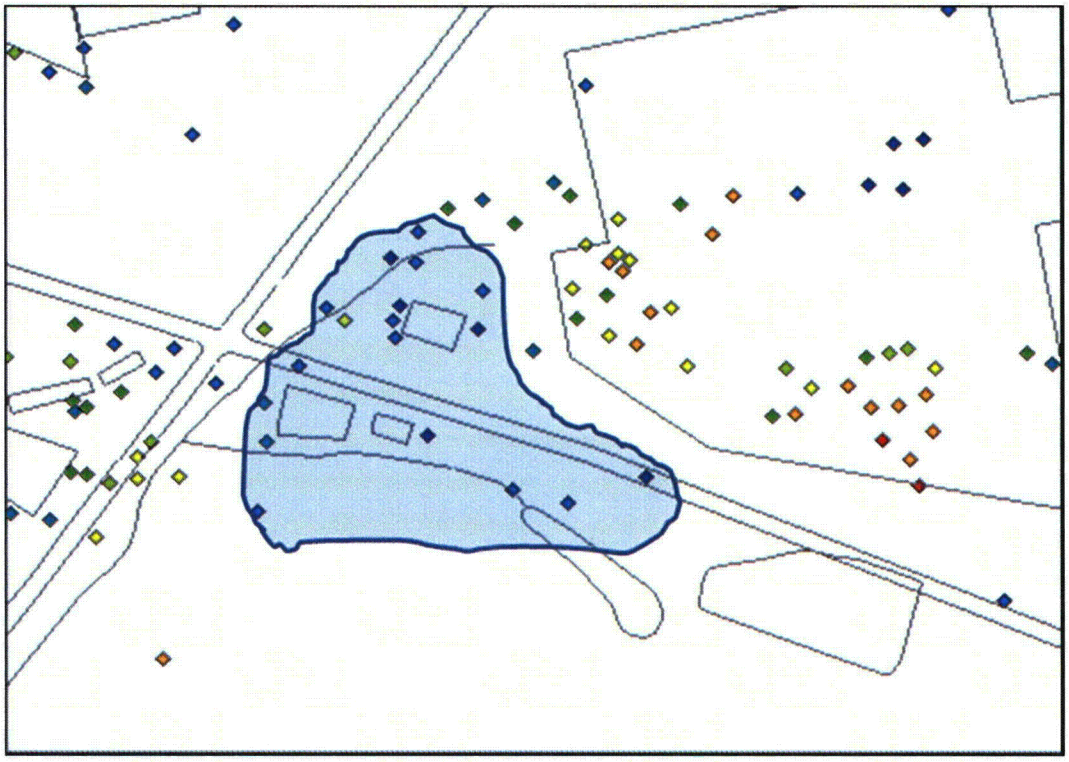

Figure RAI-FF-1.2: Low Zone within H Area near H-Canyon (Wells with Residuals > 6 foot)

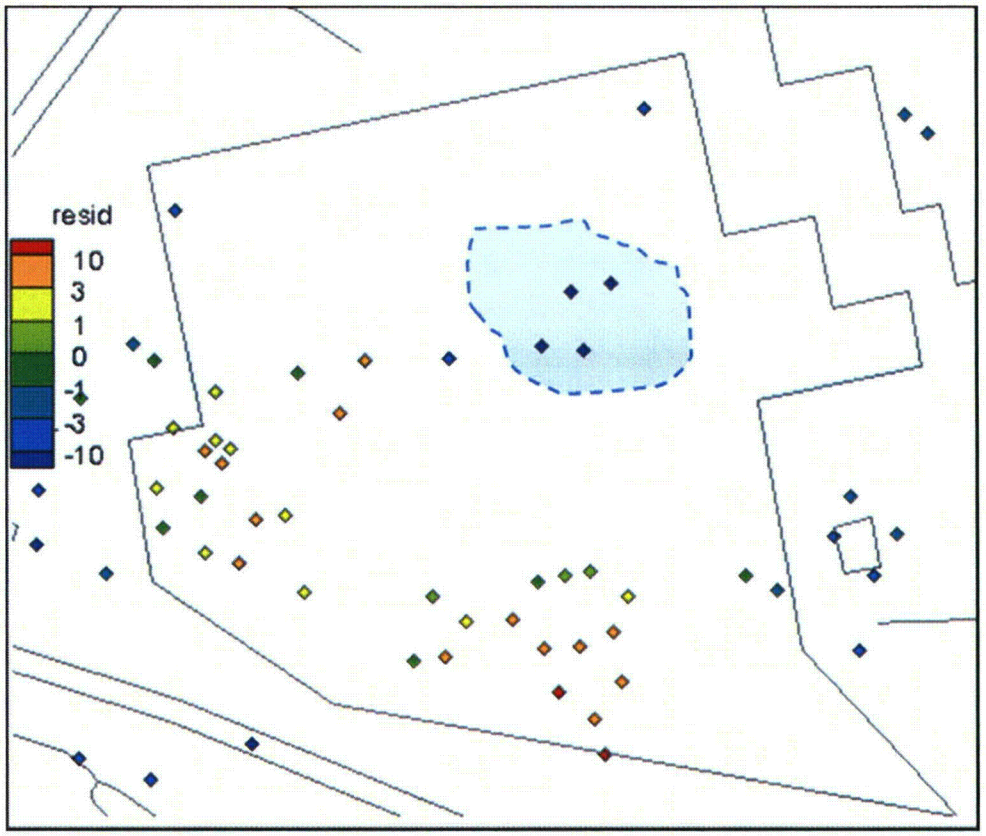

RAI-FF-2

HTF calibration targets developed during GSA model development may not represent post-closure conditions. DOE should evaluate the representativeness of HTF calibration targets to long-term conditions.

Basis

The GSA/FACT and GSA/PORFLOW® models, upon which the HTF/PORFLOW® model is based, were calibrated to what was considered long-term average water levels at the time of modeling. However, operational sources and sinks at HTF may have influenced water level measurements used to develop calibration targets. Calibration targets may also be biased high or low in comparison to long-term values given the relatively short time interval over which water level measurements were averaged. If the HTF/PORFLOW® model is not well calibrated to calibration targets representative of post-closure conditions, it is unclear if the HTF/PORFLOW® model is adequate for the purposes of simulating post-closure contaminant flow and transport at HTF.

Path Forward

GSA/FACT model documentation lists a number of potential sources local to HTF. For example, WSRC-TR-96-00399, Rev. 1, Volume 2 (page 21) lists a number of water leaks or potential sources to the model and indicates that undoubtedly unknown leaks exist at HTF. DOE should evaluate the potential for GSA/PORFLOW® calibration targets to have been influenced by potential sources and sinks, including the sources listed in the GSA/FACT model documentation.

Since the GSA/FACT and GSA/PORFLOW® models were developed, additional information has been collected at HTF that could also be used to evaluate the representativeness of the calibration targets. DOE could perform the following types of activities related to consideration of new information:

- Develop new calibration targets based on a longer or more representative period of record.
- Develop uncertainty ranges for calibration targets.
- Evaluate the goodness of fit of the HTF/PORFLOW® model to new calibration targets.
- If necessary, recalibrate the GSA/PORFLOW® model[3].

Finally, DOE could provide arguments as to why the HTF/PORLOW® model is adequate for the purposes of making long-term dose predictions for the HTF Performance Assessment (e.g., sufficient accuracy or biased towards higher dose predictions).

[3]Model recalibration is a long-term effort that is not expected to be accomplished during the RAI resolution period.

Response RAI-FF-2

The HTF PA presents in Table 4.2-17 the GSA/PORFLOW calibration statistics for well water level data through 1995, which was used to develop the original GSA model, and updated monitoring data through 2006. These data comparisons are reproduced here as Tables RAI-FF-2.1 and RAI-FF-2.2, respectively. Both data sets indicate the presence of double-digit residuals as evidenced by the minimum and maximum values. These large residuals could be a concern to the extent that the underlying well targets are representative of long-term average conditions and had an influence on model calibration. To investigate the former, well water levels were reevaluated for reliability as model calibration targets, focusing on shallow wells used to define the water table in 2003 as discussed in the Calibration Target Study section of RAI-FF-1.

Table RAI-FF-2.1: Summary Statistics for GSA/PORFLOW Hydraulic Head Residuals for Well Targets (through 1995)

Aquifer Zone	Number of Wells	Residual Median	Residual Average	Residual RMS	Residual min	Residual max
Gordon	79	-0.0	-0.5	+1.7	-4.7	+2.5
lower UTR	173	+0.8	+0.6	+4.6	-9.4	+27.0
upper UTR	386	-0.1	-0.5	+3.4	-15.2	+10.0

RMS = Root-Mean-Square

Table RAI-FF-2.2: Summary Statistics for GSA/PORFLOW Hydraulic Head Residuals for Well Targets (updates through 2006)

Aquifer	Number of Wells	Residual Median	Residual Average	Residual RMS	Residual min	Residual max
Gordon	94	+0.3	-0.0	+1.5	-3.8	+2.6
UTRA-LZ	272	+1.1	+1.0	+4.7	-11.9	+27.0
UTRA-UZ	551	+0.8	+0.1	+3.5	-16.8	+14.5

RMS = Root-Mean-Square

As discussed in the response to RAI-FF-1, a review of ERDMS well data across the GSA was performed as a first step toward investigating the "goodness of fit" of the GSA model to calibration targets (e.g., water levels) local to the area of interest at HTF. The results of this study are documented in Table RAI-FF-1.1 of the response to RAI-FF-1. Out of wells available for calibration (data was not available for all of the wells within the model domain), 21 wells were determined or suspected to be unreliable model calibration targets, as discussed in the response to RAI-FF-1. Table RAI-FF-2.3 presents summary statistics for hydraulic head omitting the 21 unreliable wells. The minimum and maximum residuals for the 2003 well targets documented in *An Updated Regional Water Table of the Savannah River Site and Related Coverages,* WSRC-TR-2003-00250, are observed in Table RAI-FF-2.3 to be much improved over Table RAI-FF-2.2. Figure RAI-FF-2.1 shows the spatial distribution of residuals corresponding to Table RAI-FF-2.3. Focusing on the HTF and surroundings, Figure RAI-FF-2.2 shows residuals within a 3,500-foot radius of H Area, and Table RAI-FF-2.4 summarizes statistics for this subgroup using the 2003 well targets.

The GSA model reasonably fits the underlying well data and the fit with available well data is improved when unreliable well data is removed. DOE believes the GSA model is adequate for the purposes of fate and transport modeling in the HTF PA, considering the risk significance of hydraulic conductivity and flow field variability, as discussed in the response to RAI-FF-3.

Table RAI-FF-2.3: Summary Statistics for GSA/PORFLOW Hydraulic Head Residuals for 2003 Well Targets

Aquifer Zone	Number of Wells	Residual Median	Residual Average	Residual RMS	Residual min	Residual max
Gordon	-	-	-	-	-	-
UTRA-LZ	52	+2.7	+1.6	+4.3	-9.8	+9.0
UTRA-UZ	406	+0.4	-0.0	+3.4	-15.2	+7.5

RMS = Root-Mean-Square

Table RAI-FF-2.4: Summary Statistics for GSA/PORFLOW Hydraulic Head Residuals for 2003 Well Targets near H Area

Aquifer Zone	Number of Wells	Residual Median	Residual Average	Residual RMS	Residual min	Residual max
Gordon	-	-	-	-	-	-
UTRA-LZ	-	-	-	-	-	-
UTRA-UZ	85	-0.8	-2.0	+5.4	-15.2	+5.9

RMS = Root-Mean-Square

Figure RAI-FF-2.1: GSA/PORFLOW Hydraulic Head Residuals for 2003 Well Targets

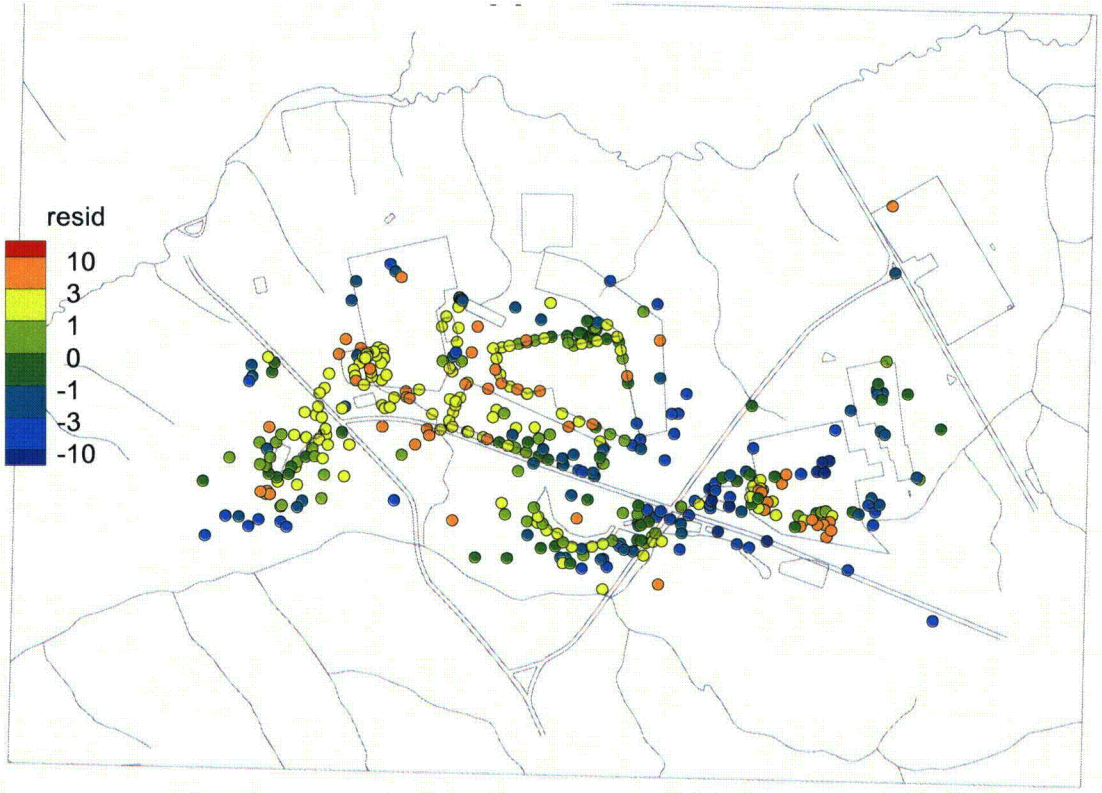

Figure RAI-FF-2.2: GSA/PORFLOW Hydraulic Head Residuals for 2003 Well Targets near H Area

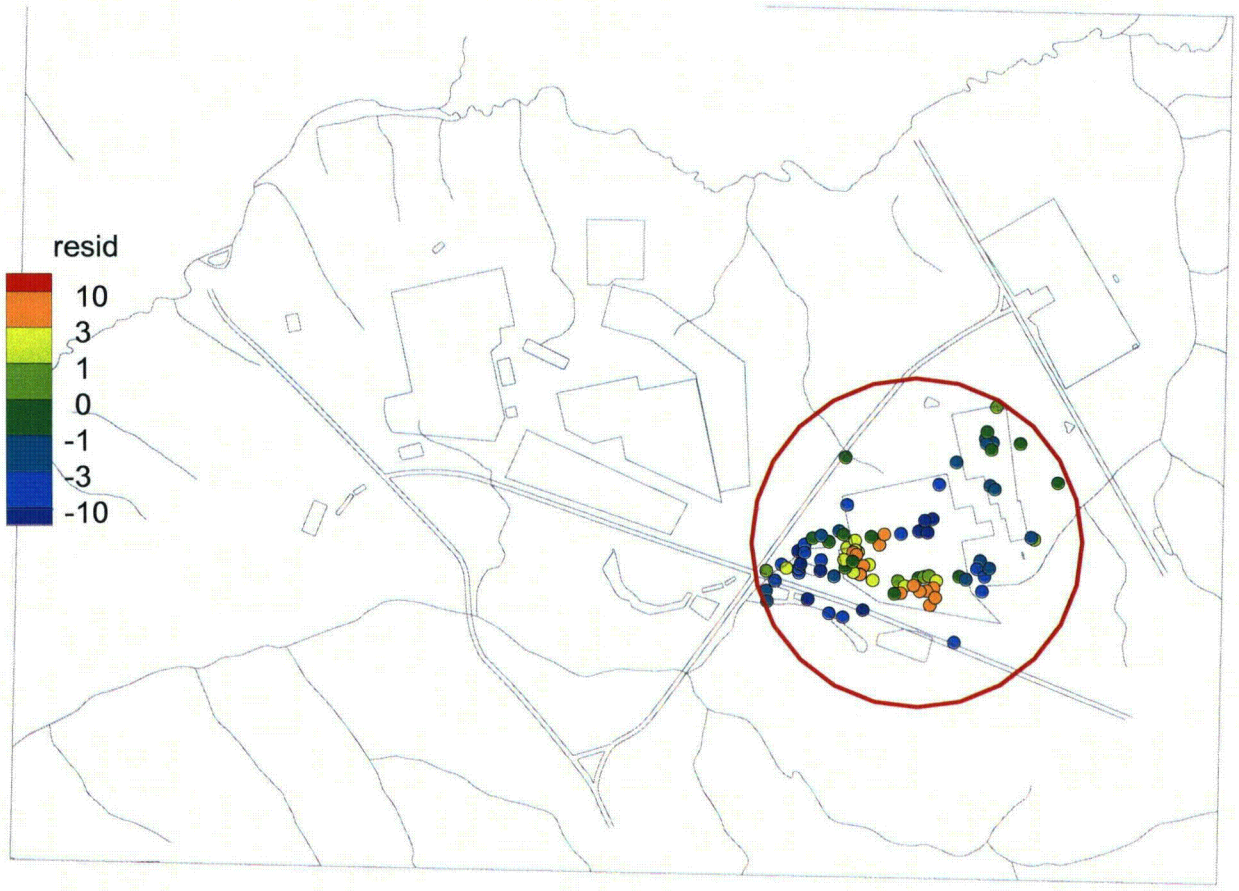

RAI-FF-3

A strong physical basis for adjustments to the Upper Three Runs Aquifer hydraulic conductivity at HTF during GSA/PORFLOW® model calibration was not provided. DOE should provide additional support for hydraulic conductivity assignments at HTF.

Basis

Adjustments to hydraulic conductivity during the GSA/PORFLOW® model calibration process may not be adequately supported and could lead to significant impacts to the flow field at HTF. Changes in hydraulic conductivity could lead to increased or decreased dilution factors and travel times. Dose predictions could be under- or over-estimated depending on such factors as source location and radionuclide.

GSA/PORFLOW® model documentation (WSRC-TR-2004-00106, Rev. 0) indicates that during model recalibration, hydraulic conductivity was lowered and artificial recharge sources[4] omitted at HTF. The documentation indicates that a low permeability confining zone or generally lower hydraulic conductivity was thought to exist at HTF but supporting details were lacking. More recently, DOE indicated that there may be evidence of low permeability zones and perched water at HTF but upon further investigation stated that there appears to be a lack of corroborating evidence for perched zones at HTF (ML13126A127; ML13154A327).

Path Forward

DOE should perform the following activities to clarify and provide additional support for the hydraulic conductivity assignments at HTF:

- Clarify the horizontal and vertical extent of hydraulic conductivity adjustments at HTF.
- Provide additional support for the hydraulic conductivities assumed for HTF.
- Evaluate the impact of hydraulic conductivity adjustments on key radionuclide concentrations and dose at the compliance boundaries.

[4]Artificial recharge sources at HTF were added during predecessor model, GSA/FACT, calibration.

Response RAI-FF-3

Clarification of Hydraulic Conductivity Adjustments

Section 2.9 of *Pre- And Post-Processing Software Associated with the GSA/FACT Groundwater Flow Model,* WSRC-TR-99-00106, describes the overall process for developing the GSA/PORFLOW model conductivity fields, and Section 2.9.5 of the document describes the tools available for making hydraulic conductivity adjustments to match calibration targets. Figure RAI-FF-3.1 provides a full listing of the hydraulic conductivity adjustments made in the GSA/PORFLOW model to the initial conductivity field based primarily on mud fraction data from sediment cores, as requested in the RAI-FF-3 *Path Forward* (see WSRC-TR-99-00106, Section 2.9.5 for further explanation of the adjustment process).

Figure RAI-FF-3.1: Contents of "Cal.dat" Defining Adjustments to the Initial GSA/PORFLOW Hydraulic Conductivity Field

```
!
! GLOBAL ADJUSTMENTS TO BASELINE
./Polygons/All.ply
'../Hydrostrat/surf1.out',0.0
'../Hydrostrat/surf2.out',0.0
                              1.    38.     38.      1.    0.005   1.e+20   1.e+20
1.   'au'  .true.
./Polygons/All.ply
'../Hydrostrat/surf2.out',0.0
'../Hydrostrat/surf3.out',0.0
                              1.    1.e-3   1.e-3    1.    1.e-5   1.e-5    1.e+20
1.   'cu'  .true.
./Polygons/All.ply
'../Hydrostrat/surf3.out',0.0
'../Hydrostrat/surf4.out',0.0
                              1.15  1.e-20  1.e+20   1.    0.05    1.e+20   1.e+20
1.   'au'  .true.
./Polygons/All.ply
'../Hydrostrat/surf4.out',0.0
'../Hydrostrat/surf5.out',0.0
                              1.    1.e-20  1.e+20   1.    0.005   0.05     1.e+20
1.   'cu'  .true.
./Polygons/All.ply
'../Hydrostrat/surf5.out',0.0
'../Hydrostrat/surf7.out',0.0
                              1.15  1.e-20  1.e+20   1.    0.05    1.e+20   1.e+20
1.   'au'  .true.
!
! PERTURBATIONS ON BASELINE
./Polygons/LA_1.ply
'../Hydrostrat/surf3.out',0.0
'../Hydrostrat/surf4.out',0.0
                              1.3   1.e-20  1.e+20   1.    0.05    1.e+20   1.e+20
1.   'au'  .true.
./Polygons/LA_2.ply
'../Hydrostrat/surf3.out',0.0
'../Hydrostrat/surf4.out',0.0
                              1.    1.e-20  5.       1.    0.05    1.e+20   1.e+20
1.   'au'  .true.
./Polygons/TC_1.ply
'../Hydrostrat/surf4.out',0.0
'../Hydrostrat/surf5.out',0.0
                              1.    1.e-20  1.e+20   1.    0.001   0.01     1.e+20
1.   'cu'  .true.
./Polygons/TC_2.ply
'../Hydrostrat/surf4.out',0.0
'../Hydrostrat/surf5.out',0.0
                              1.    1.e-20  1.e+20   1.    0.01    0.05     1.e+20
1.   'cu'  .true.
./Polygons/TC_3.ply
'../Hydrostrat/surf4.out',0.0
'../Hydrostrat/surf5.out',0.0
                              1.    1.e-20  1.e+20   1.    0.0001  0.001    1.e+20
1.   'cu'  .true.
./Polygons/UA_1.ply
'../Hydrostrat/surf5.out',0.0
'../Hydrostrat/surf7.out',0.0
                              0.8   1.e-20  1.e+20   1.    0.05    1.e+20   1.e+20
1.   'au'  .true.
./Polygons/UA_2.ply
'../Hydrostrat/surf5.out',0.0
'../Hydrostrat/surf7.out',0.0
                              1.    1.e-20  4.       1.    0.05    1.e+20   1.e+20
```

The adjustment process involved multiple steps. In the first step, global adjustments were made to the five-hydrostratigraphic zones. These perturbations are summarized, by zone, as follows:

- Gordon Aquifer: set horizontal hydraulic conductivity (K_h) = 38 ft/d and require vertical hydraulic conductivity (K_v) > 0.005 ft/d (i.e., values less than 0.005 ft/d are set to 0.005 ft/d)
- Gordon Confining Unit: set K_h = 1.0E-03 ft/d and K_v = 1.0E-05 ft/d
- UTRA-LZ: increase K_h by 1.15 × and require K_v > 0.05 ft/d
- TCCZ, UTR Aquifer: Require 0.005 < K_v < 0.05 ft/d
- UTRA-UZ: increase K_h by 1.15 × and require K_v > 0.05 ft/d

In the second step of the adjustment process, adjustments were made to specific zones based on more local calibration needs. Figures RAI-FF-3.2, RAI-FF-3.3, and RAI-FF-3.4 illustrate the selection polygons defining the targeted zones (the Gordon Confining Unit and Gordon Aquifer did not need adjustments).

Figure RAI-FF-3.2: Key Model Calibration Selection Polygons for the UTRA-UZ

Figure RAI-FF-3.3: Key Model Calibration Selection Polygons for the TCCZ

Figure RAI-FF-3.4: Key Model Calibration Selection Polygons for the UTRA-LZ

The hydraulic conductivity adjustments made near H Area were based on calibration to well water levels and were summarized by the following:

- LA_2 polygon: Require K_h < 5 ft/d and K_v > 0.05 ft/d
- TC_3 polygon: Require 0.0001 < K_v < 0.001 ft/d
- UA_2 polygon: Require K_h < 4 ft/d and K_v > 0.05 ft/d
- UA_4 polygon: Require K_h < 1.5 ft/d and K_v > 0.005 ft/d
- In the third step of the adjustment process, global adjustments were made to accommodate porting the GSA model from the FACT code to the PORFLOW code. [WSRC-TR-2004-00106] These adjustments, by zone, were:
- UTRA-LZ: Increase K_h by 1.35×
- TCCZ: Decrease K_v by 0.5×
- UTRA-UZ: Increase K_h by 1.25×

The remaining adjustments impose conductivity values specific to alluvium and pumping test areas. The resulting conductivity field is partially depicted by the vertically averaged values within the UTR Aquifer shown in Figures RAI-FF-3.5 through RAI-FF-3.7. The UTRA-UZ average includes values above the water table.

Figure RAI-FF-3.5: Vertically Averaged Horizontal Conductivity in the UTRA- UZ

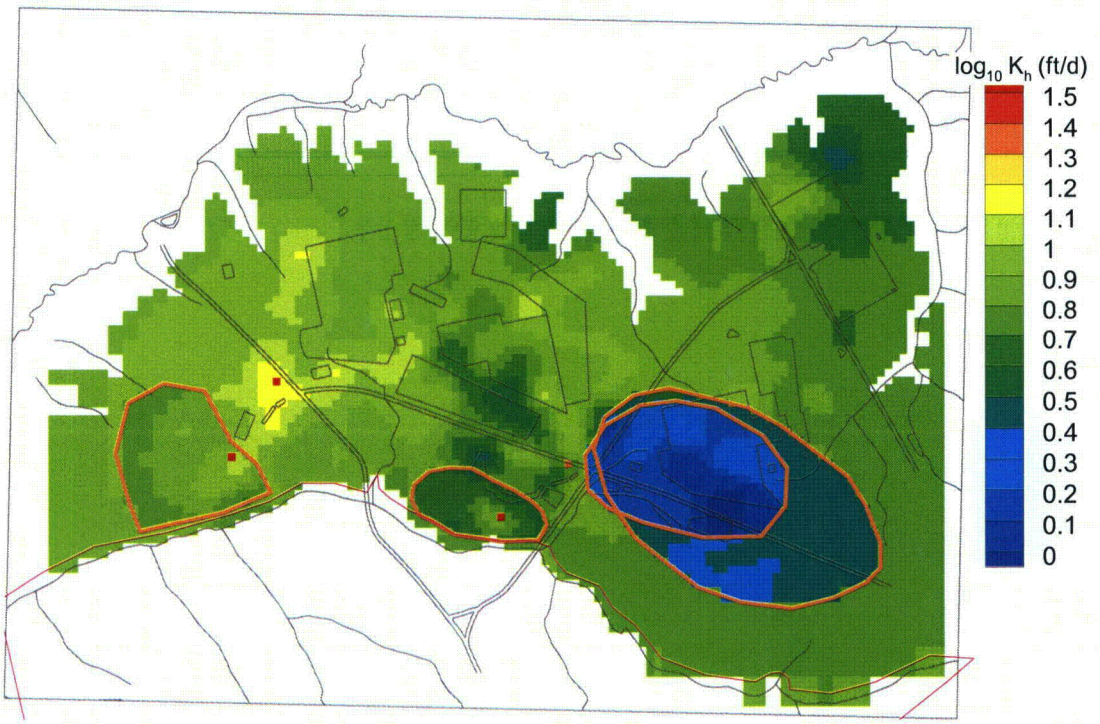

Figure RAI-FF-3.6: Vertically Averaged Vertical Conductivity in the UTR Aquifer TCCZ

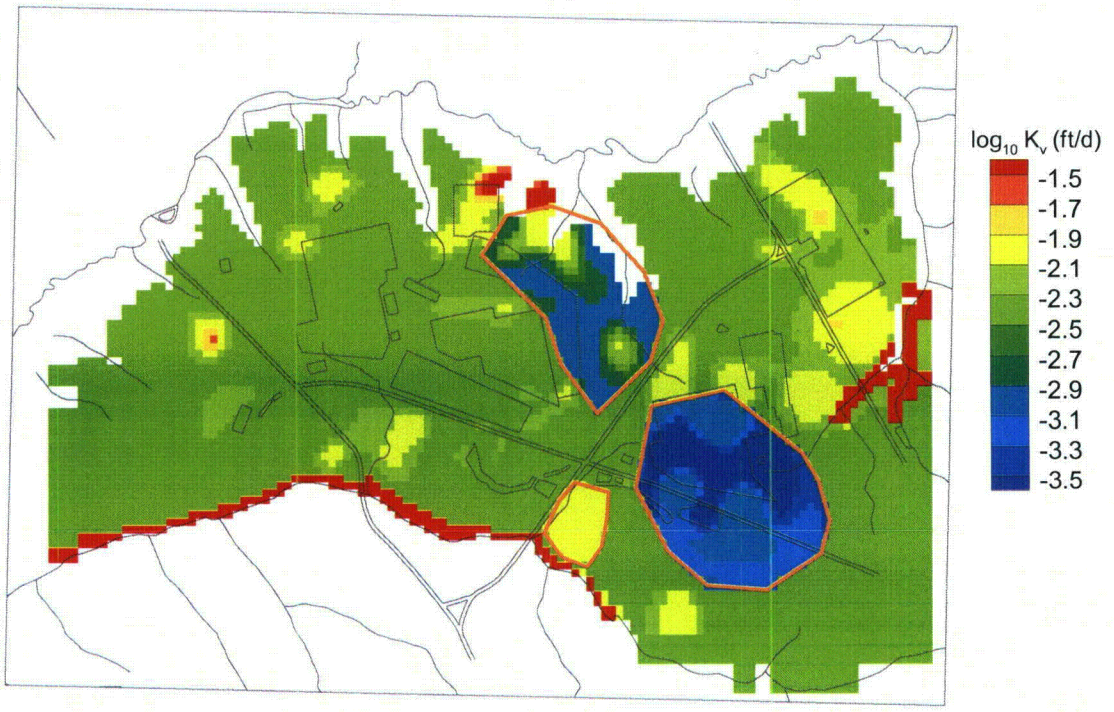

Figure RAI-FF-3.7: Vertically Averaged Horizontal Conductivity in the UTRA-LZ

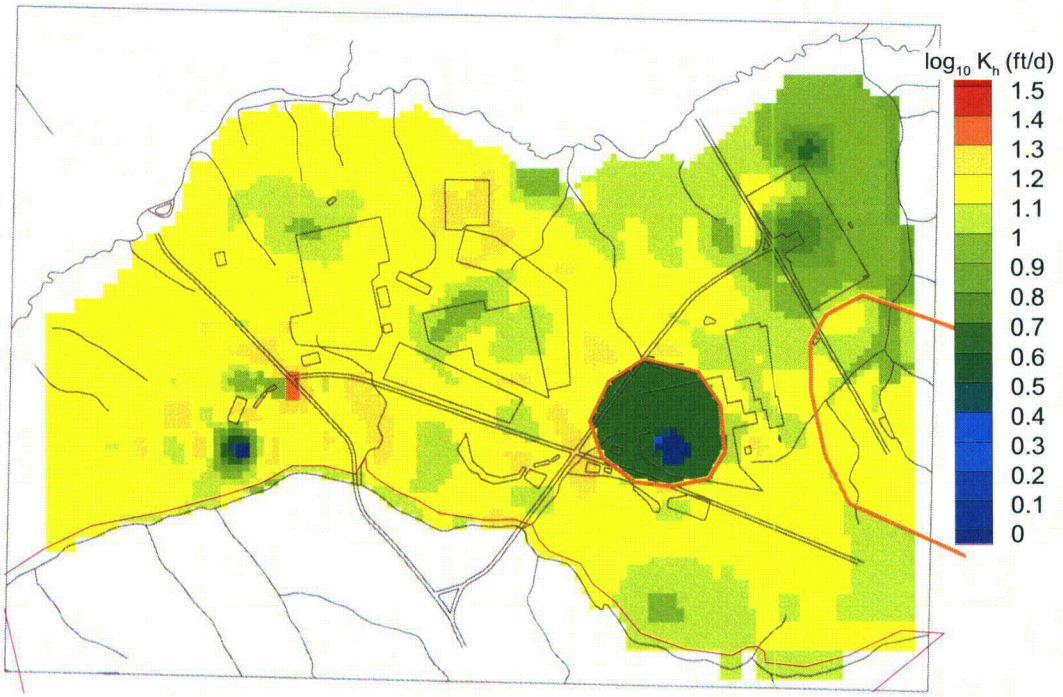

Impact of Far Field Flow Variability

The risk significance of hydraulic conductivity adjustments and other settings in the GSA/PORFLOW far field flow model can be assessed by considering the sensitivity of solute transport simulations to potential variations in the aquifer velocity field, which affects plume travel time and distance. The potential variability in aquifer flow rate in the GSA was considered in the response to RAI-47 of *Response To Additional Information Request on Draft Section 3116 Determination For Salt Waste Disposal at Savannah River Site*, CBU-PIT-2005-00131. In the RAI-47 response, "Fast" and "Slow" velocity fields were generated to complement the "Nominal" GSA/PORFLOW simulation by adjusting 1) recharge, 2) leakage through the Gordon Confining Unit, and 3) effective porosity. For the off-nominal scenarios, each of the three parameters was adjusted to its plus or minus 95 % confidence level value to produce the fastest and slowest possible solute travel times. The UTR hydraulic conductivity field was then re-adjusted to maintain approximate calibration to hydraulic head targets. Particle tracking for the HTF and the Nominal, Fast, and Slow aquifer flow fields are shown in Figures RAI-FF-3.8 through RAI-FF-3.10. The three alternatives exhibit a wide variation in travel time to a point 100 meters from the HTF facility boundary corresponding to a significant variation in the average UTR Aquifer flow rate.

Figure RAI-FF-3.8: Groundwater Pathlines and 10-Year Time Markers for the Nominal GSA/PORFLOW Flow Field

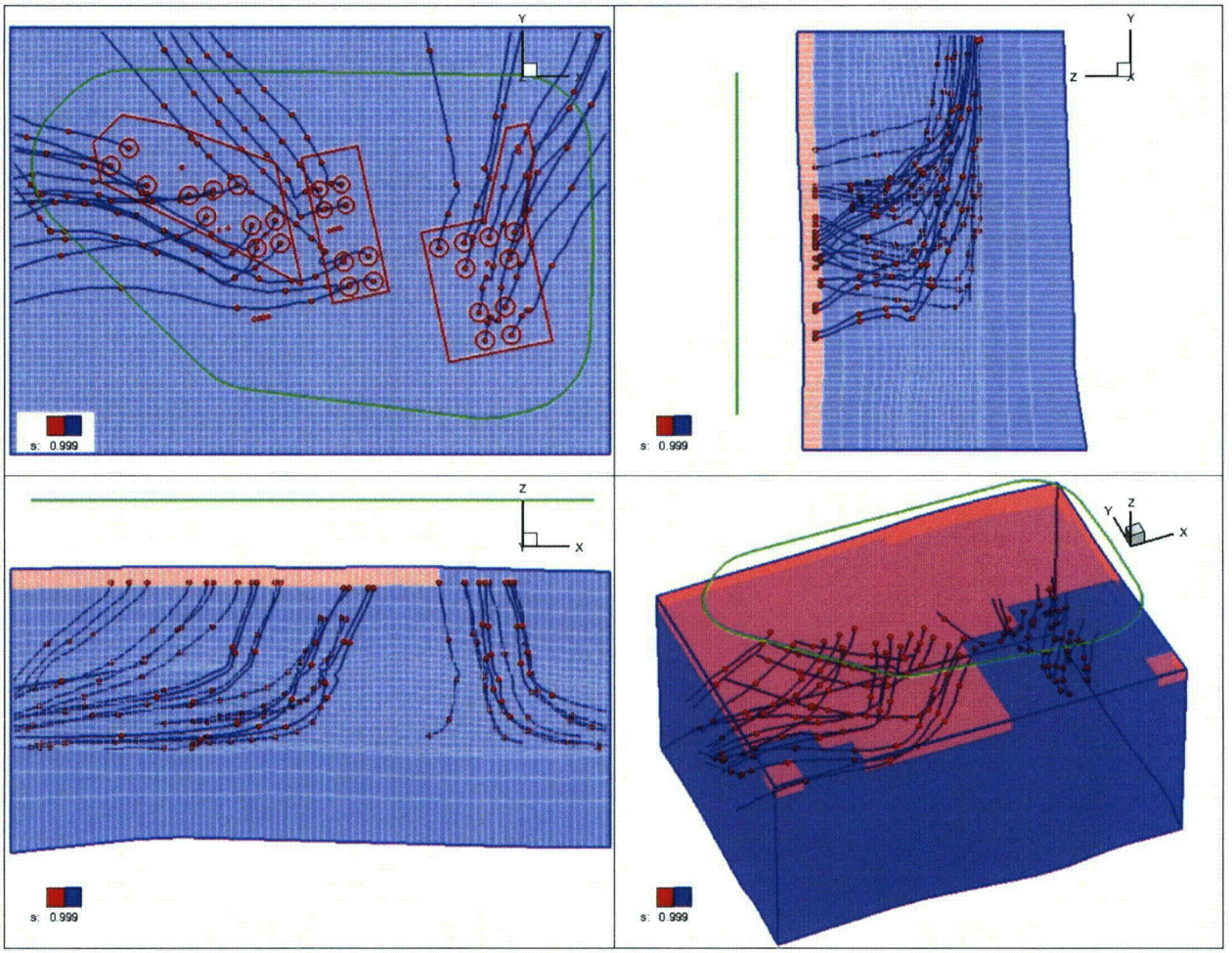

Figure RAI-FF-3.9: Groundwater Pathlines and 10-Year Time Markers for the Alternative Fast GSA/PORFLOW Flow Field

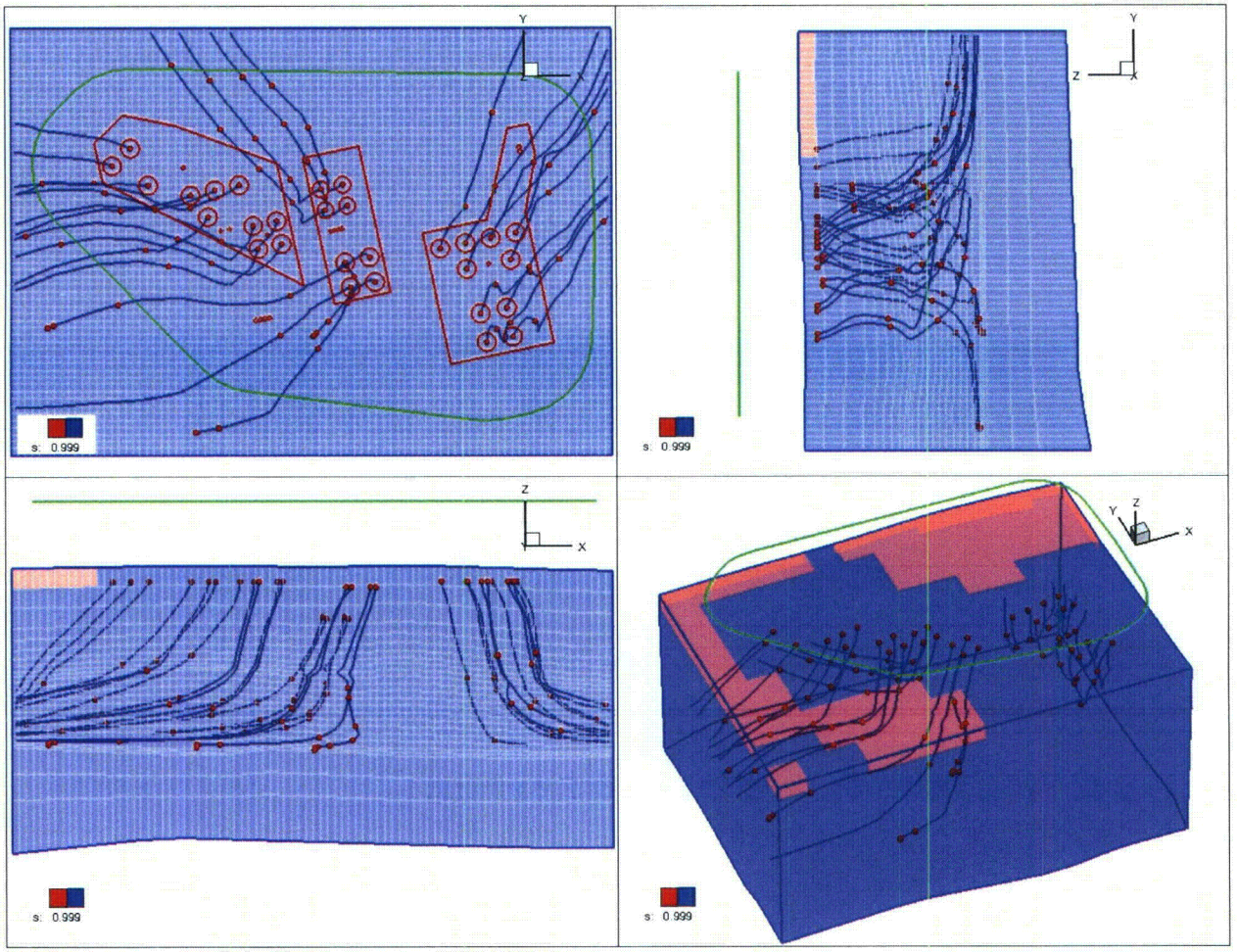

Figure RAI-FF-3.10: Groundwater Pathlines and 10-Year Time Markers for the Alternative Slow GSA/PORFLOW Flow Field

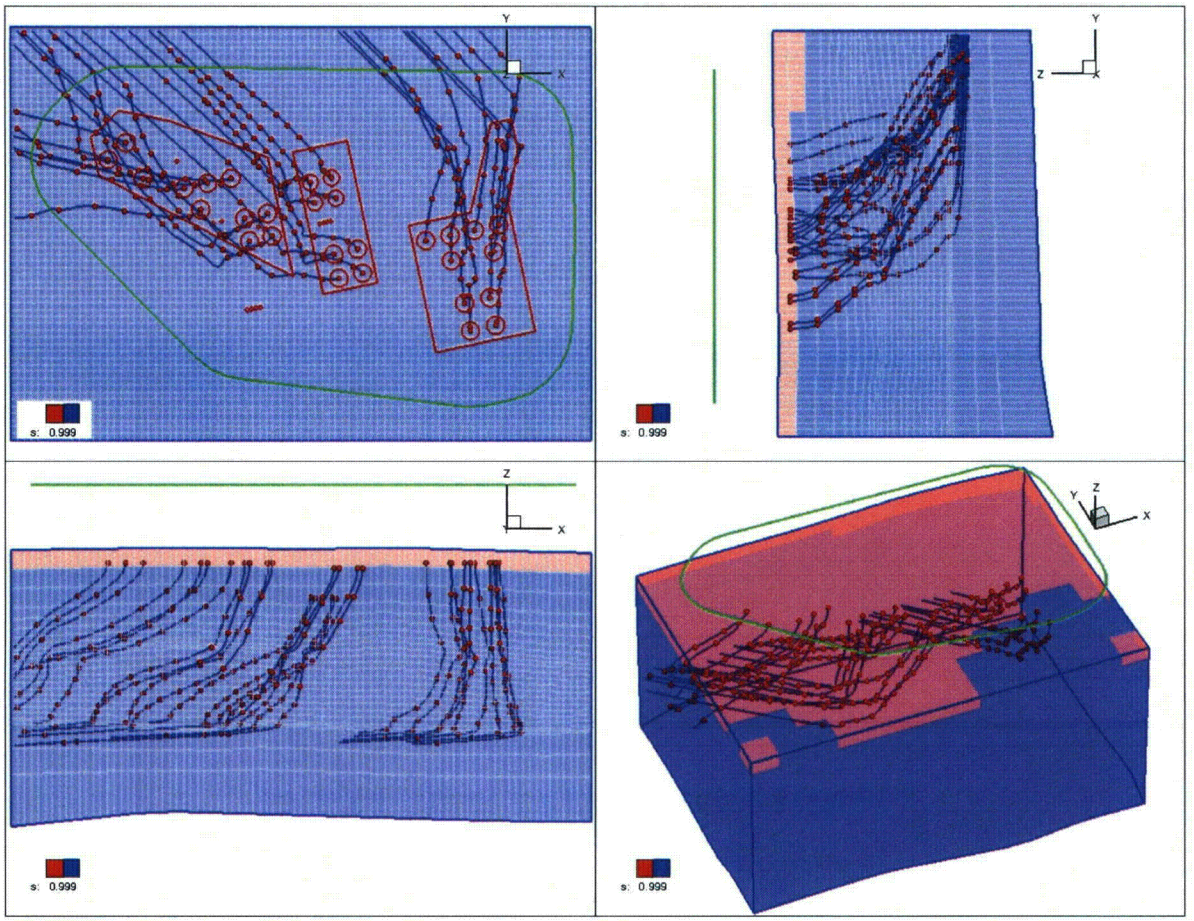

The HTF PA GoldSim Model was used to perform additional deterministic sensitivity runs using flow variability. These new modeling runs provide insights to the sensitivity of peak doses relative to variability in aquifer flow rate. For this analysis, all of the Base Case (Case A) assumptions were used except that the Darcy velocities along the pathlines were varied for each run. The objective of this analysis was to evaluate, non-mechanistically, the flow variability independent of cause, to understand the relative risk importance of various inputs to hydrogeology (hydraulic conductivities, recharge rates, barrier degradation rates) better.

The HTF GoldSim Model was deterministically executed three times, each time using a different set of pathline specific Darcy velocities (displayed in Table RAI-FF-3.1). The three sets of Darcy velocities represent the nominal set used in the PA, a fast set, and a slow set. The Darcy velocities were based on the times that breakthrough curve peaks, generated by instantaneous releases of conservative tracers at the individual waste tanks, reached the 100-meter distance from the HTF (the 100-meter distance from HTF is shown in Figure 5.2-1 of the HTF PA). The Darcy velocities were in turn, generated by dividing the pathline distance to the 100-meter distance from the HTF by the peak breakthrough times to generate a pore velocity and multiplying the pore velocity by the porosity. Note that because the nominal pathline distances were used to generate all three velocity fields, the sets represent approximations, which can be (and are) used only to examine specific effects on processes such as dilution.

Table RAI-FF-3.1: Darcy Velocities Used in the Far Field Flow Variability Study

Tank or Ancillary Structure	Slow Darcy Velocity Rates (ft/yr)	Nominal Darcy Velocity Rates (ft/yr)	Fast Darcy Velocity Rates (ft/yr)
T9	2.6	4.3	4.4
T10	2.4	3.7	4.0
T11	3.0	4.4	4.4
T12	2.8	3.9	3.7
T13	6.4	10.8	14.3
T14	3.8	4.2	5.9
T15	6.3	9.8	11.4
T16	7.0	13.1	14.1
T21	4.3	10.7	10.7
T22	3.7	10.0	11.7
T23	4.0	9.0	9.8
T24	4.0	10.5	11.6
T29	3.8	6.2	7.9
T30	5.1	6.2	7.7
T31	4.0	6.5	7.9
T32	3.8	5.9	7.6
T35	7.1	8.1	9.4
T36	7.6	8.3	9.9
T37	7.6	8.8	9.5
T38	4.9	5.9	5.9
T39	5.3	6.8	6.8
T40	5.8	8.2	8.5
T41	5.6	9.2	10.3
T42	4.6	5.5	6.5
T43	4.4	7.3	9.7
T48	4.3	5.0	7.1
T49	3.5	5.2	7.3
T50	4.1	4.5	6.0
T51	2.7	4.2	6.1
HPT2	3.4	4.1	4.3
HPT3	3.3	4.0	4.2
HPT4	3.3	3.8	4.0
HPT5	6.8	11.9	13.6
HPT6	7.0	11.4	13.0
HPT7	7.7	11.2	12.4
HPT8	7.3	10.8	12.9
HPT9	7.1	11.3	13.6
HPT10	7.9	11.0	11.9
E242_H	4.3	11.3	12.5
E242_16H	4.8	6.7	8.4
E242_25H	6.4	6.7	7.7
HTF_T_Line1	10.9	19.1	29.9
HTF_T_Line2	3.2	5.1	5.8
HTF_T_Line3	12.5	15.7	27.4
HTF_T_Line4	6.9	12.0	13.0
CTSO	4.2	7.1	8.9
CTSN	4.9	8.4	10.1

Figure RAI-FF-3.11 depicts peak dose curves (from any sector) for the three runs. Comparing the dose curves presented in Figure RAI-FF-3.11 it can be seen that there is relatively little difference between the three dose curves. In early years, the slow-flow results have the highest peaks of the three runs, mainly reflecting a decrease in Tc-99 dilution, due to lower flow rates. In later years, the lower flow-rate run generates lower doses, reflecting the dose contribution of Ra-226, a radionuclide with a relatively high decay rate, that is moderately to strongly sorbed in the soil. For Ra-226, the influence of the slower flow rates on decay dominates over the influence of decreased dilution. Even when other species control the shape of the peak, such as Tc-99 at 10,000 years, the lower Ra-226 dose contributions lower the peak values. Comparing the nominal flow-rate results with the fast flow-rate results in Figure RAI-FF-3.11 shows that the faster-flow tends to produce slightly lower dose levels at early times and then increases the dose levels later on. This once again reflects the importance of dilution (which increases in the faster-flow runs) on the species controlling the early time doses, and the influence of flow rate on decay of the species controlling the later time doses.

Figure RAI-FF-3.11: Far Field Flow Variability Study Peak Doses

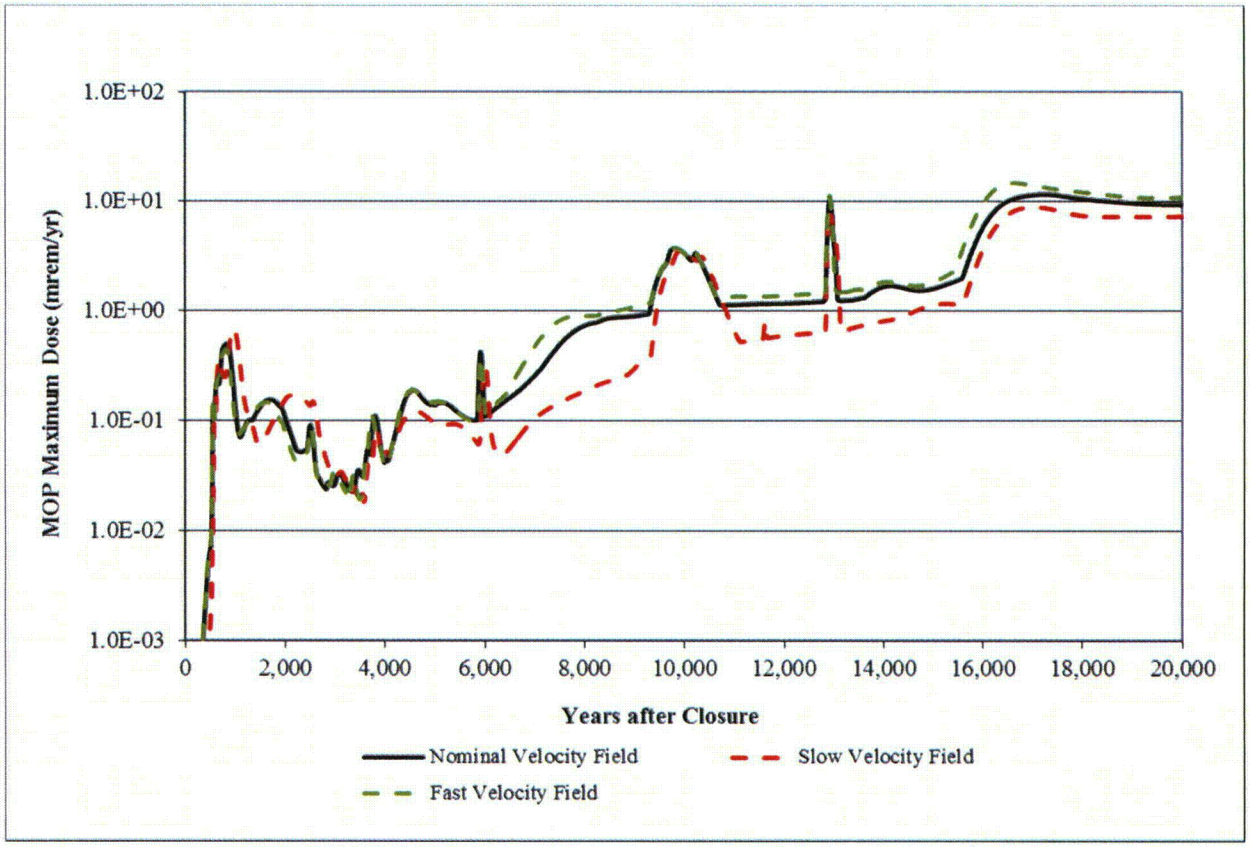

Table RAI-FF-3.2 shows the peak doses over 10,000 years and over 20,000 years from all three runs as a function of the Darcy velocity. Over a 10,000-year period, as flow rates increase from slow to nominal to fast, the peak values show a slight increase, reflecting a peak controlled by both Ra-226 and Tc-99. Over 20,000 years, increased flow rates result in a greater increase peak values reflecting the dominance of Ra-226 in dose contributions. Considering the three sets of Darcy velocities described above, the peak dose contribution does not reach 4 mrem/yr until after 10,000 years and does not exceed 15 mrem/yr within 20,000 years after HTF final facility closure.

Table RAI-FF-3.2: Summary of Far Field Flow Variability Study Results

Darcy Velocity Field	Peak Dose Over 10,000 Years (mrem/yr)	Time of Peak Dose Over 10,000 Years (yrs)	Peak Dose Over 20,000 Years (mrem/yr)	Time of Peak Dose Over 20,000 Years (yrs)
Slow	3.6	9,930	9.0	17,010
Nominal	3.8	9,810	11.7	17,230
Fast	3.8	9,800	14.8	16,630

These runs provide insight into the relationship between Darcy velocity and corresponding peak doses. The DOE recognizes that only modifying the Darcy velocity within the HTF GoldSim Model is a simplified representation of the far field flow changes represented in the Nominal, Fast, and Slow aquifer flow fields shown in Figures RAI-FF-3.8 through RAI-FF-3.10. The flow variability study performed is most informative in cases where the flow path lines did not change significantly.

DOE maintains that the nominal flow characterization currently embodied in the HTF models represents a reasonable estimate of hydrogeological behavior within the post-closure environment. As discussed in the responses to RAI-FF-1 and RAI-FF-2, the GSA model reasonably fits the underlying data and is adequate for the purposes of fate and transport modeling in the HTF PA, considering the risk significance of hydraulic conductivity and flow field variability discussed in this response.

As required by DOE Manual 435.1-1, maintenance of the HTF PA will include future updates to incorporate new information, update model codes, consider actual residual inventories, etc., as appropriate. The potential impact of new information will be evaluated using established site practices and procedures including preparation of an SA, as appropriate, consistent with DOE Manual 435.1-1 and DOE Guide 435.1-1. As waste tank-specific SAs are prepared it is anticipated that sensitivity analyses will be performed that explicitly address both individual waste tank inventories and unique waste tank conditions, such flow variability potential (e.g., waste tank-specific water level or potential for increased recharge). Because different as-modeled waste tank conditions may prove to be conservative or non-conservative (with respect to timing and/or magnitude of peak doses) depending on other corresponding waste tank conditions, these analyses are more suited to waste tank-specific sensitivity analyses than to changes to the overarching Base Case assumptions. For example, modeling assumptions that slow the far field flow may cause waste tank releases to reach the Gordon Aquifer sooner, which may increase dilution. The impact of a change in far field flow will vary depending on the quantity (total curies) and nature (short-lived versus long-lived radionuclides) of the released inventory.

RAI-FF-4

Time variant recharge rates and flow are not considered in the HTF/PORFLOW® model but may be risk-significant. DOE should evaluate the impact of time-variant recharge rates and flow on HTF Performance Assessment predictions.

Basis

HTF flow fields may be variable over time due to climatic variability or engineered barrier degradation; however, DOE uses a long-term, steady state (saturated zone) model to predict contaminant fate and transport at the HTF. Changes in flow rates and directions at HTF over time may have a significant impact on dose predictions.

While the GSA/PORFLOW® model uses a recharge rate of 19 in/yr over most areas of the model domain (WSRC-TR-2004-00106, Rev. 0), the long-term infiltration rate is assumed to be approximately 12 in/yr after degradation of the engineered closure cap. Additionally, the engineered closure cap at HTF is assumed to be effective at reducing recharge to relatively low rates for hundreds to thousands of years following HTF closure. Yet, the impact of the closure cap on recharge rates following facility closure is not considered in the far-field model.

While the closure cap is generally expected to reduce infiltration, the area between the west and east closure caps may represent an area of increased infiltration due to runoff from the caps. The impact of increased runoff from the caps was evaluated in Portage (PORTAGE-08-022, Rev. 0), but infiltration was limited in the drainage area between the west and east caps and a more detailed evaluation of the effect of the cap on HTF performance would be beneficial.

While the FTF Performance Assessment (SRS-REG-2007-00002, Rev. 1) did not consider time-variant recharge rates, in most cases releases from the tanks were not assumed to occur until after the closure cap and cementitious materials were degraded and recharge rates were near long-term, steady-state values. However, time-variant recharge rates may be more risk-significant for HTF sources due to the fact that some tank liners are assumed to be initially failed and releases could occur much earlier in time prior to closure cap and cementitious material degradation (for submerged and partially submerged tank sources).

Path Forward

DOE could perform the following activities to evaluate the impact of time-variant recharge and flow at HTF. Note that some of the activities have been partially evaluated in PORTAGE-08-022, Rev. 0. This report can be used as a starting point in addressing this request for additional information but additional detail would be helpful.

- Compare modeled or hand-contoured potentiometric surfaces at various points in time to evaluate the potential for climatic variability to effect flow rates and directions at HTF. Note that observed flow field variability may be influenced by operations as discussed in RAI-FF- 2 and would not be necessarily indicative of long-term natural variability relevant to the HTF Performance Assessment.
- If found or thought to be significant, evaluate the potential impact of climatic variability on the HTF flow field. This would include evaluation of the impact of variability on dilution, dispersion, and cumulative impacts due to changes in flow rates and directions.
- Evaluate the impact of lower recharge rates due to the presence of an engineered closure cap on HTF water levels and the HTF flow field.

- Evaluate the impact of increased recharge in drainage areas, particularly the area between the west and east engineered closure caps, on HTF water levels and the HTF flow field.
- Evaluate the impact of engineered barrier degradation (e.g., closure cap and tank cement/grout) on HTF releases and the HTF flow field over time.

Response RAI-FF-4

HTF Potentiometric Mapping

In the majority of the Atlantic Coastal Plain, groundwater flow in the water table is driven by surface recharge and tends to be a muted expression of topography. The elevation of the water table varies with recharge, but the relative shape of the surface is generally stable. In the GSA, the major discharge points for the water table remain relatively constant in elevation and location. Thus, in response to moderate changes in climate and topography, the shape of the water table, location of the groundwater divide, and the associated flow vectors are expected to remain similar to present conditions.

It is noteworthy that a groundwater contour map can vary slightly based on incomplete and uncertain input data used to create the surface. However, in the GSA, there is sufficient historical groundwater information to support the shape of the water table surface used to create the potentiometric surfaces and flow fields used in the PORFLOW modeling.

As stated above, groundwater elevations can vary vertically over time based on recharge. An evaluation of HTF monitoring well water levels in the water table (UTRA-UZ) over time versus HTF annual moving-average rainfall shows a strong correlation. In addition, these effects on the water table due to recharge are similar at all of the monitoring wells in HTF, indicating that as the water table rises and falls, the shape of the surface remains relatively unchanged. This strong correlation between rainfall and recharge would indicate that existing localized engineered barriers have very little effect on the overall water table shape and flow fields.

Contour maps of water tables and potentiometric surfaces can vary also, based on the contouring method used to create them. Most computerized contouring programs have difficulty interpreting the effects of topography, especially within the vicinity of discharge points (HTF PA Figure 4.2-21). In addition, determining contour shapes in areas of minimal data can result in a higher degree of uncertainty. However, the basic shape, orientation, and elevation of contoured surfaces in areas with abundant historical water level data, such as the GSA, can be determined with a higher degree of confidence.

A comparison of historic water table data over time is presented in Figure RAI-FF-4.1. Contour surfaces for three years (1995, 1998, and 2003) are overlain for comparison. For reference, the location of HTF and the associated groundwater divide have been denoted. For the HTF, groundwater discharge from the water table aquifer is to Crouch Branch and McQueen Branch, and ultimately to UTR, to the north and to Fourmile Branch to the south. As indicated by the contouring, slight variations exist between localized individual contours, but the overall shape (including groundwater divides), direction of flow, and discharge points remain constant. These contours are consistent with each other, indicating that there has not been a significant change in our understanding of long-term average water table conditions in the GSA since the mid-1990s. In 1995, 617 monitoring wells were used in contour mapping. In 1998, the number of wells increased to 946. Finally in 2003, the number of wells for contouring increased to 1,324. As indicated by this figure, varying the number of wells used to create the maps does not result in significant variation in shape of the overall contour map and the location, orientation and

relative intensity of the groundwater divide within the vicinity of the HTF. Therefore, it is highly unlikely that modest changes in recharge to the water table, such as those experienced over the past two decades, or additional data will result in a significant shift in the groundwater divide that would alter discharge to surface water.

Figure RAI-FF-4.1: Water Table Contour Maps for GSA

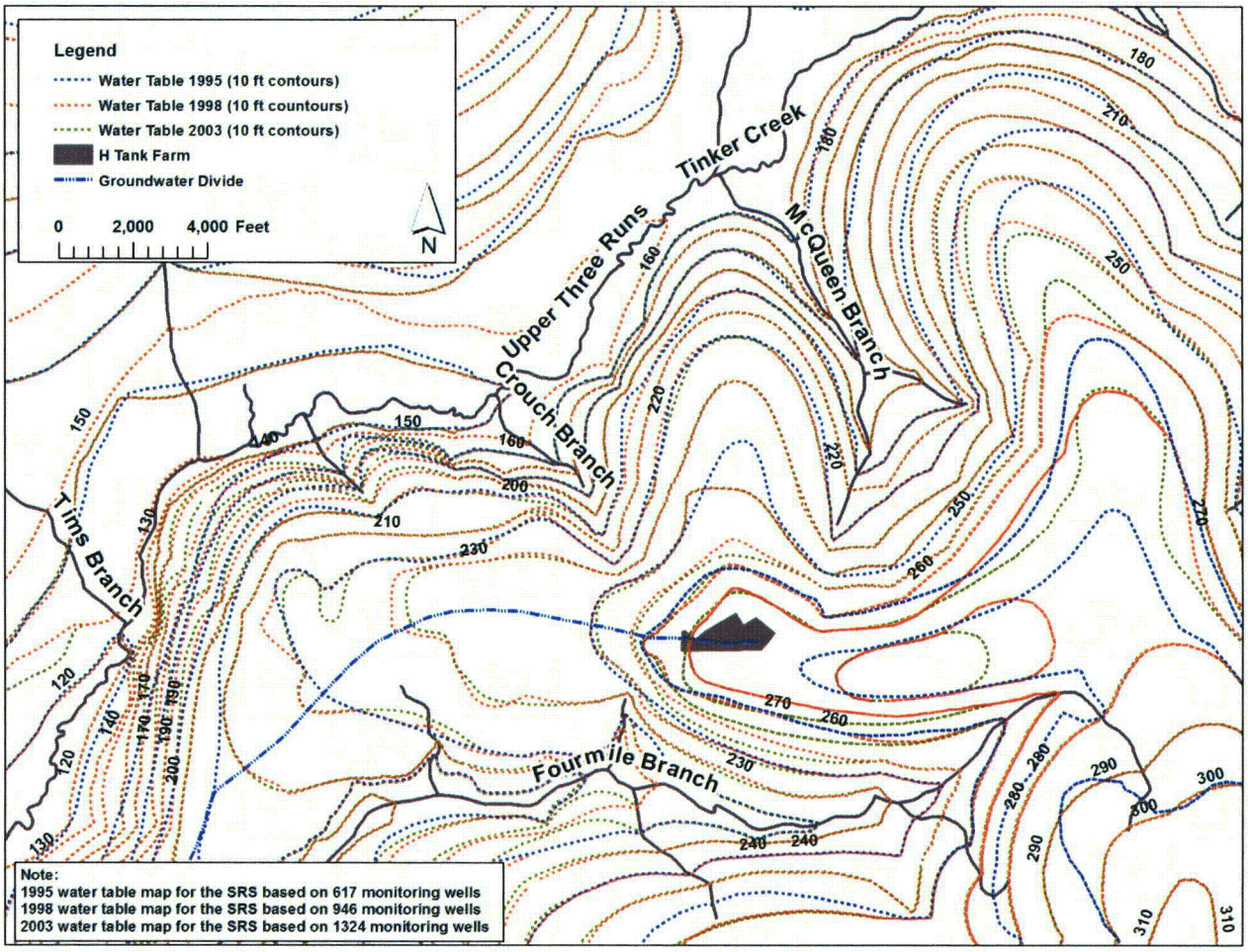

Shapes and elevations of potentiometric surfaces of the UTRA-LZ in HTF are similar to the water table (see *Hydrogeologic Data Summary in Support of the H-Area Tank Farm Performance Assessment*, SRNL-STI-2010-00148, Figures 23 and 24). This is because the TCCZ, separating the UTRA-UZ from the UTRA-LZ, is considered a semi-confining zone and is not generally considered major impedance to the vertical movement of groundwater. The PORFLOW modeling, and associated flow fields, reflects this strong correlation between the two aquifer zones.

Finally, the Gordon Aquifer is separated from the UTR Aquifer by the Gordon Confining Unit. Within the vicinity of HTF, the Gordon Aquifer only discharges to UTR. The Gordon Confining Unit acts as a significant barrier to vertical movement of groundwater in the GSA and, as such, the aquifer reflects little variation in potentiometric surface shape and discharge over time due to minimal vertical recharge (see *Hydrogeologic Data Summary in Support of the H-Area Tank Farm Performance Assessment*, SRNL-STI-2010-00148, Figure 25).

To assess the potential impact of a low-permeability cover system over the HTF after final facility closure, a sensitivity study on aquifer flow was performed. Figure RAI-FF-4.2 shows groundwater pathlines emanating from HTF waste tanks for nominal conditions. Figure RAI-FF-4.3 shows the corresponding pathlines when the surface recharge is reduced by 100× over the area coinciding with the 1-meter facility boundary used for dose calculations. The general impact of the cap is to push groundwater deeper and toward the north.

Figure RAI-FF-4.2: Groundwater Pathlines for Nominal Conditions

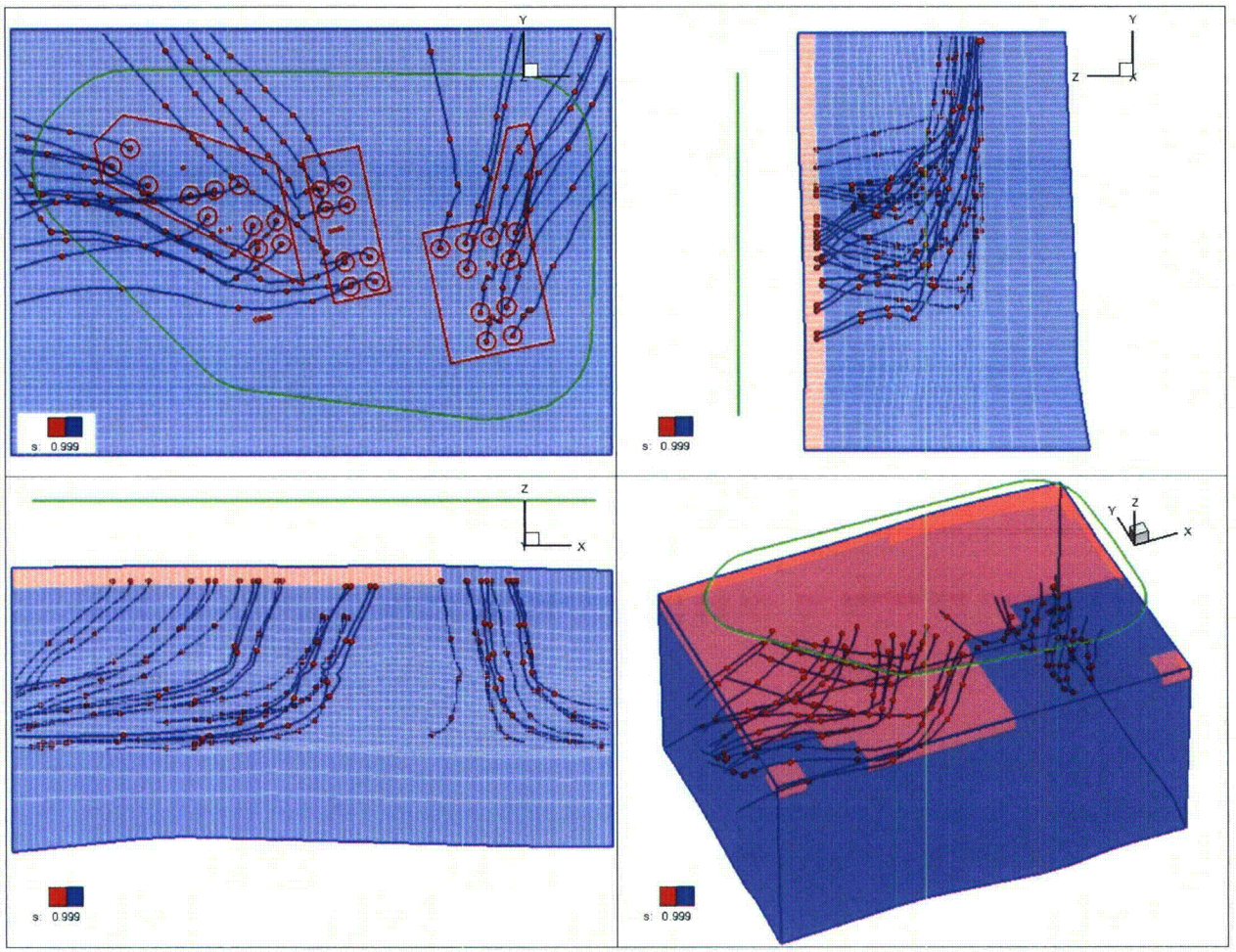

Figure RAI-FF-4.3: Groundwater Pathlines for Reduced Recharge Conditions

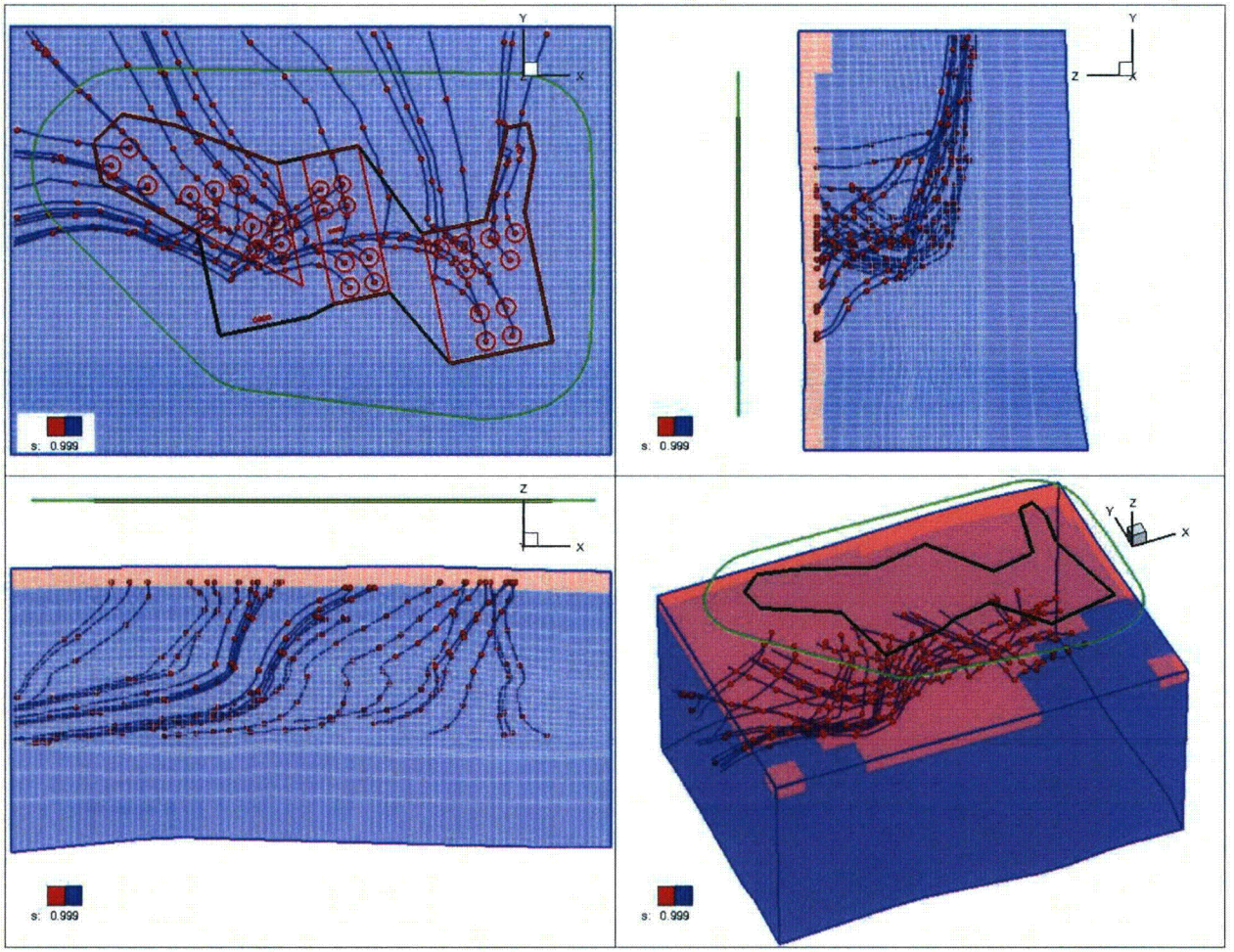

Impact of Far Field Flow Variability

As discussed in detail in the response to RAI-FF-3, the risk significance of hydraulic conductivity adjustments and other settings in the GSA/PORFLOW far field flow model can be assessed by considering the sensitivity of solute transport simulations to potential variations in the aquifer velocity field, which affects plume travel time and distance. Figure RAI-FF-3.11 depicts peak dose curves for three HTF sensitivity runs with the different runs reflecting far field flow variability (each run used a different set of pathline specific Darcy velocities). The three modeling runs represent a nominal flow set, a fast flow set, and a slow flow set. By comparing the dose curves associated with the three different sets (presented in Figure RAI-FF-3.11), it can be seen that there is relatively little difference between the dose results.

CC-FF-1

Page 59 of SRR-CWDA-2010-00093, Rev. 2 indicates that some HTF plumes are spread over both aquifers and that higher vertical dispersivities are generally needed for the eastern plumes. Clarify what tank sources are spread over both aquifers and the differences between vertical dispersion for western versus eastern sources in GoldSim® probabilistic modeling.

Response CC-FF-1

To help clarify which waste tank sources are spread over both the UTRA-UZ and UTRA-LZ, a complete series of plume plots from PORFLOW waste tank-specific simulations was generated (see Figures CC-FF-1.1 through CC-FF-1.10). The plumes were generated from initial emplacements of a conservative constituent (i.e., constituent that is not sorbed, is not solubility controlled, and does not decay) and present concentrations for the time period when the center-line concentrations would peak at a point 100 meters from the HTF boundary. Both areal and vertical plots are presented. The concentrations in the plots are in moles per liter (mol/L) and represent maximum values perpendicular to the plane being viewed. The Y-Z and X-Z plots in the upper right hand and lower left hand corners, respectively, of the figures can be used to evaluate the vertical extent of the plume at the 100-meter point. In the vertical profiles, the top eight cells represent the UTRA-UZ, the next two cells represent the TCCZ of the UTR Aquifer, the next 10 cells represent the UTRA-LZ, the following two cells represent the Gordon confining zone, and the bottom three cells represent the Gordon Aquifer.

These new plume figures (Figures CC-FF-1.1 through CC-FF-1.10) show that most of the contaminant resides in the UTRA-LZ at the 100-meter point. Low concentrations (< 3E-10 mol/L) of contaminant occur in the UTRA-UZ in plumes emanating from Tanks 39, 40, 49, and 51 as shown in Figures CC-FF-1.2, CC-FF-1.3, CC-FF-1.8, and CC-FF-1.10, respectively. Higher concentrations (> 3E-10 mol/L) of contaminant occur in the UTRA-UZ in plumes emanating from Tanks 41 and 43 as shown in Figures CC-FF-1.4 and CC-FF-1.6, respectively.

Peak dose results from benchmarking (shown in Section 5.6.2.2. of the HTF PA) validate the modification of vertical dispersivity to improve the match between the PORFLOW and GoldSim models. The eastern waste tank releases followed relatively straight pathlines, and the waste tank release plumes did not show the same high degree of transverse spreading as found in the western waste tank releases, therefore the horizontal transverse dispersivity was not adjusted during the benchmarking process.

Figure CC-FF-1.1: Concentration Plume (mol/L) Formed by the Release of a Conservative Constituent from Tank 38

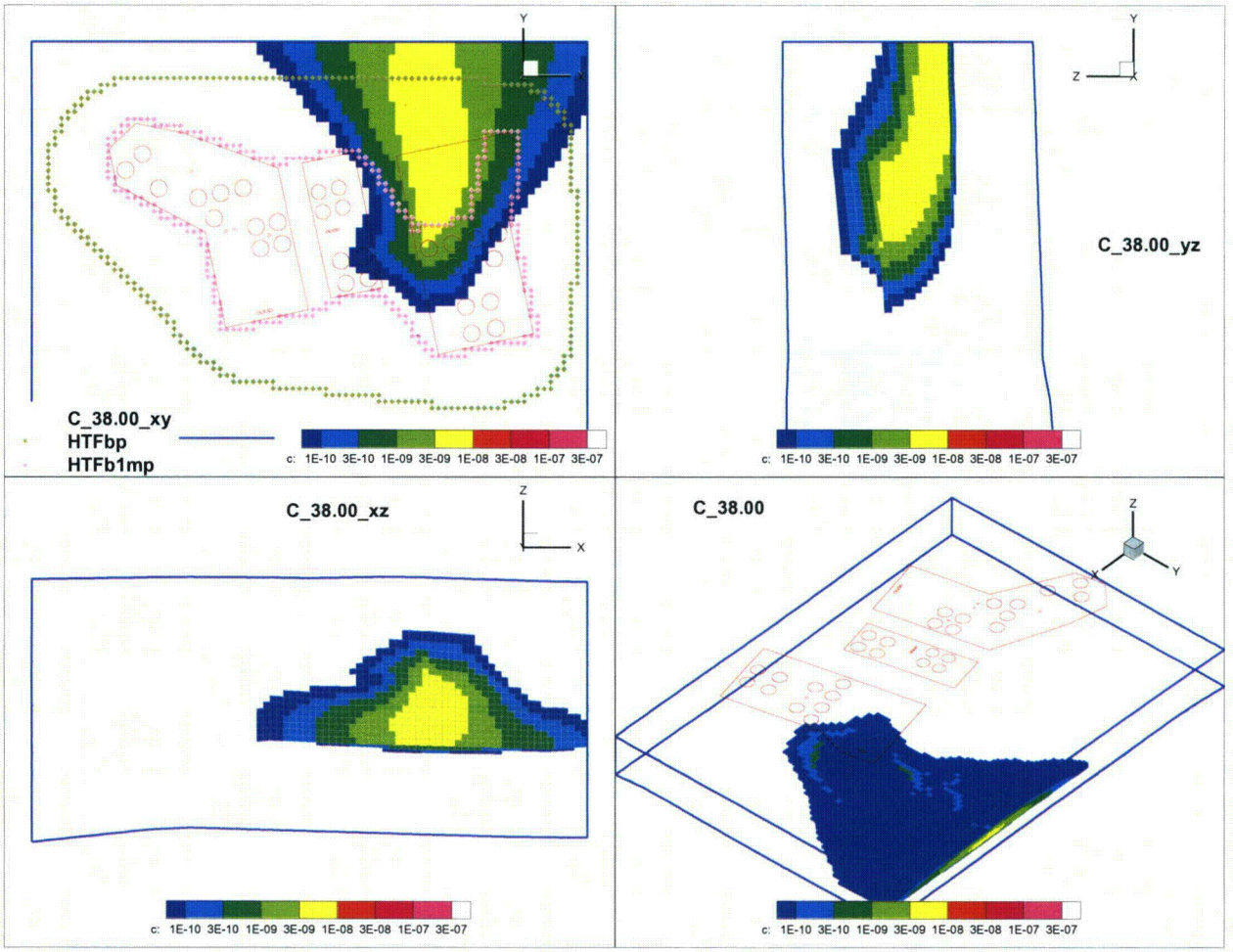

Figure CC-FF-1.2: Concentration Plume (mol/L) Formed by the Release of a Conservative Constituent from Tank 39

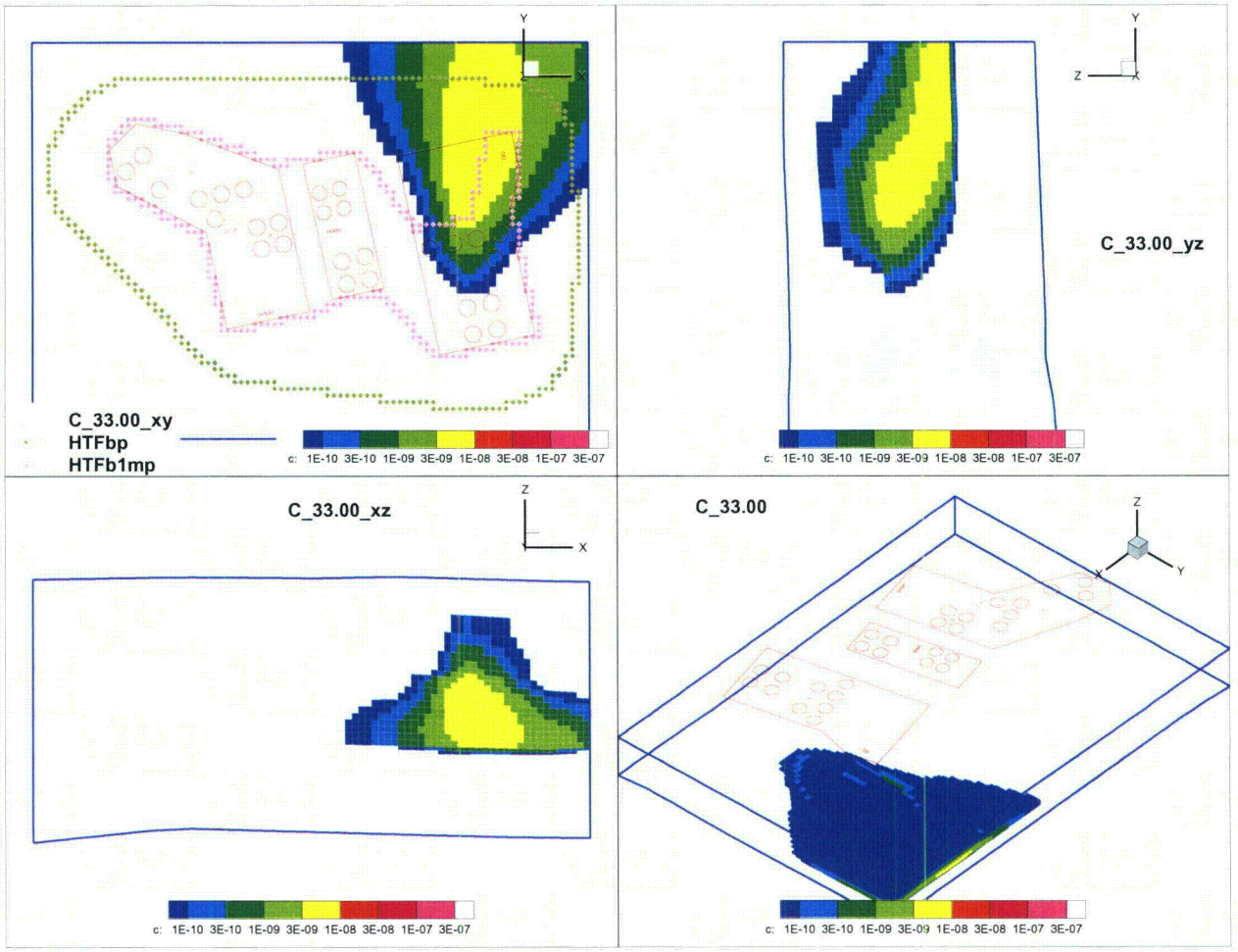

Figure CC-FF-1.3: Concentration Plume (mol/L) Formed by the Release of a Conservative Constituent from Tank 40

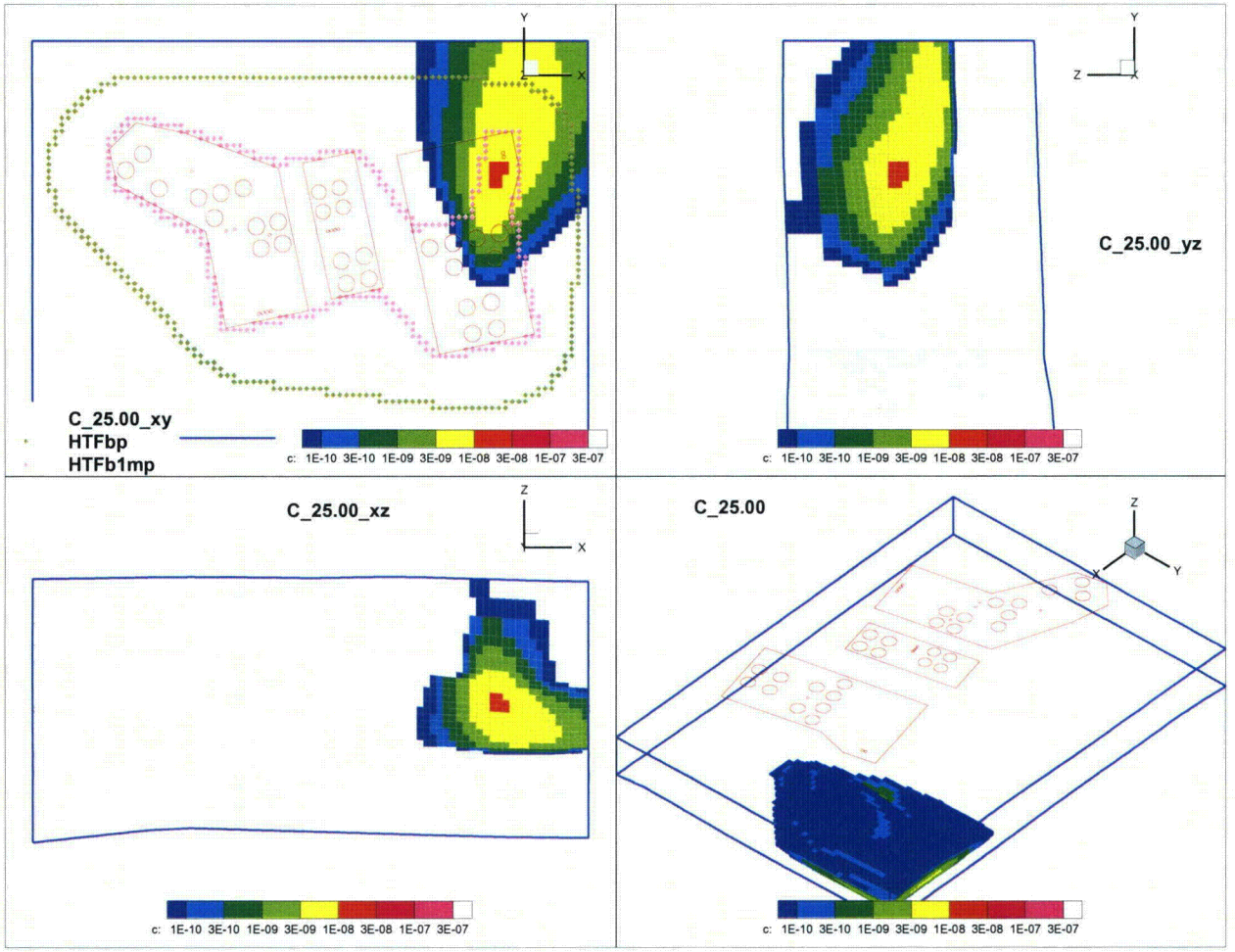

Figure CC-FF-1.4: Concentration Plume (mol/L) Formed by the Release of a Conservative Constituent from Tank 41

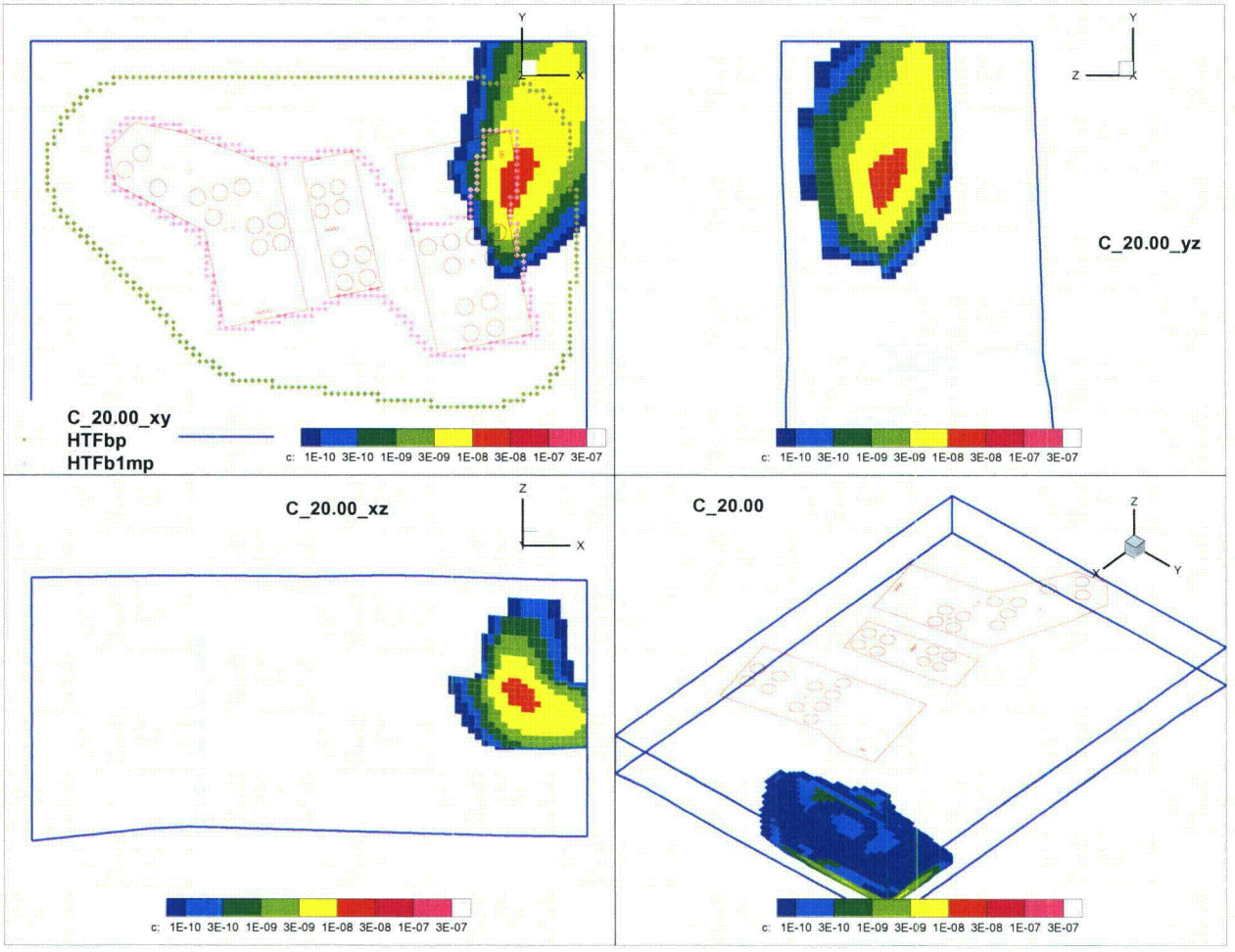

Figure CC-FF-1.5: Concentration Plume (mol/L) Formed by the Release of a Conservative Constituent from Tank 42

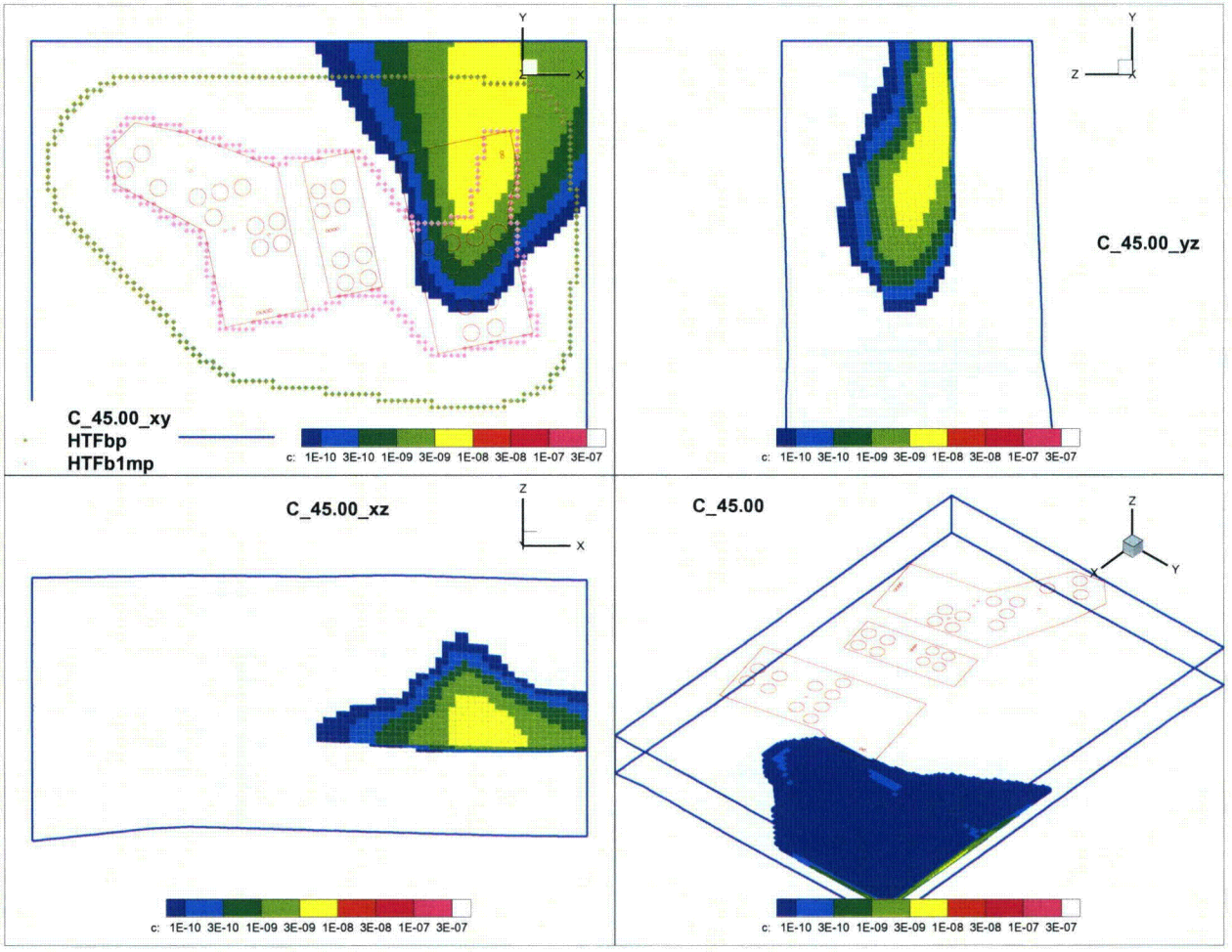

Figure CC-FF-1.6: Concentration Plume (mol/L) Formed by the Release of a Conservative Constituent from Tank 43

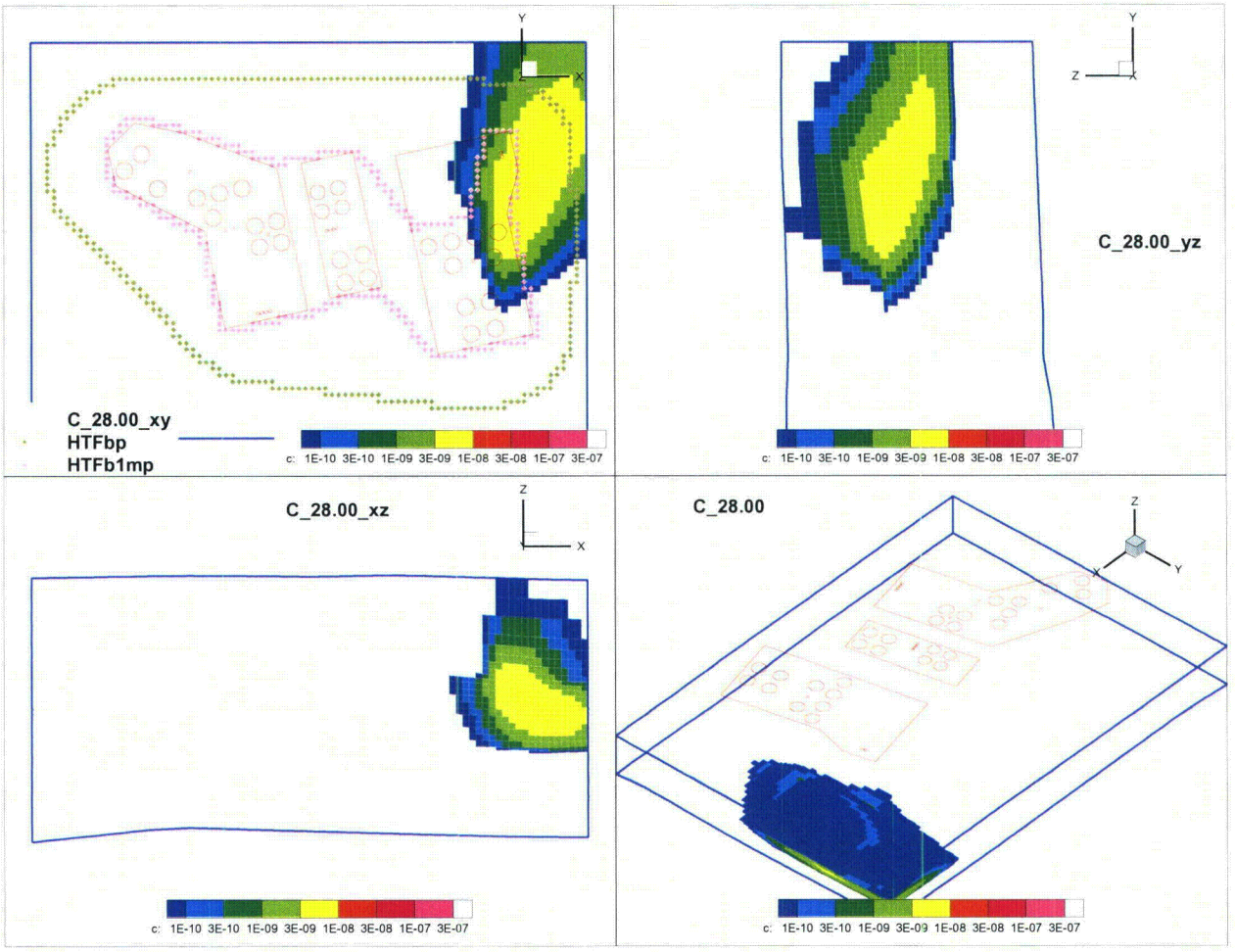

Figure CC-FF-1.7: Concentration Plume (mol/L) Formed by the Release of a Conservative Constituent from Tank 48

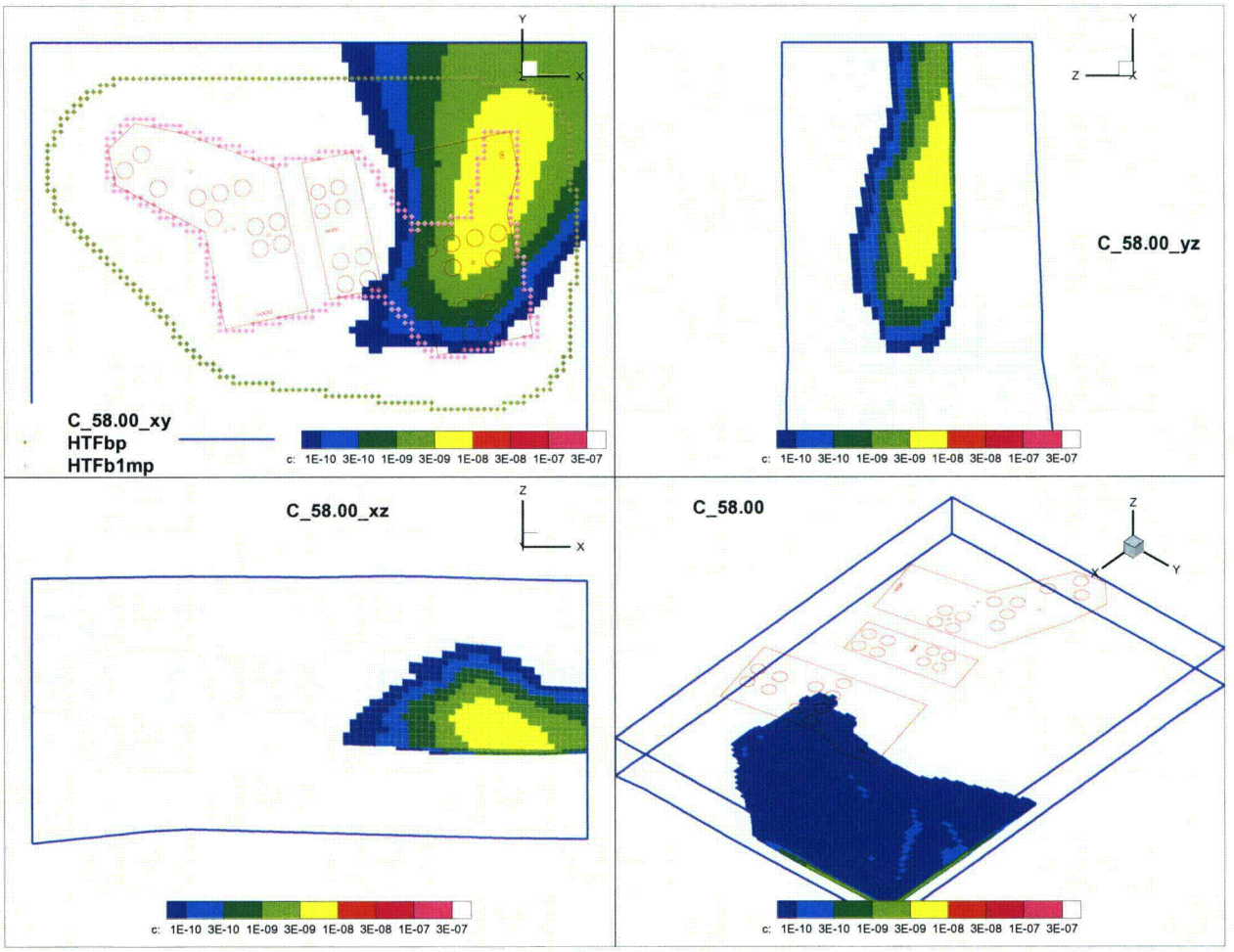

Figure CC-FF-1.8: Concentration Plume (mol/L) Formed by the Release of a Conservative Constituent from Tank 49

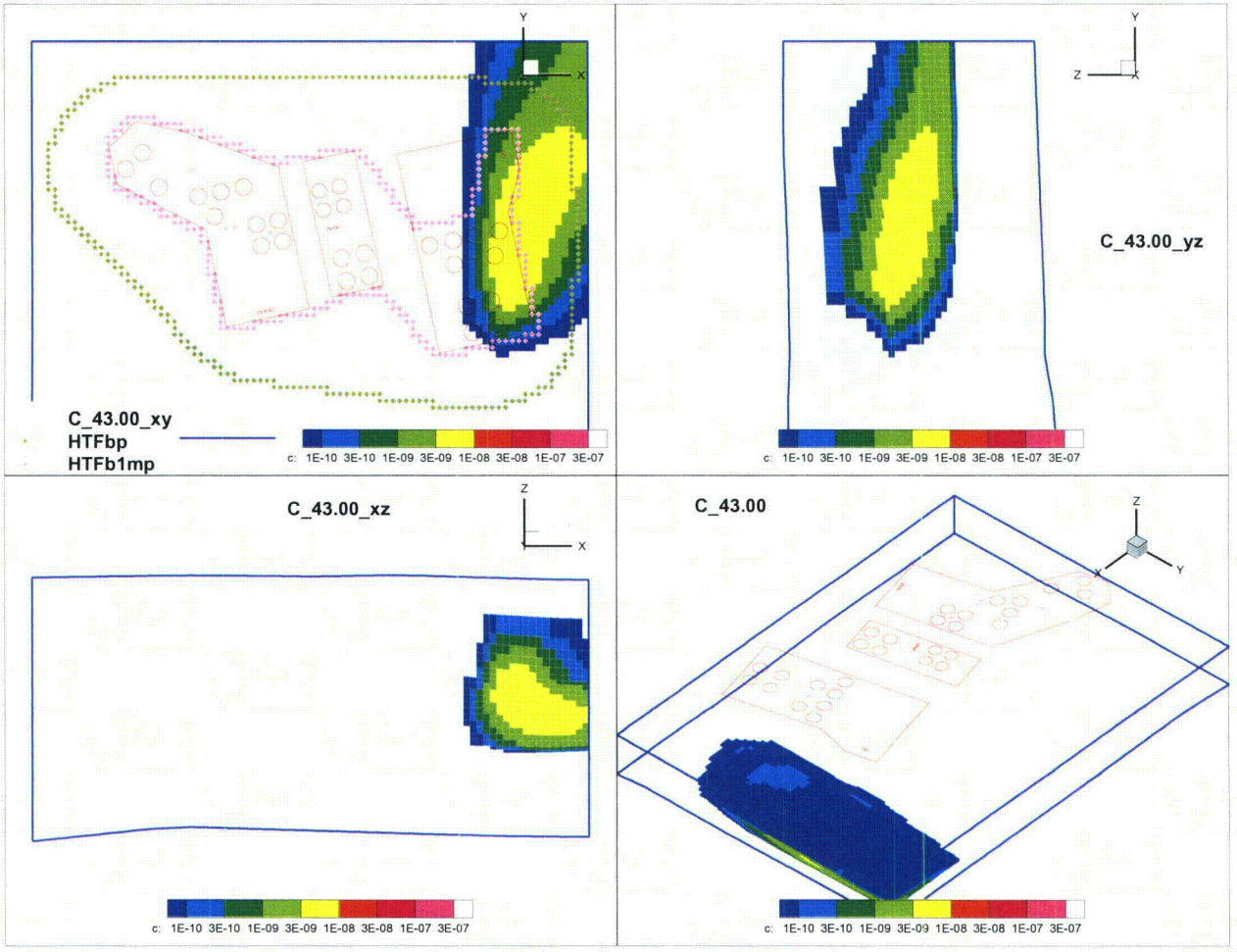

Figure CC-FF-1.9: Concentration Plume (mol/L) Formed by the Release of a Conservative Constituent from Tank 50

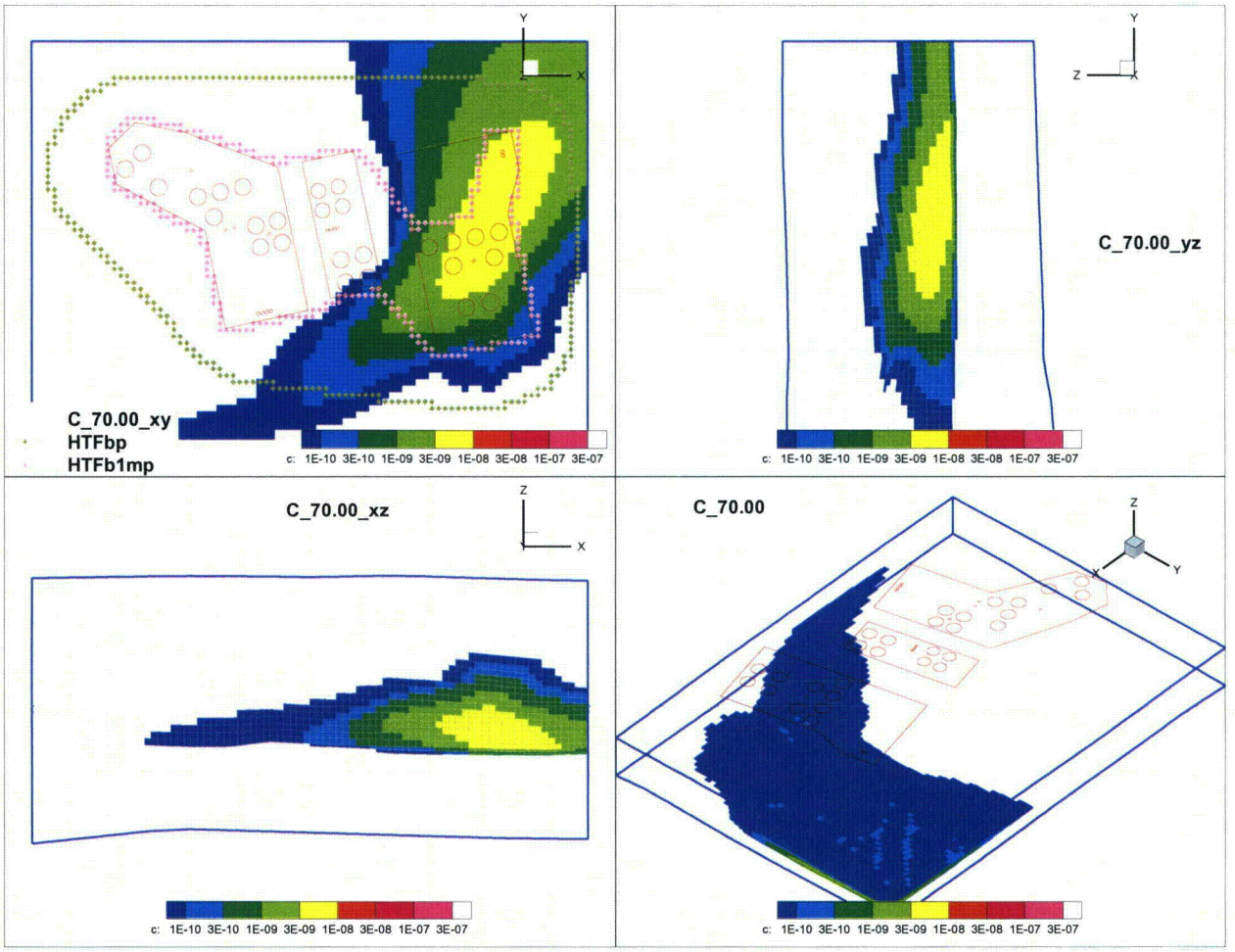

Figure CC-FF-1.10: Concentration Plume (mol/L) Formed by the Release of a Conservative Constituent from Tank 51

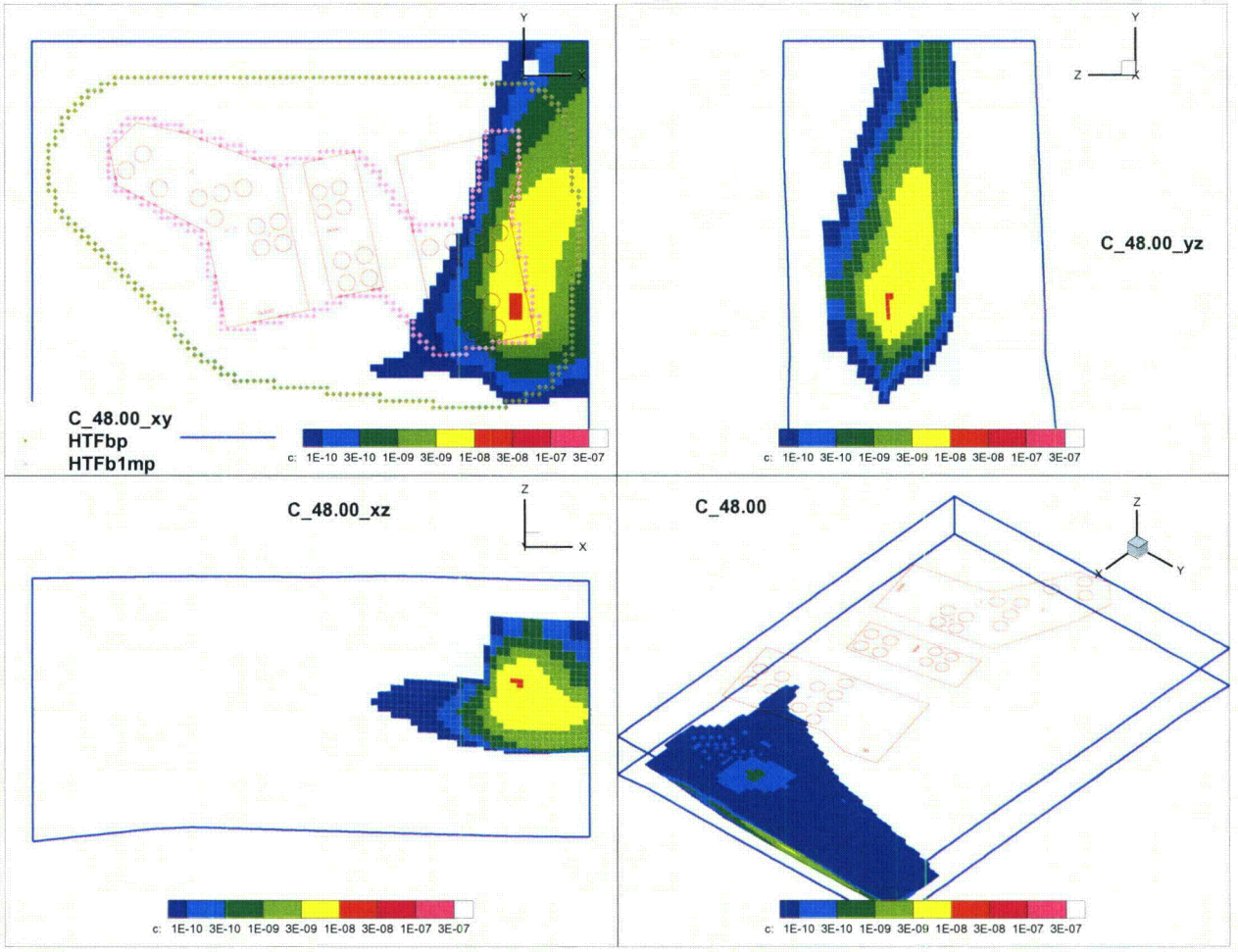

CC-FF-2

Page 60 of SRR-CWDA-2010-00093, Rev. 2 indicates that differences in flow directions were more significant for western sources, leading to the need for higher transverse dispersivities for western sources. Clarify the degree of transverse spreading for various sources at HTF and how changes in transverse dispersivity in GoldSim® probabilistic modeling are used to simulate the effect of changing flow directions.

Response CC-FF-2

When carrying out HTF modeling, it is difficult to match the degree of plume spreading and associated increase in dilution generated by the fully, 3-D PORFLOW model, with the quasi-3-D GoldSim abstraction of the PORFLOW model. On the western side of the HTF, a groundwater divide, spatially divergent flow, and changes in flow direction enhance the lateral spreading of the plumes generated by waste tank releases. The PORFLOW model solves the advective-dispersive transport equations in a fully, 3-D framework, and thus considers both lateral dispersion and the divergence of the flow field in its calculations. The GoldSim model is a quasi-3-D abstraction of the PORFLOW model that solves for 1-D advective-dispersive transport along a pathline, and approximates the influences of horizontal and vertical transverse dispersion with Green's function solutions. In this configuration all the effects of the flow field are not fully captured. Confined to evaluating advective-dispersive transport in a unidirectional flow field, the GoldSim model generates typical cigar shaped plumes for steady and instantaneous releases (Figure CC-FF-2.1 (a) and (b)).

Figure CC-FF-2.1: Plume Generation in Uniform Flow Fields for (a) Steady and (b) Instantaneous Sources

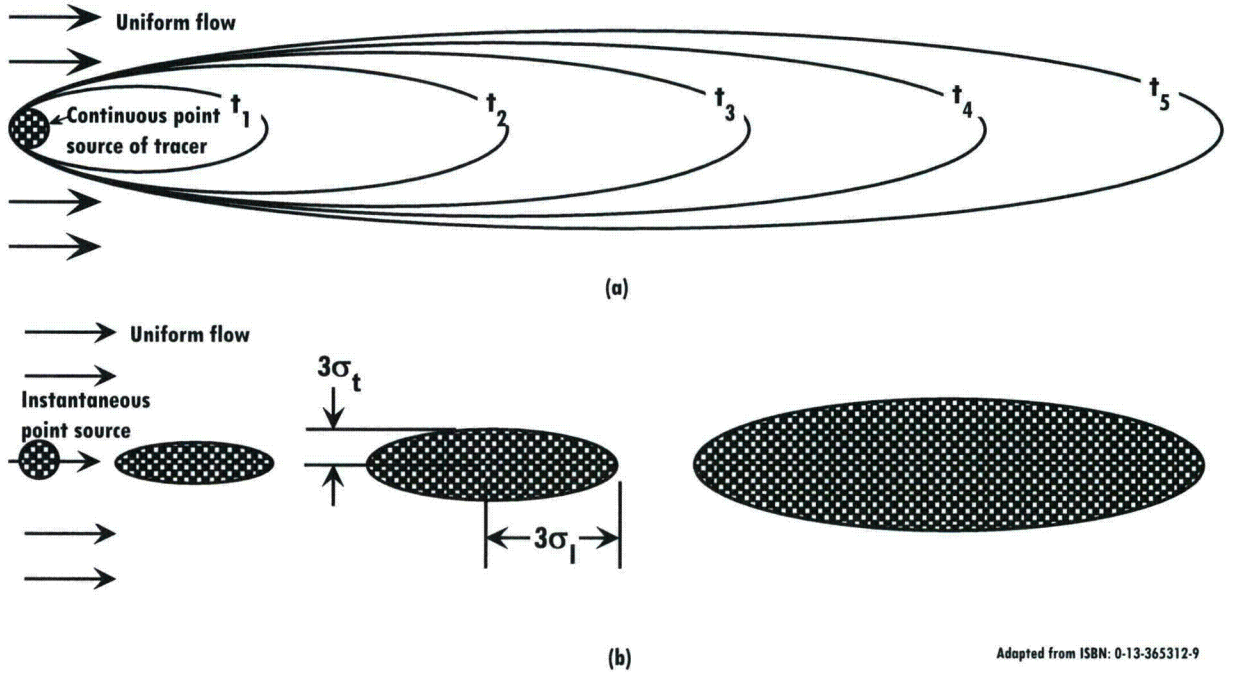

The waste tanks located on the western side of the HTF include the Type I tanks (9, 10, 11, and 12), the Type II tanks (13, 14, 15, and 16), the Type IV tanks (21, 22, 23, and 24), and some of the Type III and IIIA tanks (29, 30, 31, 32, 35, 36, and 37). Releases from these waste tanks tend to form plumes that are wider than would be expected for a system with a longitudinal to horizontal-transverse dispersivity ratio of 10:1 as used in the PORFLOW model. The influence of the spatially variant aspects of the flow field on plume spreading can be observed in waste tank-specific plume plots. These PORFLOW generated plots (see Figures CC-FF-2.2 through CC-FF-2.20) show plumes formed by a pulse release of a conservative constituent (i.e., constituent that is not sorbed, is not solubility controlled, and does not decay). The GoldSim pipe element, which assumes a steady unidirectional flow field, used in conjunction with the plume function will generate a cigar shaped plume as depicted in Figure CC-FF-2.1 (a) and (b) depending on whether the source is steady (a) or instantaneous (b). For each source release, the flow-fields increase spreading of the plumes (as modeled in PORFLOW), which decreases the radionuclide concentrations (and associated dose contributions) at a point 100 meters from the HTF boundary.

Figure CC-FF-2.2: Concentration Plume (mol/L) Formed by the Pulse Release of a Conservative Constituent from Tank 9

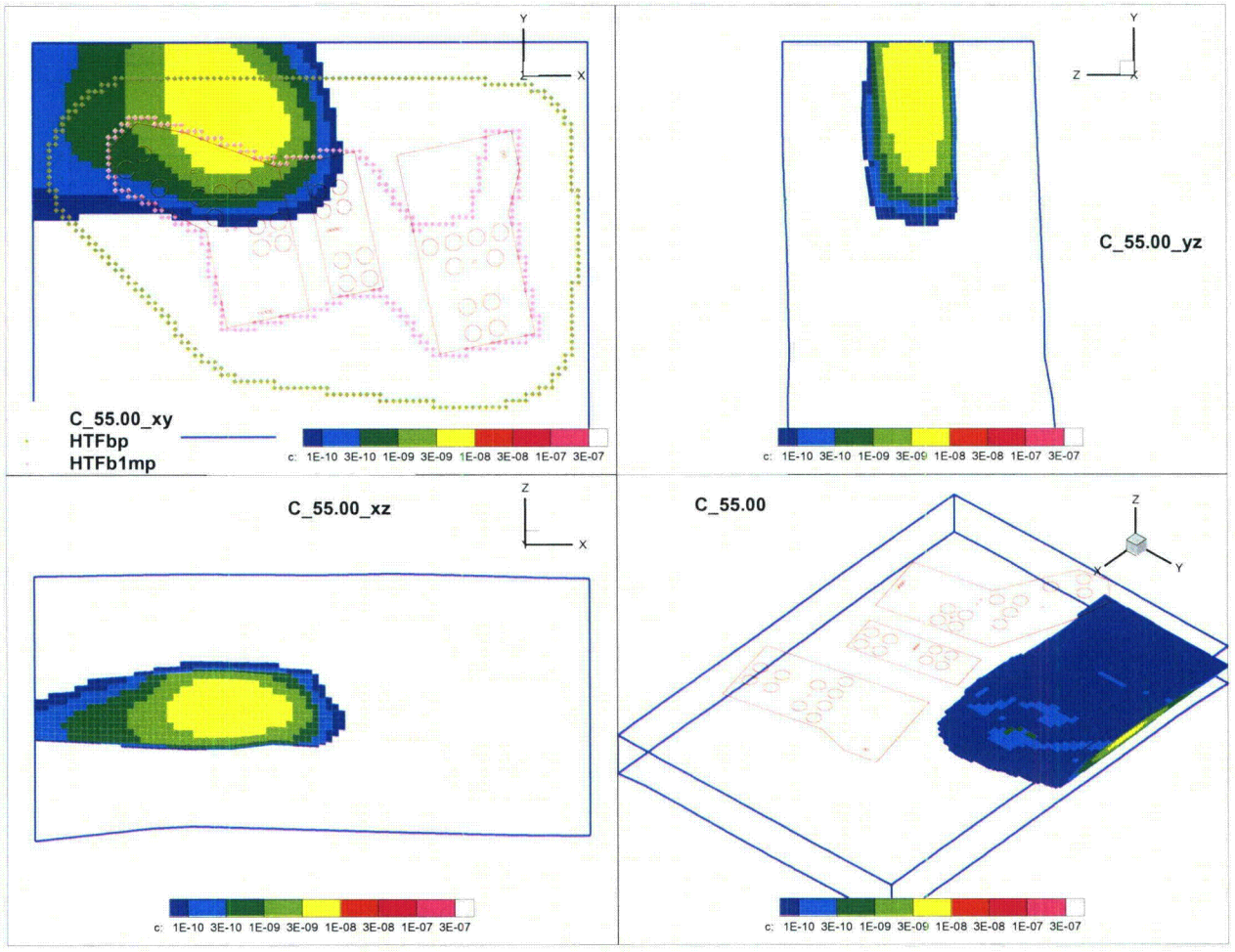

Figure CC-FF-2.3: Concentration Plume (mol/L) Formed by the Pulse Release of a Conservative Constituent from Tank 10

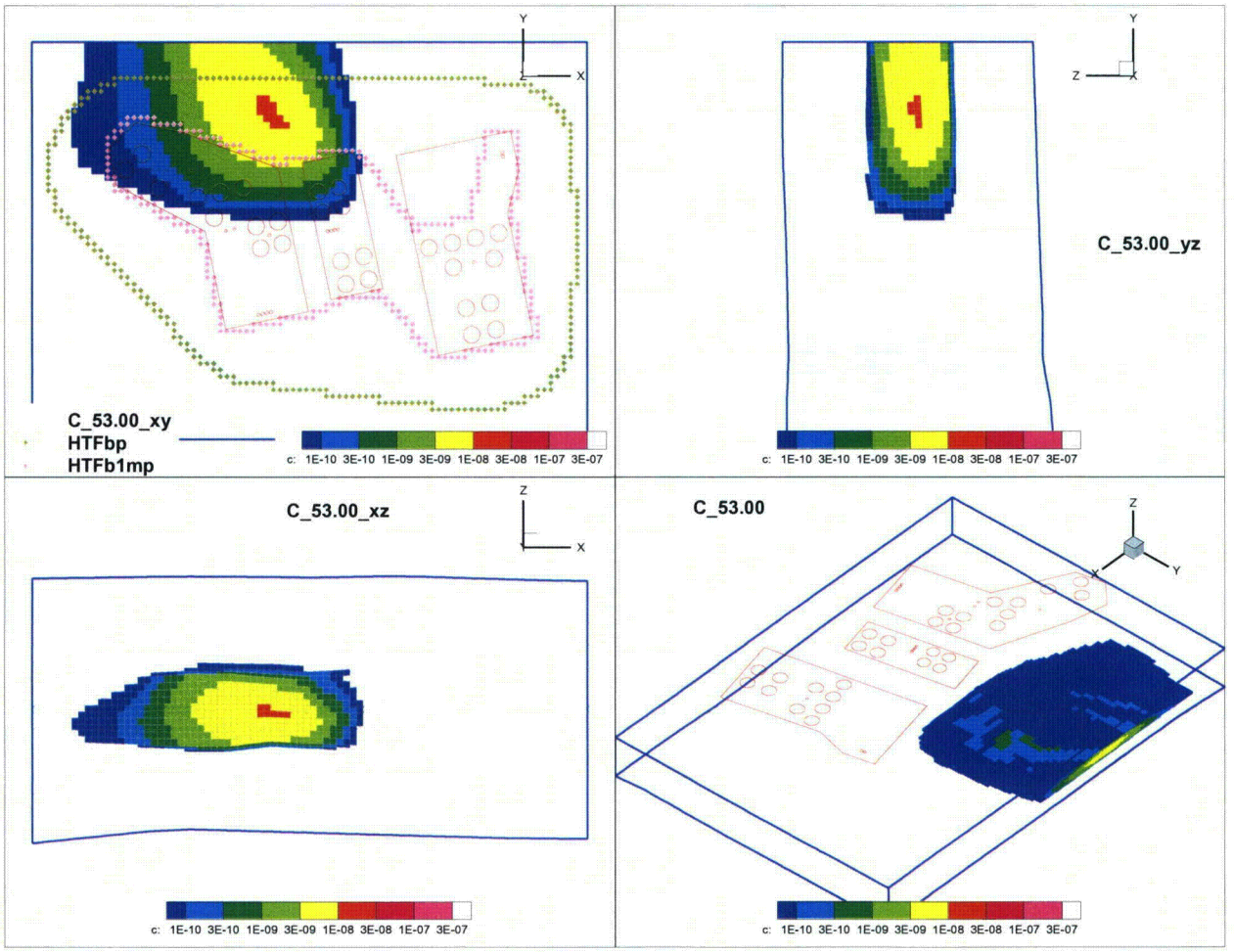

Figure CC-FF-2.4: Concentration Plume (mol/L) Formed by the Pulse Release of a Conservative Constituent from Tank 11

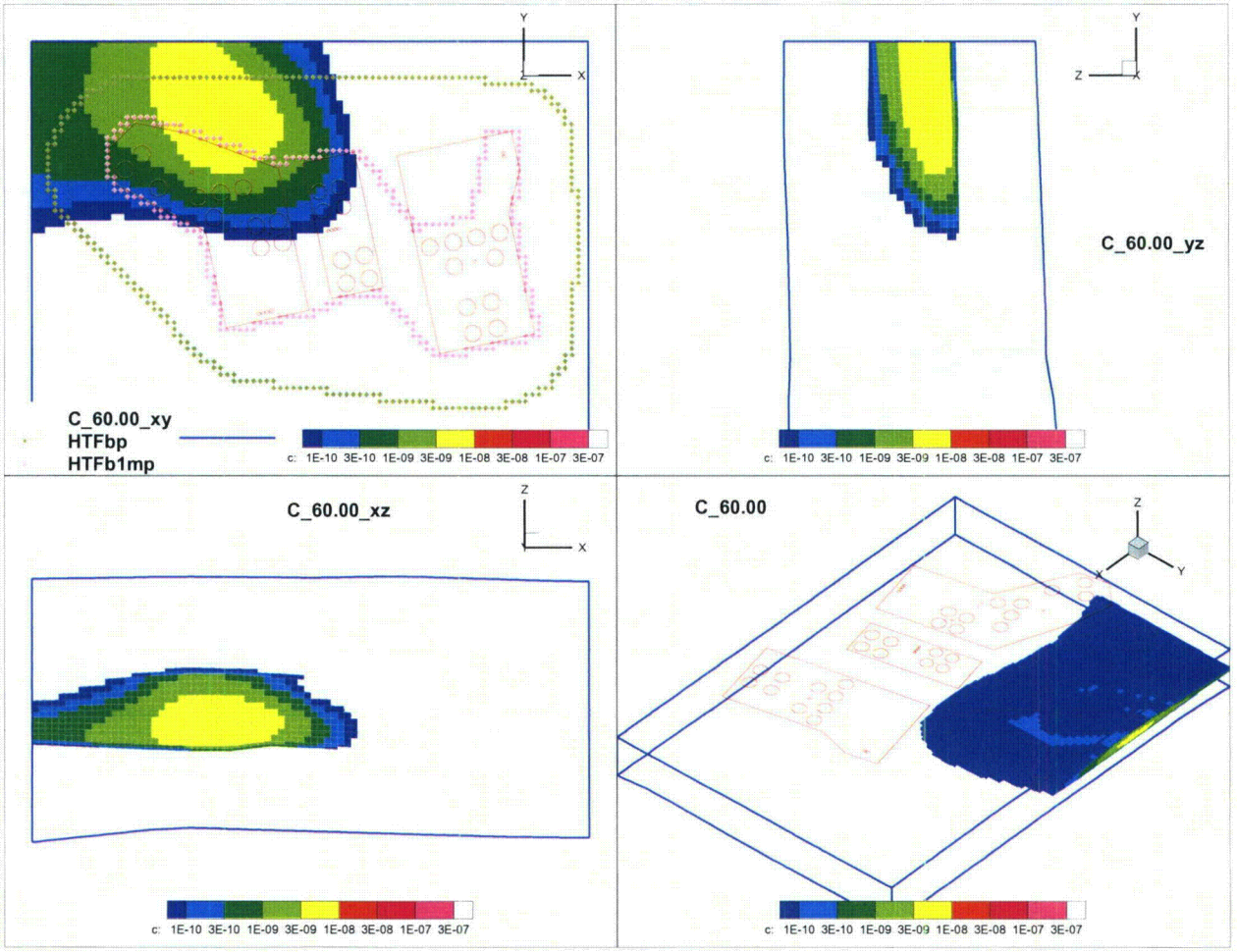

Figure CC-FF-2.5: Concentration Plume (mol/L) Formed by the Pulse Release of a Conservative Constituent from Tank 12

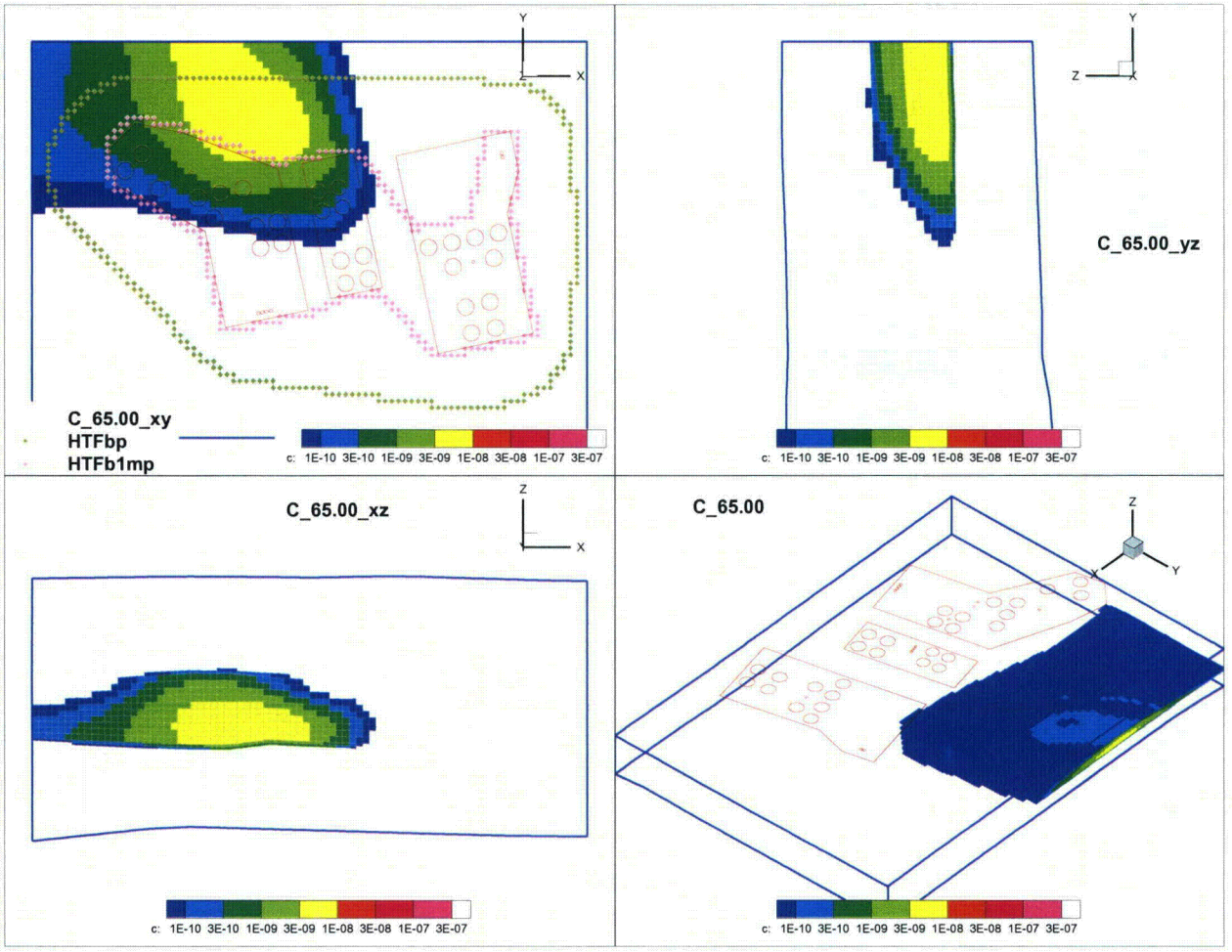

Figure CC-FF-2.6: Concentration Plume (mol/L) Formed by the Pulse Release of a Conservative Constituent from Tank 13

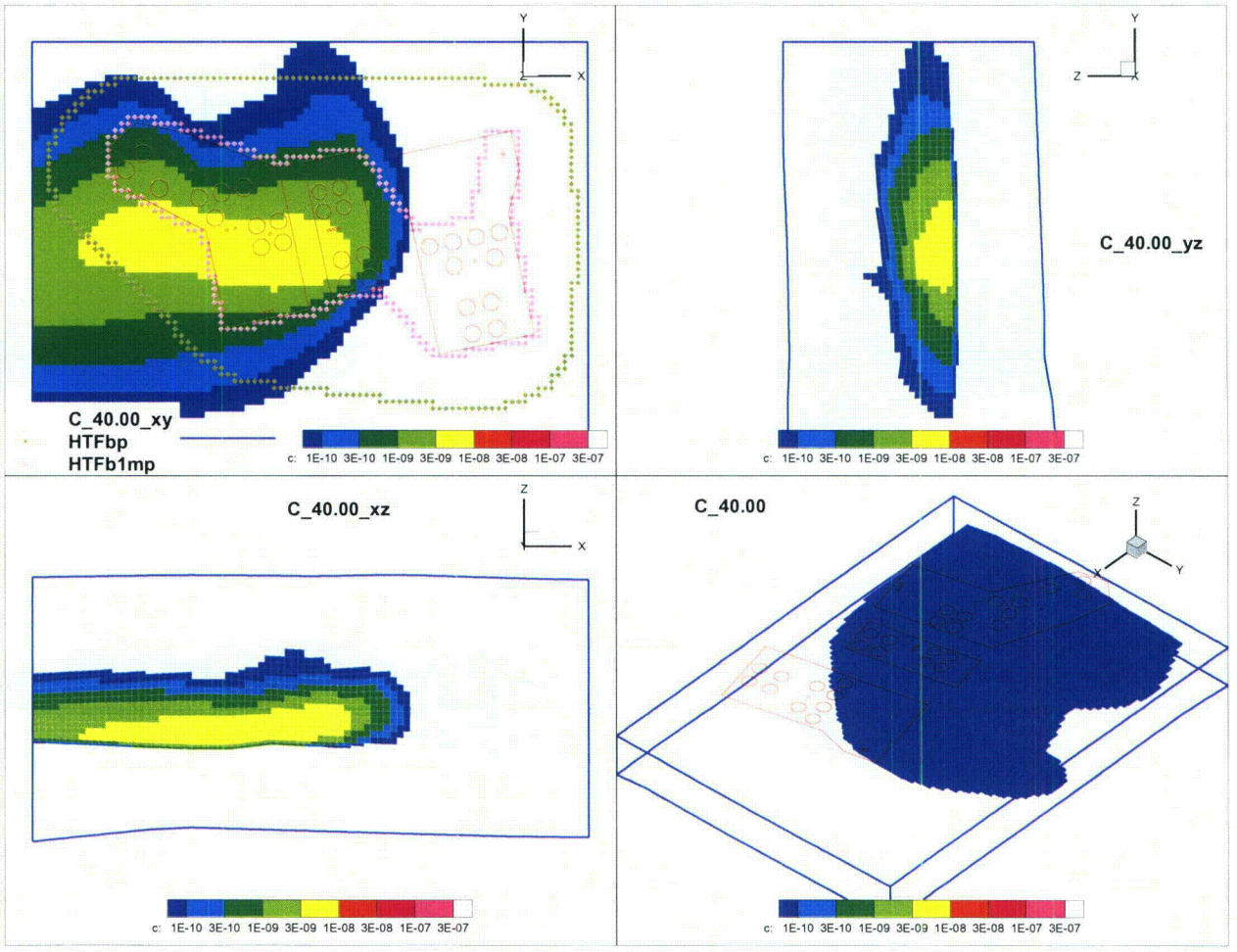

Figure CC-FF-2.7: Concentration Plume (mol/L) Formed by the Pulse Release of a Conservative Constituent from Tank 14

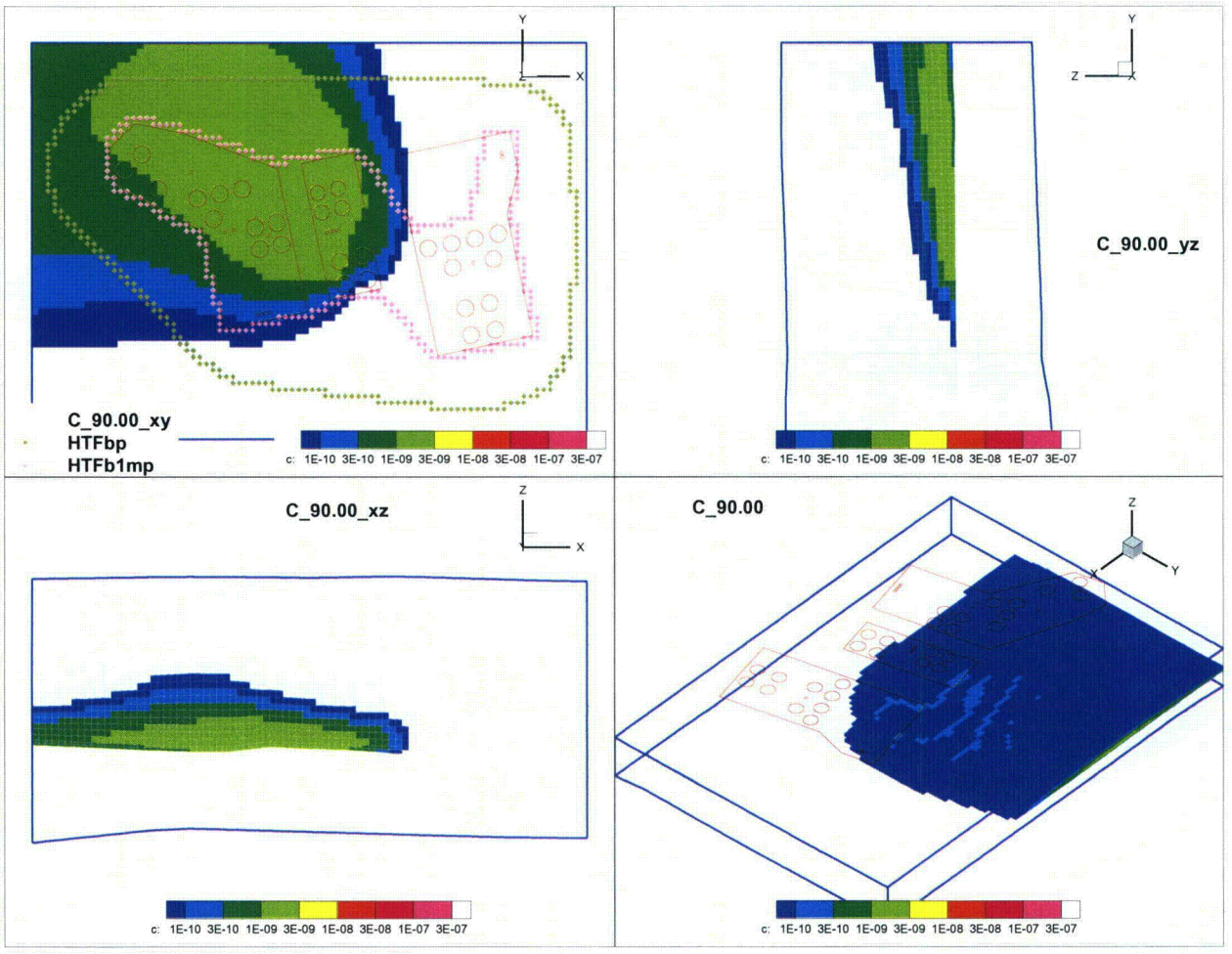

Figure CC-FF-2.8: Concentration Plume (mol/L) Formed by the Pulse Release of a Conservative Constituent from Tank 15

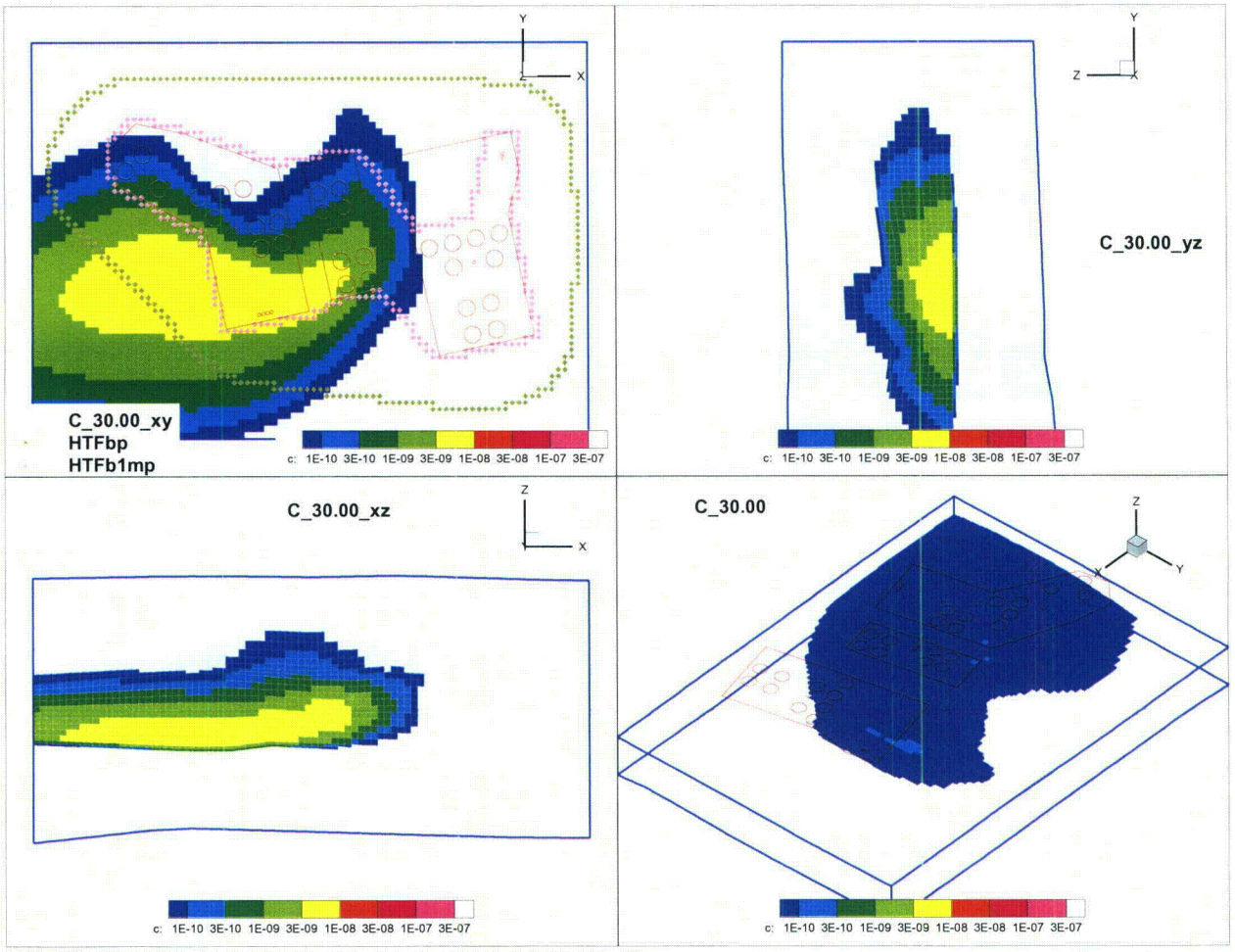

Figure CC-FF-2.9: Concentration Plume (mol/L) Formed by the Pulse Release of a Conservative Constituent from Tank 16

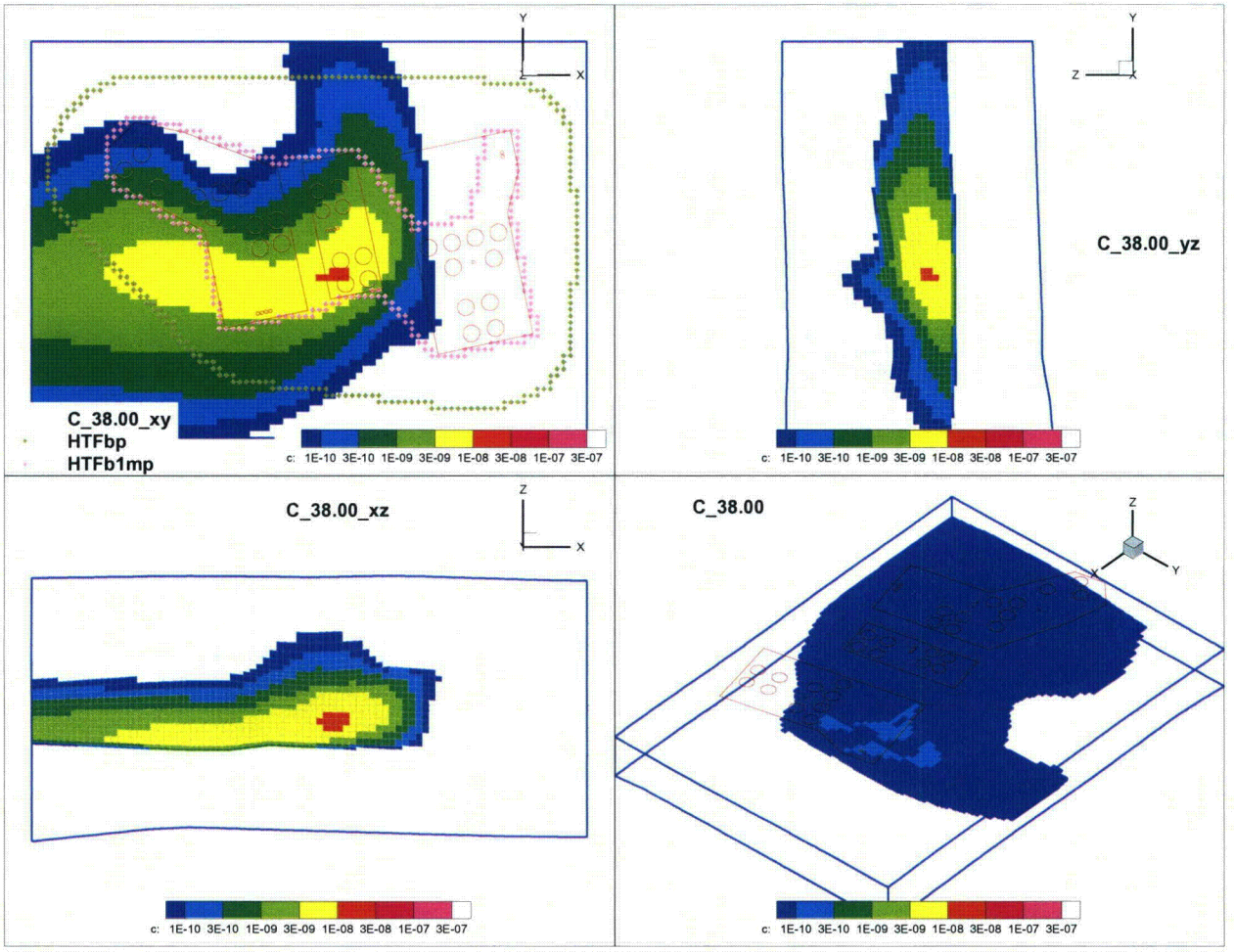

Figure CC-FF-2.10: Concentration Plume (mol/L) Formed by the Pulse Release of a Conservative Constituent from Tank 21

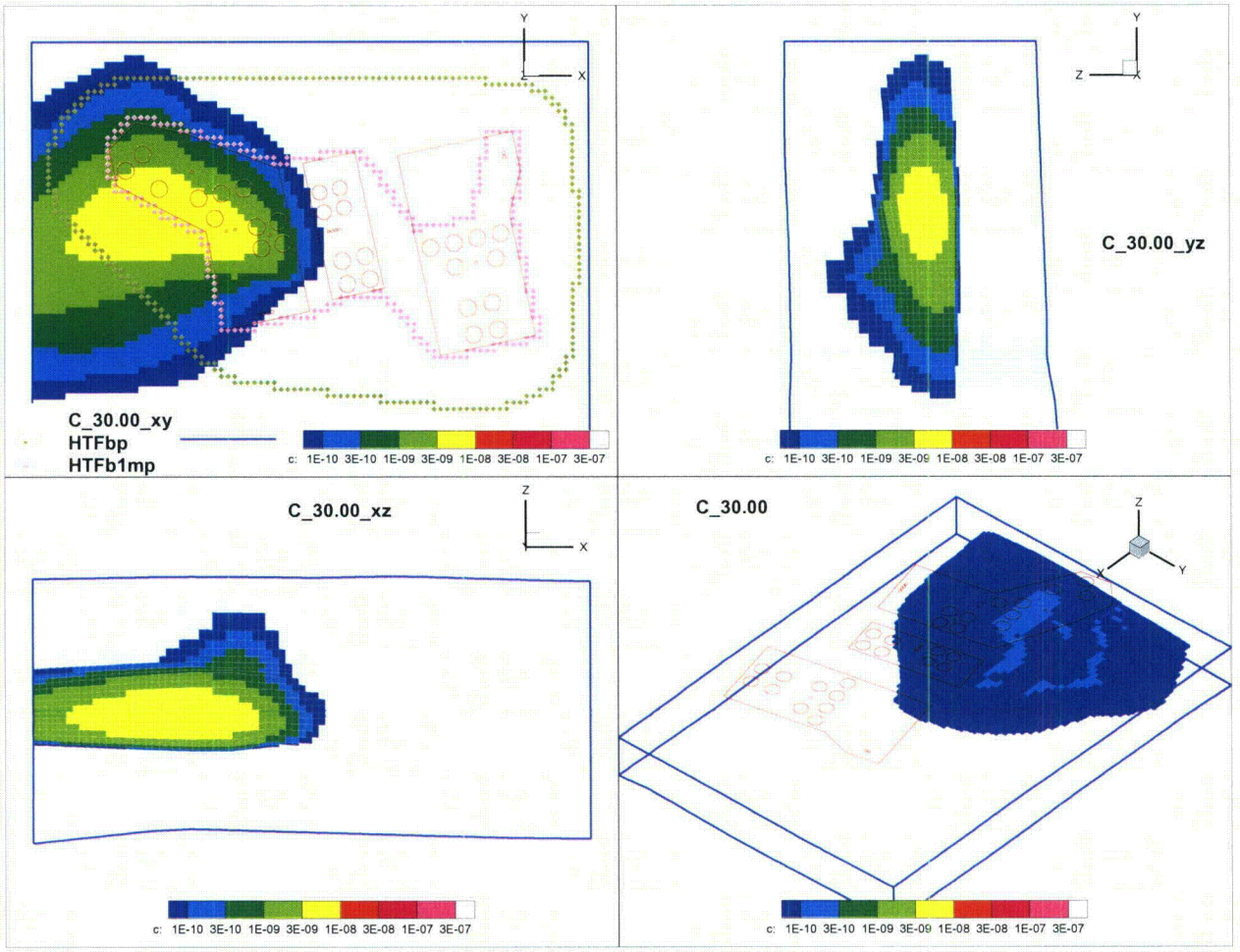

Figure CC-FF-2.11: Concentration Plume (mol/L) Formed by the Pulse Release of a Conservative Constituent from Tank 22

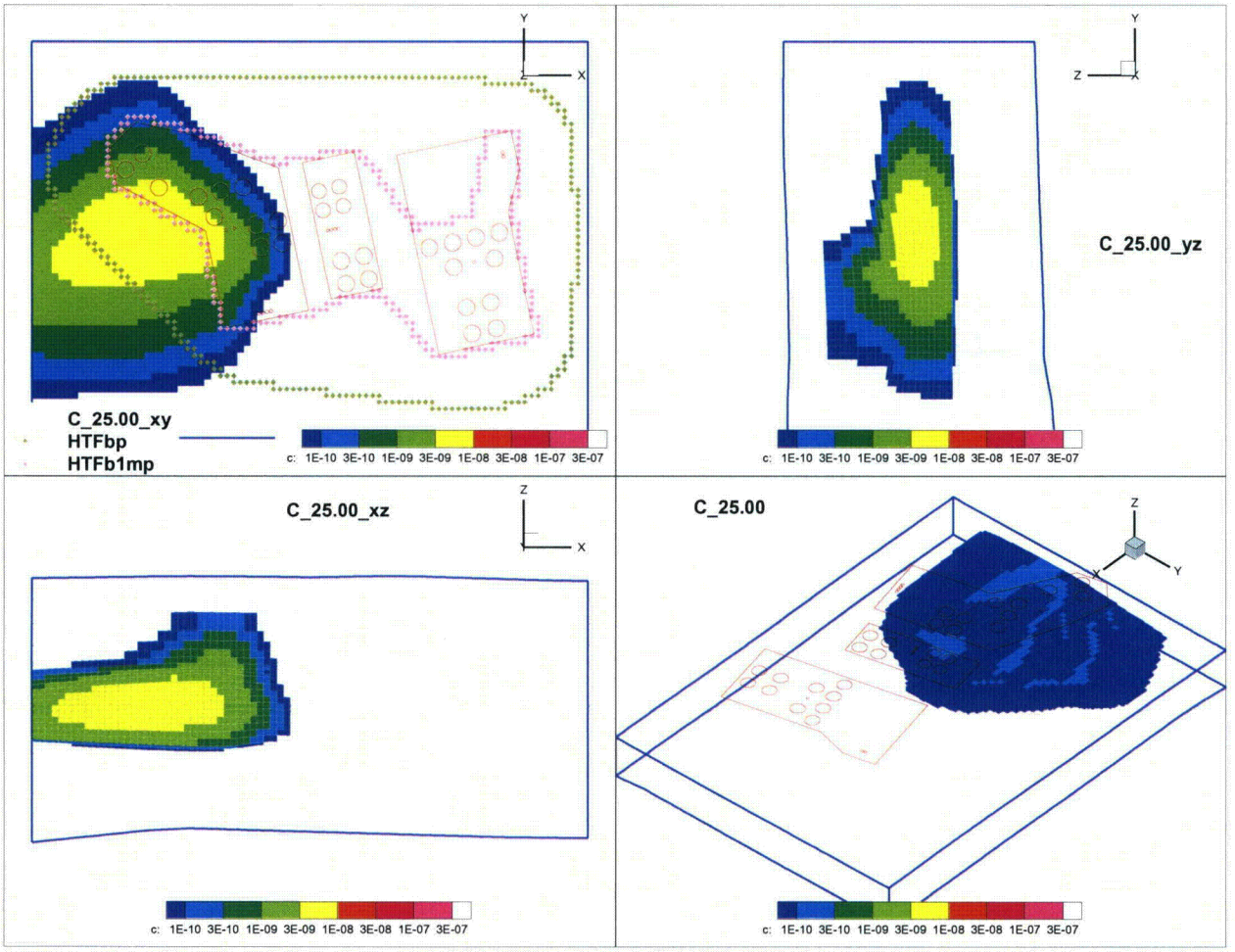

Figure CC-FF-2.12: Concentration Plume (mol/L) Formed by the Pulse Release of a Conservative Constituent from Tank 23

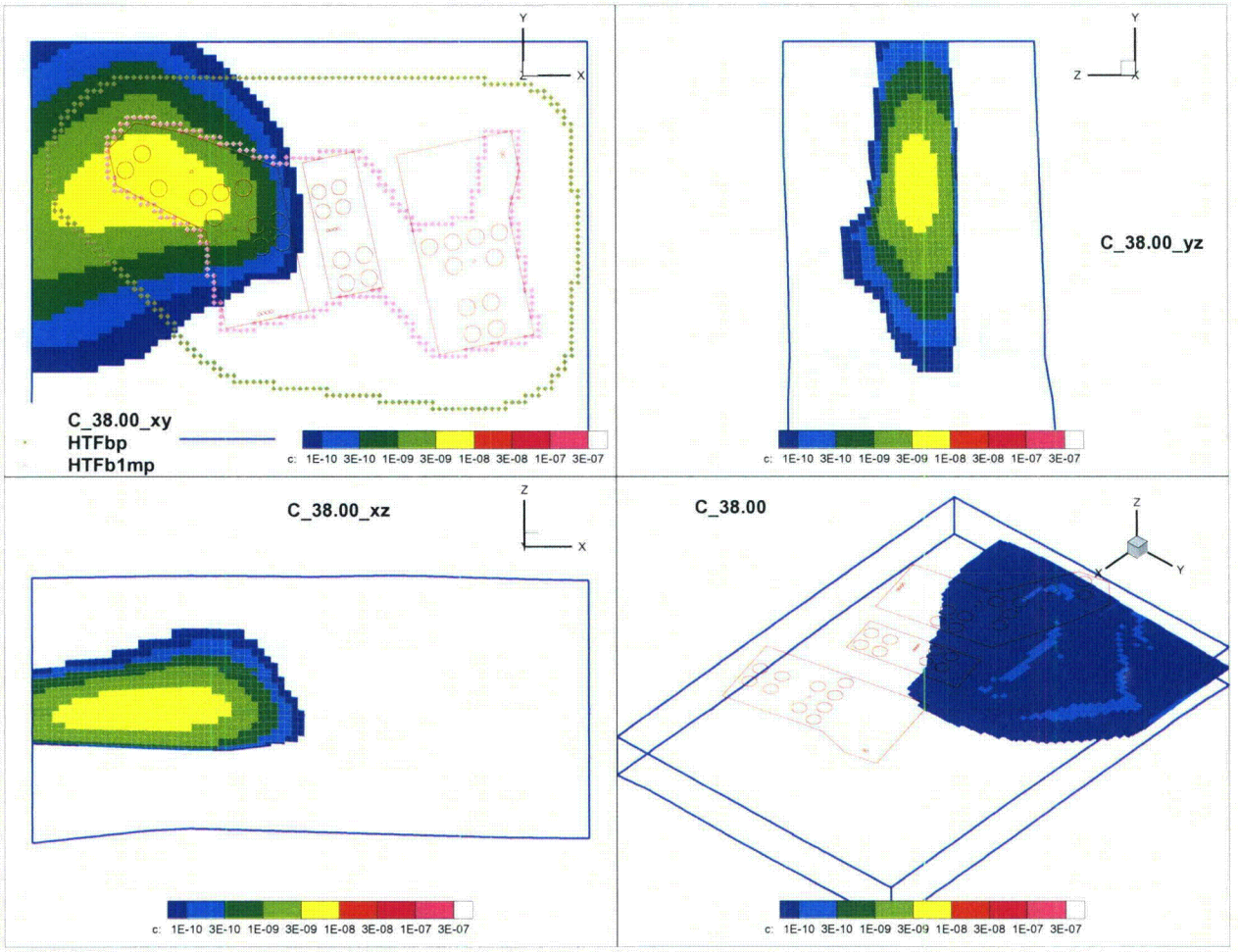

Figure CC-FF-2.13: Concentration Plume (mol/L) Formed by the Pulse Release of a Conservative Constituent from Tank 24

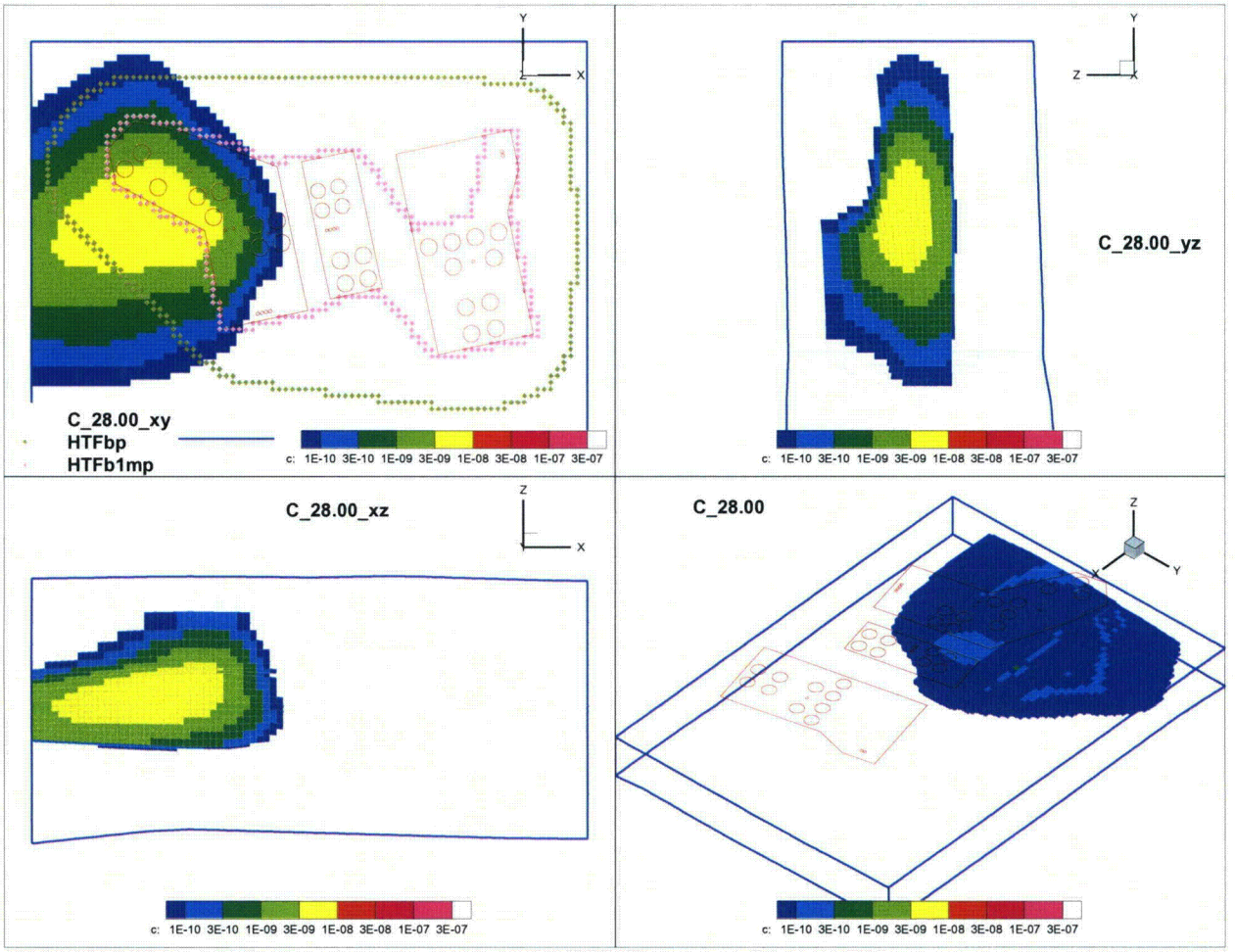

Figure CC-FF-2.14: Concentration Plume (mol/L) Formed by the Pulse Release of a Conservative Constituent from Tank 29

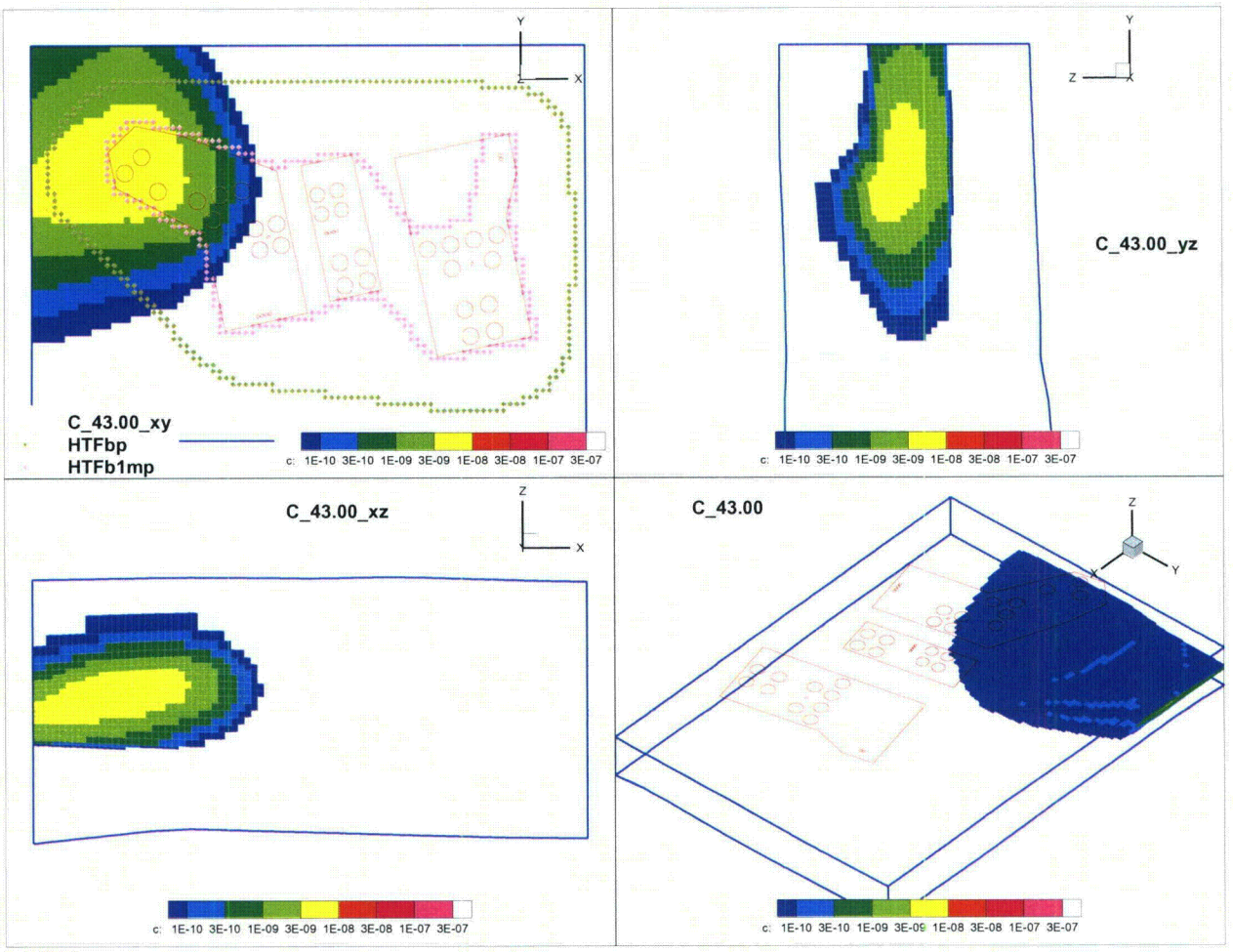

Figure CC-FF-2.15: Concentration Plume (mol/L) Formed by the Pulse Release of a Conservative Constituent from Tank 30

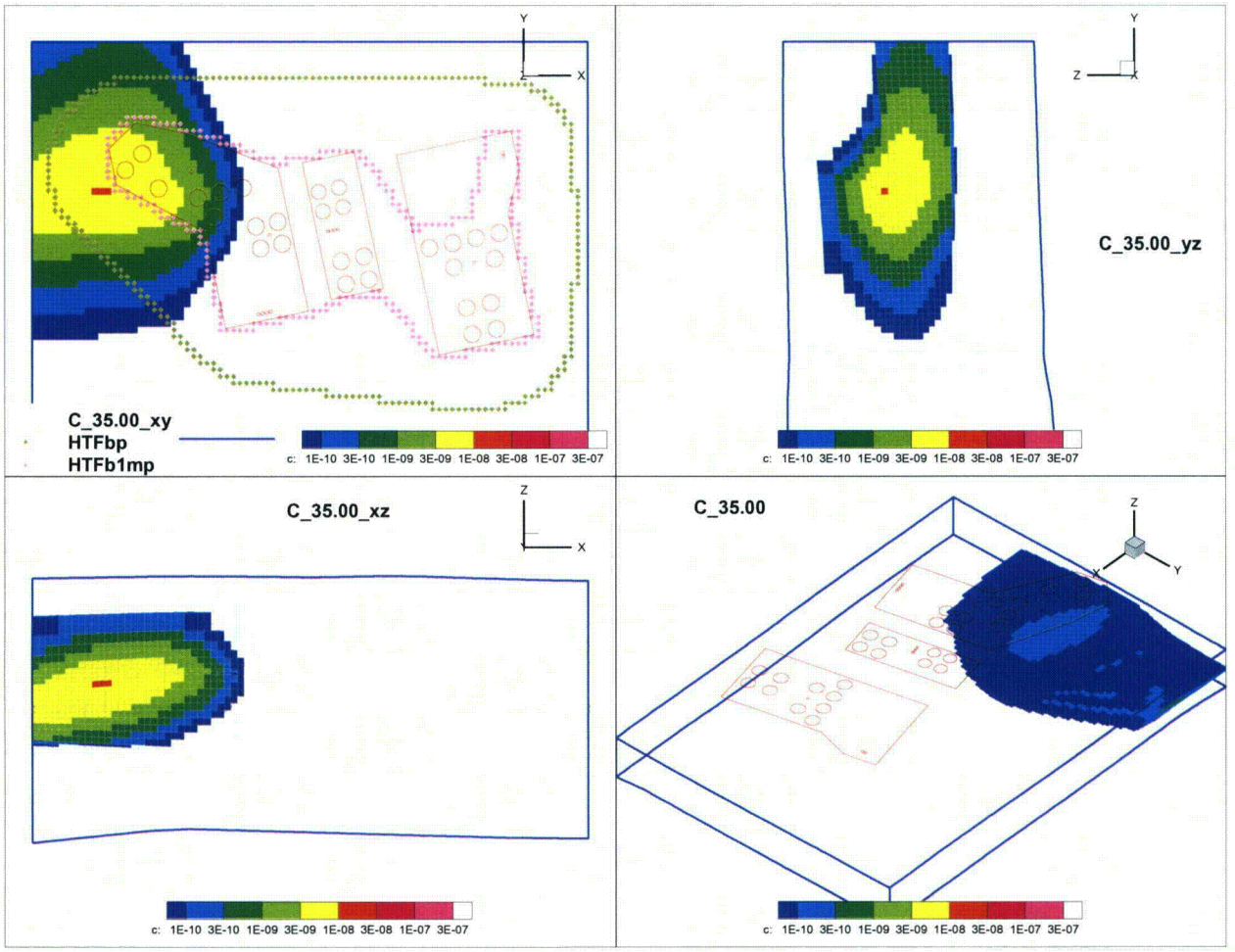

Figure CC-FF-2.16: Concentration Plume (mol/L) Formed by the Pulse Release of a Conservative Constituent from Tank 31

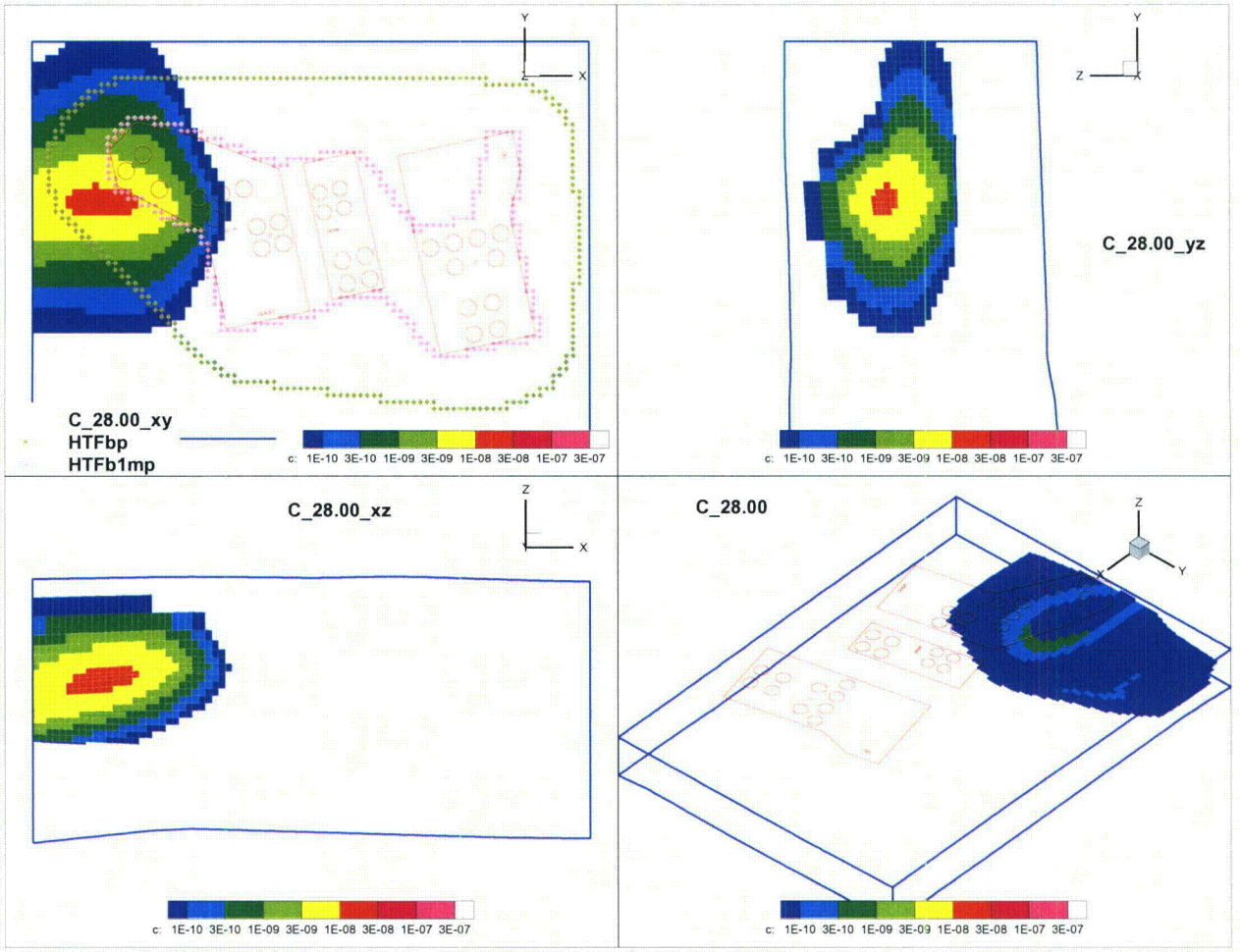

Figure CC-FF-2.17: Concentration Plume (mol/L) Formed by the Pulse Release of a Conservative Constituent from Tank 32

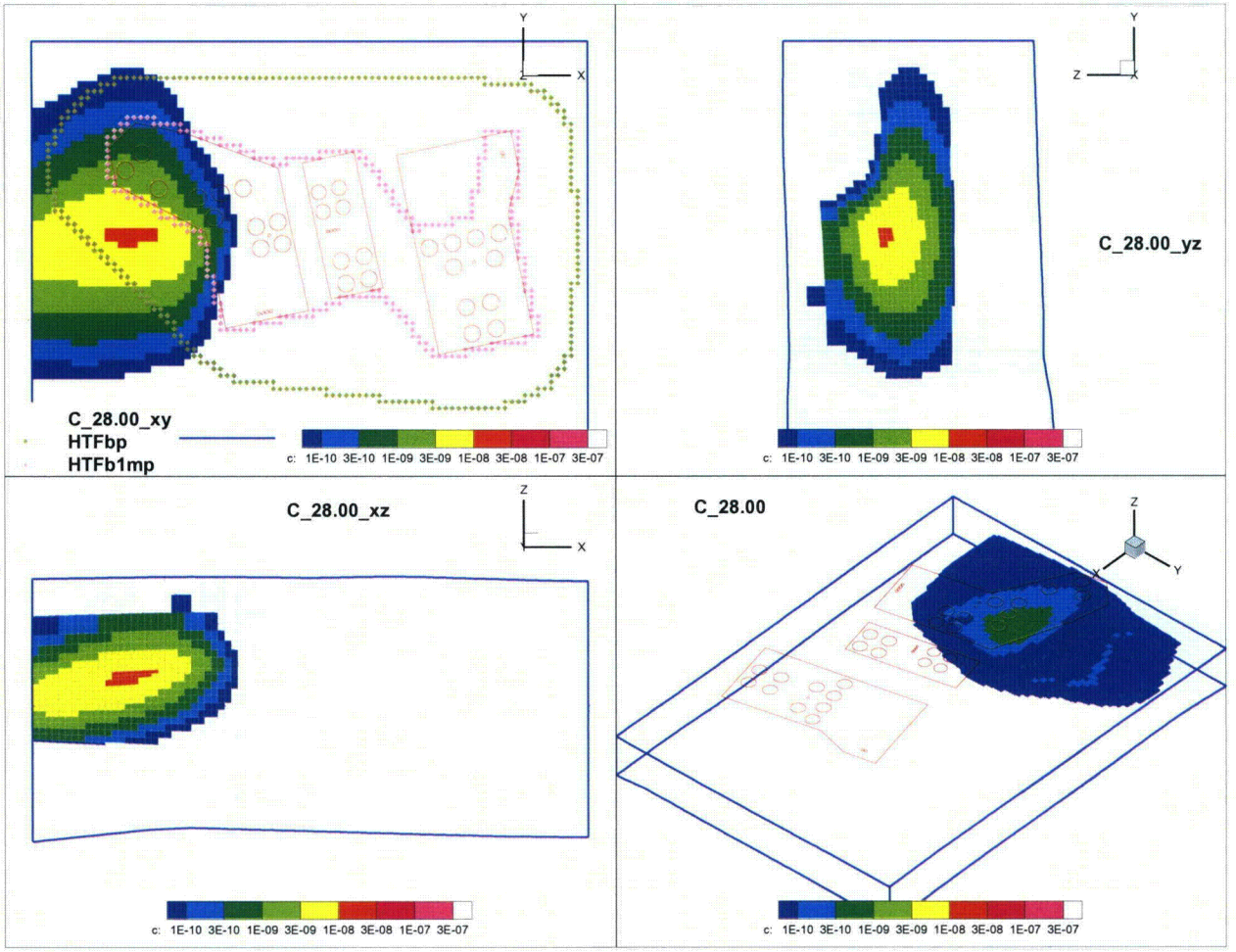

Figure CC-FF-2.18: Concentration Plume (mol/L) Formed by the Pulse Release of a Conservative Constituent from Tank 35

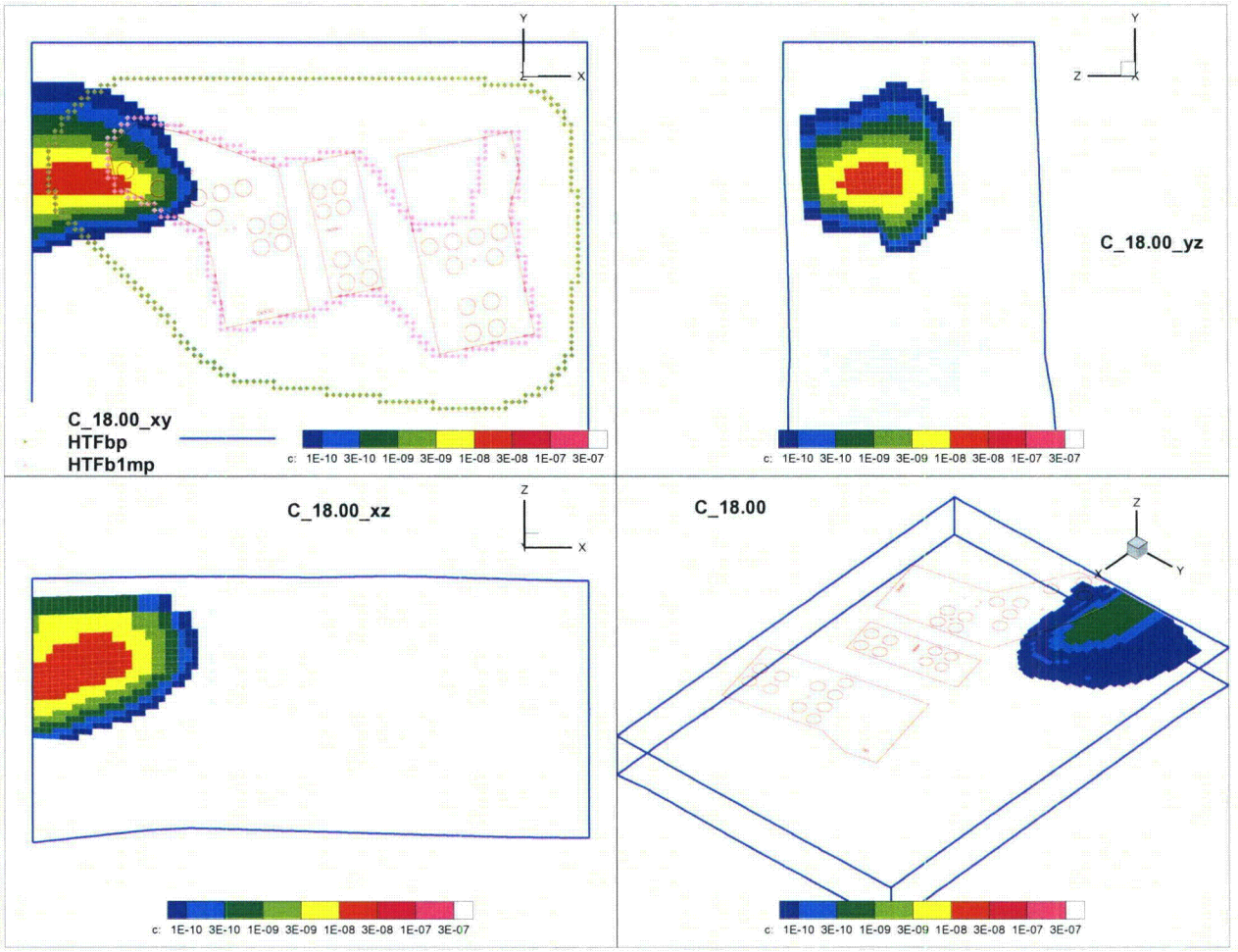

Figure CC-FF-2.19: Concentration Plume (mol/L) Formed by the Pulse Release of a Conservative Constituent from Tank 36

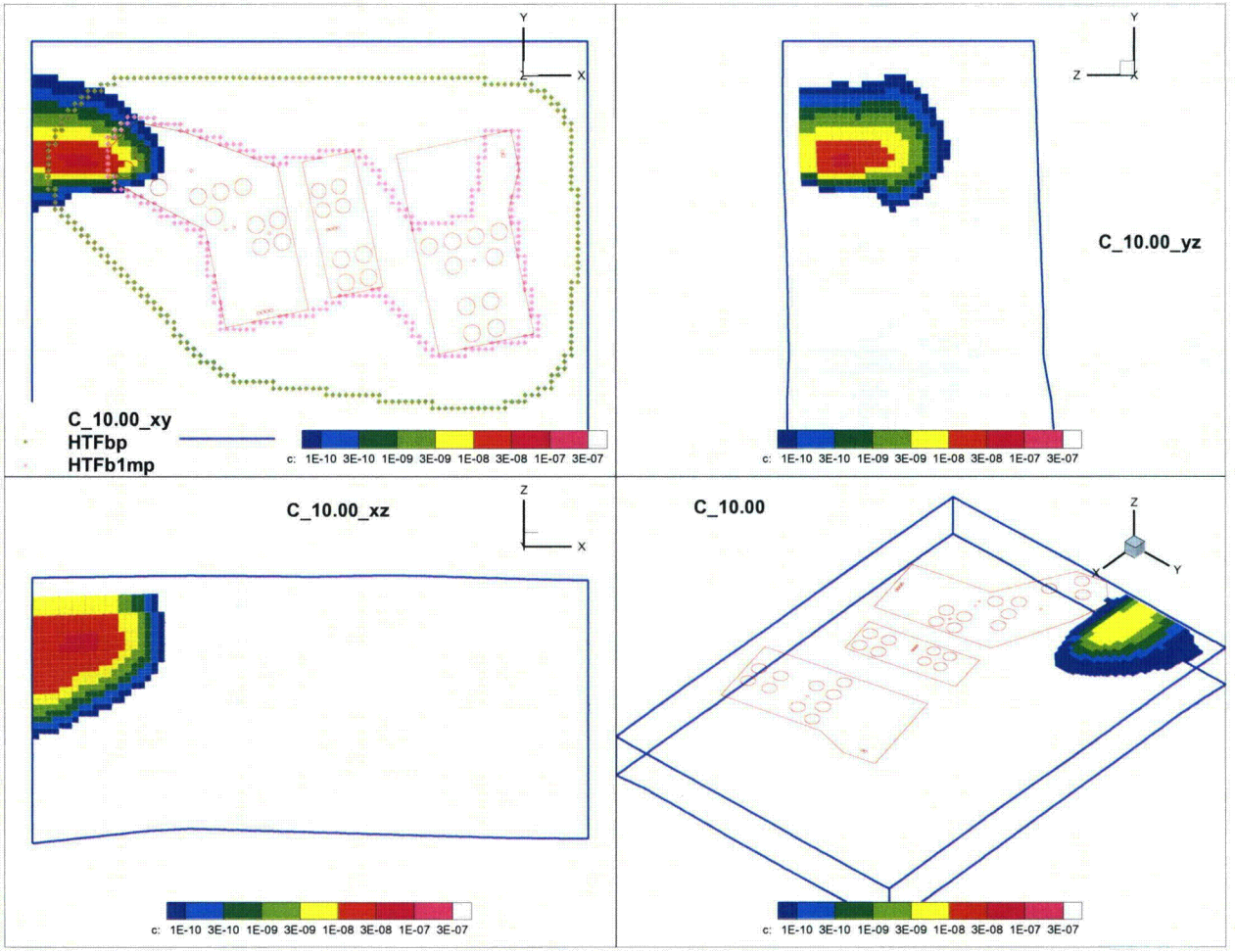

Figure CC-FF-2.20: Concentration Plume (mol/L) Formed by the Pulse Release of a Conservative Constituent from Tank 37

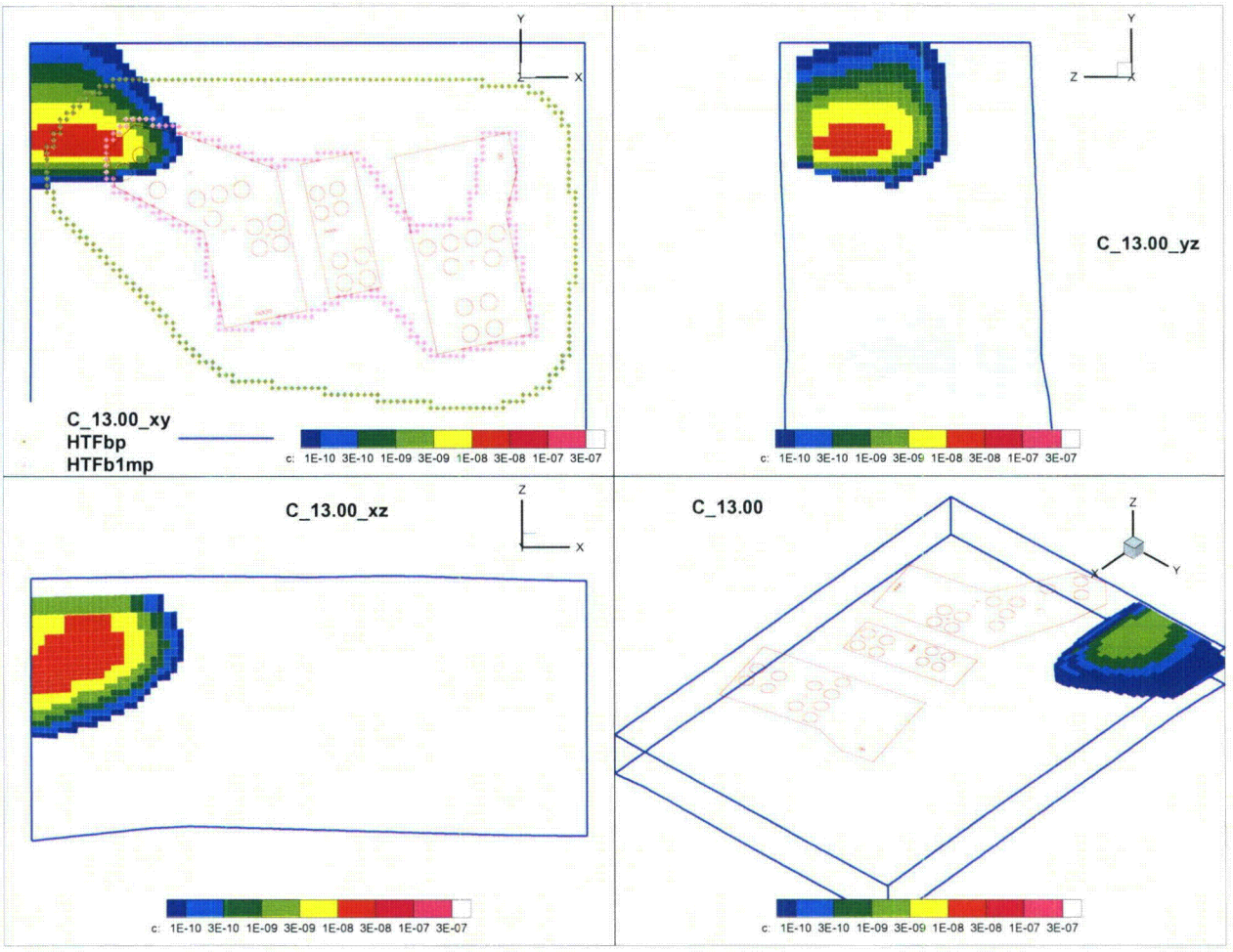

In addition, some source release plumes (Figures CC-FF-2.2 through CC-FF-2.20) show two lobes, indicating that part of the mass released does not follow the pathline defined by a particle track initiated at the center of the source (see the response to RAI-FF-3 for the pathlines used for each waste tank). This pattern is seen in instantaneous (pulse) releases from Tanks 13, 15, and 16 as shown in Figures CC-FF-2.6, CC-FF-2.8, and CC-FF-2.9, respectively. The implications of this pattern of release can be seen in the plot of a steady release from Tank 16 as shown Figure CC-FF-2.21. In GoldSim model simulations, this bimodal release of mass will lead to an overestimation of the waste tank-specific dose contribution in the sector transected by the flow pathline and an underestimation of dose contribution to any secondary sectors. Since the plots of the pulse releases with bimodal pathways showed a dominant path of migration, the addition of a secondary source and pathline was not considered in the GoldSim model.

Figure CC-FF-2.21: Concentration Plume (mol/L) Formed by the Steady Release of a Conservative Constituent from Tank 16

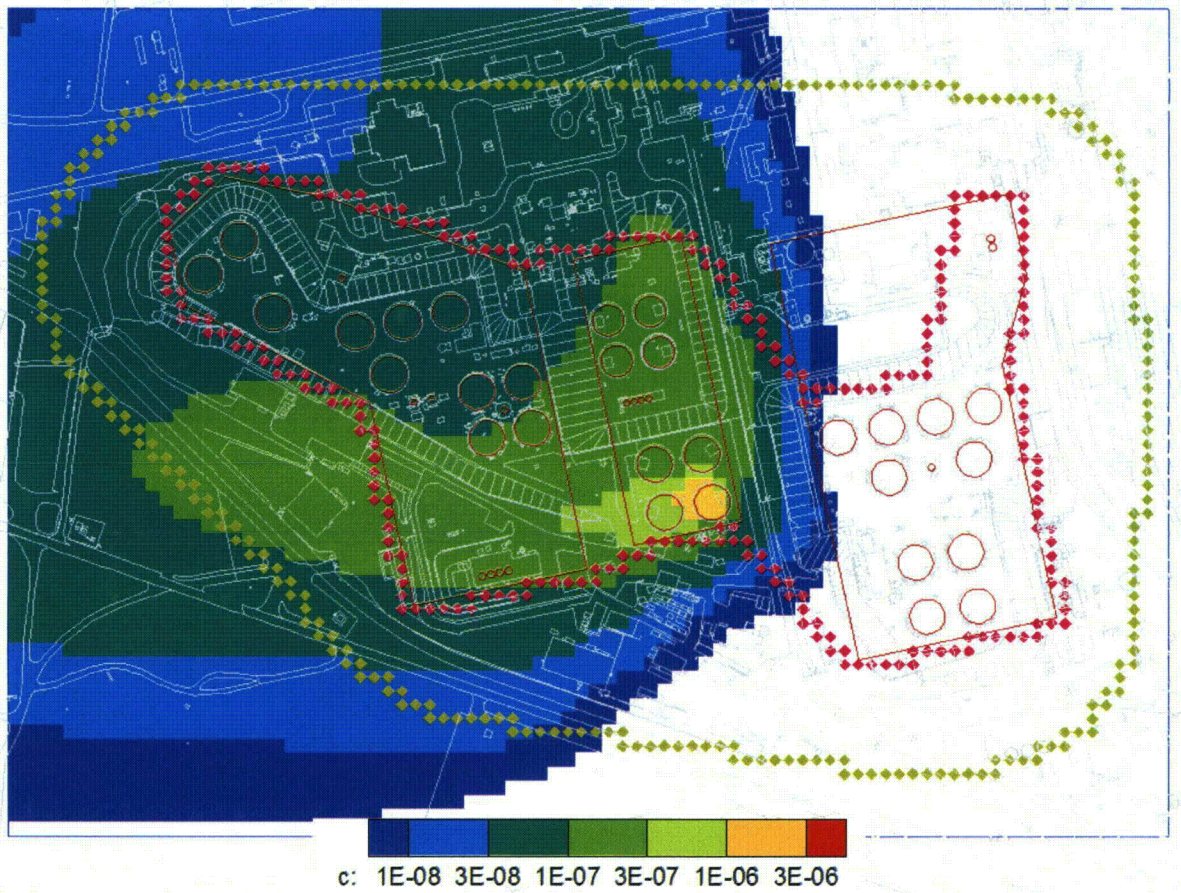

To compensate for the increased spreading of the plumes in the western zone of the HTF, the transverse dispersivity was increased by a factor of three from the PORFLOW value from 1.04 feet (0.316 meter) to 3.12 feet (0.948 meter). This increase improved the match between the PORFLOW and GoldSim models in Sectors A through C. Because of the similar scale of the plumes, complexity of the flow fields and the distortion of plume shapes, a single factor was chosen for the western side.

Note that the plumes from Tanks 35, 36, and 37, presented in Figures CC-FF-2.18, CC-FF-2.19, and CC-FF-2.20, respectively, seem like they might not be as influenced by the flow field. Because the plumes from these three waste tanks are close to the model boundary and are truncated it is hard to discern how much they are affected by the flow field. The decision to use the larger transverse dispersivity for these waste tank releases is based on the benchmarking exercise and the very close match (between the PORFLOW and GoldSim models) for the I-129 dose peaks in Sector B as shown in Figures A-2-3 and A-2.4 of the report, *H-Area Tank Farm Stochastic Fate and Transport Model*, SRR-CWDA-2010-00093.

CC-FF-3

DOE indicated during the June 6, 2013 (ML13183A410) site visit that additional mixing is performed at the end of the flow path in GoldSim® probabilistic modeling to account for increased velocities. Clarify effective dilution factors applied at the end of the flow path near the compliance boundary in GoldSim® modeling.

Response CC-FF-3

In the HTF GoldSim Model, radionuclide transport in the saturated zone is evaluated using GoldSim analytical-solution based pipe elements. The conceptual model uses a 1-D solution for the advective-dispersive transport of dissolved species in a porous medium subject to sorption, simple decay, and/or ingrowth. The solution utilized by GoldSim is a Laplace transformed solution which is evaluated in the Laplace domain, and the results are subsequently inverted numerically back to the time domain. The 1-D analytical solution is based upon a spatially invariant steady flow field and therefore, a representative flow rate must be approximated by the user. In the HTF GoldSim Model, individual Darcy velocities for each waste tank are developed along PORFLOW generated pathlines going from the waste tank centroid to a point a 100-meters from the HTF boundary. The Darcy velocities (V_{Darcy}) are based upon the time it takes for the peak of a breakthrough curve generated from a pulse release at the waste tank of a conservative species to reach the 100-meter point (T_{Pulse}), the length of the surface trace of the pathline from HTF to the 100-meter point ($S_{pathline}$), and, the effective porosity (φ). The derivation is as follows:

(Eq. 1)

$$V_{Darcy} = \frac{S_{pathline}\varphi}{T_{Pulse}}$$

The derived velocity represents a harmonically averaged Darcy velocity along the pathline. This Darcy velocity will accurately account for the time it will take the center of mass of a pulse release to reach the 100-meter point but may not accurately represent the degree of dilution in the migrating species by the time it reaches the 100-meter point. The degree of dilution at the 100-meter point is also a function of changes in flow rates along the pathline. For example, consider a simple 1-D conceptual model for dissolved species transport in a constant thickness aquifer where the velocity increases in the downgradient direction as a function of a spatially invariant infiltration rate. The governing equation for 1-D advective-dispersive transport of a dissolved species in a 1-D flow field can be written as:

(Eq. 2)

$$\frac{\partial(\varphi RC)}{\partial t} = D\frac{\partial^2 C}{\partial l^2} - \frac{\partial(vC)}{\partial l} - \varphi R\lambda C + \sum_{i=1}^{Np} \varphi R\lambda_{pi} C_{pi}$$

which can be rewritten in the form:

(Eq. 3)

$$\frac{\partial(\varphi RC)}{\partial t} = D\frac{\partial^2 C}{\partial l^2} - v\frac{\partial C}{\partial l} - C\frac{\partial v}{\partial l} - \varphi R\lambda C + \sum_{i=1}^{Np} \varphi R\lambda_{pi} C_{pi}$$

where,

R is the retardation coefficient, C is the concentration, D is the dispersion coefficient, λ is the decay coefficient, v represents the Darcy velocity, l is distance along the flowpath, and N_p is the number of parent species. The third term on the right hand side of Equation 3 is a first-order term that represents the effects of the spatial change in velocities on derived concentrations. For the above HTF GoldSim conceptual model, if v is the Darcy velocity at an upgradient point, by replacing $\partial v/\partial l$, with i/L where i is the infiltration rate and L is the aquifer thickness, the third term of the right hand side of Equation 3 represents the dilution due to the infiltration of clean water along the pathline. Note that the third and fourth terms on the right hand side of Equation 3 can be combined when solving the equation. The solution of the Equation 3 for the 1-D conceptual model then derives concentrations at downgradient points which result from dilution due to recharge along the pathline while using a constant velocity required by the analytical solution. Note that for this choice of velocity, the mass arrival time will not be accurate. Similarly, results at downgradient points can also be obtained by omitting the third right hand side term in Equation 3 and multiplying the derived concentrations at downgradient points by the following dilution factor (*DF*):

(Eq. 4)

$$DF = \frac{Q_I}{Q_I + Q_A}$$

where,

Q_I is the infiltration flux along the pathline (m^3/yr) and Q_A is the aquifer flux (m^3/yr). If the Darcy velocity is known at the downgradient point, the *DF* in Equation 4 could be redefined as:

(Eq. 5)

$$DF = \frac{v}{V_{DarcyDowngradient}}$$

In this form, any increase in velocity along a pathline does not have to change in a linear manner. The upgradient velocity, v, could be replaced by a harmonically averaged velocity.

The HTF GoldSim Model takes advantage of the use of the *DF* defined in Equation 5 by multiplying the concentrations derived at the 100-meter point by a *DF* equal to the ratio of the harmonically averaged Darcy velocity along the pathline to the Darcy velocity at the 100-meter point. By using this *DF* in conjunction with results based upon the harmonically averaged flow rate, the HTF model maximizes the accuracy of the breakthrough time and degree of dilution obtained at the 100-meter point for this simplified transport model abstraction.

CC-FF-4

Provide approximate (effective) dilution factors for various HTF sources in GoldSim® probabilistic model considering vertical and horizontal dispersion, as well as additional mixing due to increased dilution at the end of the flow path. Evaluate dilution for various source release profiles such as pulse or continuous releases with respect to peak dose for various source locations and radionuclides.

Response CC-FF-4

In the HTF GoldSim Model, mass released from individual HTF waste tanks is transported by advection, through the unsaturated zone to a sink cell. The mass release is integrated over time, and the integrated mass is applied as a cumulative input source term to a 1-D advective-dispersive analytical solution used in GoldSim pipe pathways. In the HTF GoldSim Model, the cross section over which the 1-D solution is evaluated is equivalent to the product of the waste tank-width and a vertical source thickness assumed to be 3 meters. The solution used in the pipe-pathway element considers the effects of longitudinal dispersion, but a separate function, the GoldSim plume function is used to evaluate the influence of horizontal- and vertical-transverse dispersion on the dilution of dissolved radionuclides transported in the aquifer. The GoldSim plume function uses a series of Green's function and spatially integrates Green's function solutions to evaluate the influence of transverse dispersion on a source release from rectangular planar or rectangular prismatic sources. In the HTF GoldSim Model, the 3-D aspects of dispersion are implemented by taking the product of the plume function values and the 100-meter concentrations (i.e., the concentrations at a point 100 meters from the HTF) generated by the pipe pathway analytical solution. The total degree of dilution of mass migrating from the waste tank to the plume becomes a function of:

- The mixing of the mass released to the saturated zone in the analytical model;
- The influence of longitudinal dispersion in the derivation of concentrations in the pipe-pathway solution; and
- The influence of horizontal- and vertical-transverse dispersion as determined by the plume function.

In addition, a dilution factor, which represents downgradient changes in flow rates (as described in the response to CC-FF-3), is applied in the HTF GoldSim Model to evaluate the total attenuation due to dilution.

Because the degree of attenuation (due to longitudinal dispersion) depends upon the temporal nature of the source term, the influence of longitudinal diffusion will be evaluated separately in this report. By disregarding attenuation (due to longitudinal dispersion) approximate (effective) dilution factors were defined for the HTF waste tank sources by evaluating the influence of the transverse spreading due to dispersion and the flow rates in the aquifer. The effective dilution factor associated with the processes discussed above can be described by Equation 1:

(Eq. 1)

$$DF_{Effective} = \frac{V_{SZ} W_{Source} T_{Source} DF_{Boundary}}{\pi r_{tank}^2 V_{UZ} PF_{Plume}}$$

where,

V_{SZ} is the Darcy velocity in the saturated zone, V_{UZ} is the Darcy velocity in the unsaturated zone, W_{Source} is the diameter of the waste tank, r_{tank} is the waste tank radius, and T_{Source} is the source thickness. Additionally, the plume function (PF_{plume}) is the product of the Green's function solutions describing horizontal and vertical transverse dispersion at the end of the pipe and $DF_{Boundary}$ is the dilution factor, associated with changes in flow rate along the pathway.

Table CC-FF-4.1 presents the approximate (effective) dilution factors evaluated using Equation 1 in conjunction with the data used in the Base Case (Case A) of the HTF GoldSim Model. Table CC-FF-4.2 presents the approximate (effective) dilution factors, excluding the boundary dilution factor ($DF_{Boundary}$).

Table CC-FF-4.1: Effective Dilution Factors for HTF (Including $DF_{Boundary}$)

Waste Tank Number	Dilution Factor (DF_{Total})
T9	33
T10	28
T11	38
T12	35
T13	92
T14	47
T15	69
T16	118
T21	77
T22	68
T23	82
T24	69
T29	60
T30	50
T31	42
T32	37
T35	33
T36	24
T37	27
T38	53
T39	52
T40	50
T41	45
T42	59
T43	68
T48	69
T49	72
T50	100
T51	67

Table CC-FF-4.2: Effective Dilution Factors for HTF (Excluding $DF_{Boundary}$)

Waste Tank Number	Dilution Factor (DF_{Total})
T9	6
T10	4
T11	7
T12	6
T13	27
T14	9
T15	16
T16	37
T21	20
T22	13
T23	17
T24	15
T29	9
T30	7
T31	7
T32	5
T35	7
T36	5
T37	6
T38	7
T39	8
T40	9
T41	9
T42	8
T43	7
T48	9
T49	12
T50	8
T51	5

These partial dilution factors are applicable for continuous or pulse releases and for all radionuclides. The dilution factors were calculated for each HTF waste tank as the source. Note that the dilution factors presented below are based on the final values of Darcy velocity in the unsaturated zone and are evaluated at the points where flow pathlines cross the 100-meter point.

The total degree of dilution to which radionuclides are subject to while migrating through the aquifer is also a function of longitudinal dispersion or spreading. The degree of attenuation determined by the GoldSim pipe pathway analytical model is a function of the longitudinal dispersivity, the pipe length, and the temporal nature of the source term. Because this portion of the dilution is dependent on the release profile of the source term, the process was evaluated for a typical path length, Darcy velocity, and other parameters consistent with the HTF GoldSim Model aquifer parameters. The pipe pathway model was used to evaluate the attenuation of a conservative species migrating along a 1,000-foot pathway from the waste tank center to the 100-meter point using a Darcy velocity of 10 ft/yr, a porosity of 25 %, and the 10.4-foot HTF model longitudinal dispersivity. Note that the degree of attenuation is independent of the Darcy velocity, which controls only the timing of the breakthrough curve.

The evaluation used source pulse lengths of 0.5, 1, 2.5, 5, 10, 15, 20, and 25 years as well as a steady source. The results are presented as normalized doses that are normalized with respect to the steady-state results for a constant flux. The attenuation for each source pulse length is

defined by a separate attenuation factor, and presented in Table CC-FF-4.3. The 100-meter concentration breakthrough curves for each simulation are presented in Figure CC-FF-4.1. Note that the attenuation factors are the inverses of the peak values of the normalized breakthrough curves presented in Figure CC-FF-4.1. Due to the model parameters used, the dilution factor for a 25-year pulse essentially equals the steady pulse after 25 years. A complete dilution factor can then be defined as the product of $DF_{Effective}$ and the attenuation factor.

Table CC-FF-4.3: Attenuation Factors for HTF

Pulse Length (yr)	Attenuation Factor
0.5	17.89
1	8.99
2.5	3.65
5	1.94
10	1.20
15	1.04
20	1.01
25	1.00
Steady Pulse	1.00

Figure CC-FF-4.1: Normalized 100-Meter Concentration Breakthrough Curves for Modeled Source Pulses

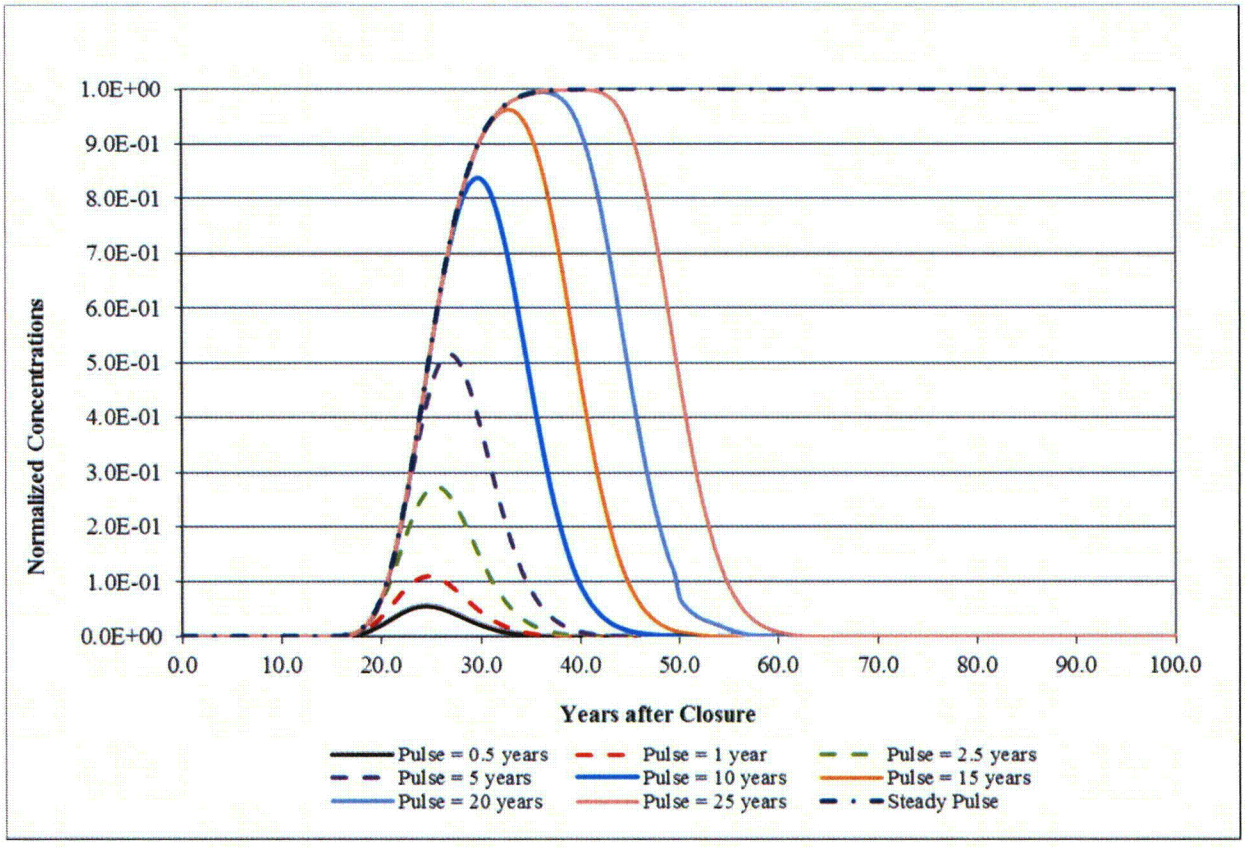

Inadvertent Intrusion (INT)

CC-INT-1

Clarify whether intruder doses presented in Section 6 of the HTF Performance Assessment (SRR-CWDA-2010-00128, Rev. 1) consider alternative cases.

Response CC-INT-1

Section 6.5.1 of the HTF PA includes the following IHI alternative scenarios:

1. The impact of drilling into a 4-inch line rather than a 3-inch line (Section 6.5.1.1)
2. The impact of drilling into a waste tank rather than a 3-inch line (Section 6.5.1.2)
3. The impact of drilling into locations closer to specific waste tanks rather than at the 1-meter boundary (Section 6.5.1.3)

However, Section 6 of the HTF PA did not include intruder dose results for the alternative waste tank configurations (i.e., Cases B, C, D, and E). Provided in Table CC-INT-1.1 and Figures CC-INT-1.1 through CC-INT-1.8 are the chronic IHI dose results for each of these alternative configurations (by sector and by key radionuclides). The 1-meter boundaries for each of the six sectors (Sectors A through F) are shown on Figure 5.2-5 of the HTF PA.

These Alternative Case modeling runs were developed using the HTF PORFLOW Model and the same GoldSim dose calculator as used for the Base Case (Case A of the HTF PA modeling configurations). These models only include the sensitivity run radionuclides, as identified in Table 5.2-9 of the HTF PA. This is why the Base Case value is lower than that reported in Section 6.4 of the HTF PA. Case E is discussed further in the response to CC-INT-2.

The acute IHI dose is based on exposure to drill-cuttings and does not rely upon contaminant transport via groundwater. In addition, applying an alternative waste tank configuration does not alter the acute IHI dose. Therefore, the acute IHI dose results are not discussed in this response.

Table CC-INT-1.1: Chronic IHI Peak Doses for the Base Case and Alternative Cases

Case	1,000-Year Peak Dose	10,000-Year Peak Dose	100,000-Year Peak Dose
A	40 mrem/yr at year 100	50 mrem/yr at year 10,000	348 mrem/yr at year 50,520
B	40 mrem/yr at year 100	41 mrem/yr at year 10,000	214 mrem/yr at year 19,070
C	40 mrem/yr at year 100	83 mrem/yr at year 9,070	286 mrem/yr at year 42,400
D	40 mrem/yr at year 100	63 mrem/yr at year 6,190	312 mrem/yr at year 45,370
E	367 mrem/yr at year 1,000	1,127 mrem/yr at year 2,160	1,127 mrem/yr at year 2,160

Case A = Base Case

Figure CC-INT-1.1: Case B Chronic IHI Dose

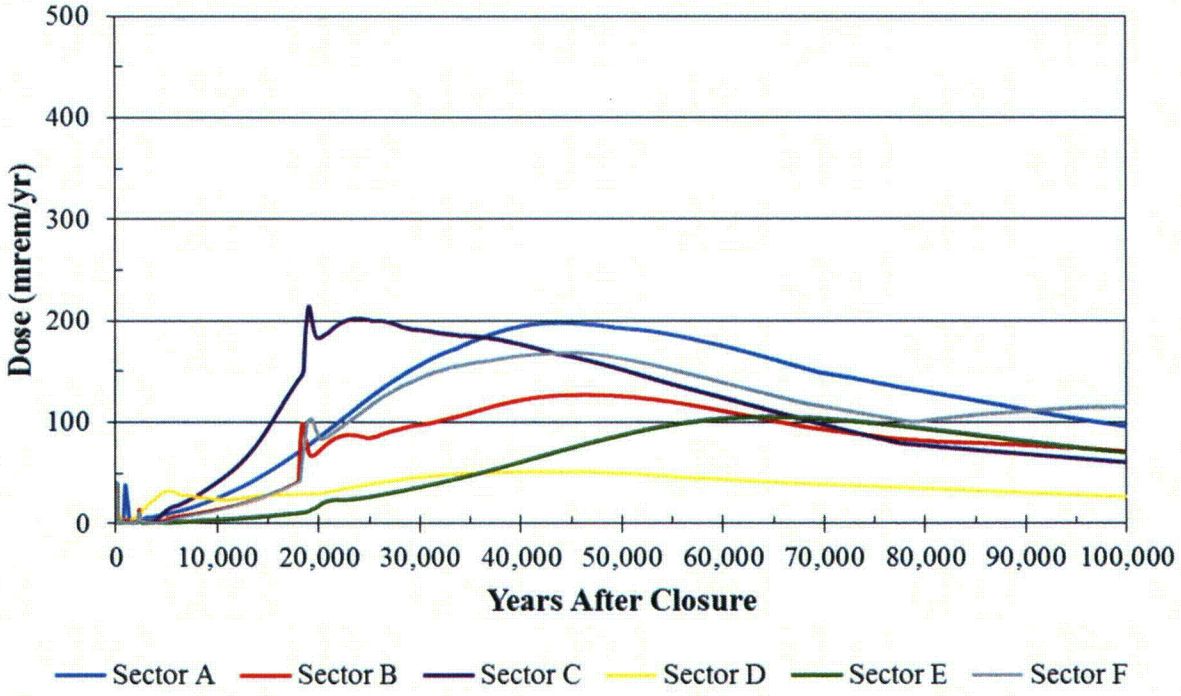

Figure CC-INT-1.2: Case B Individual Radionuclide Contributors to Chronic IHI Dose

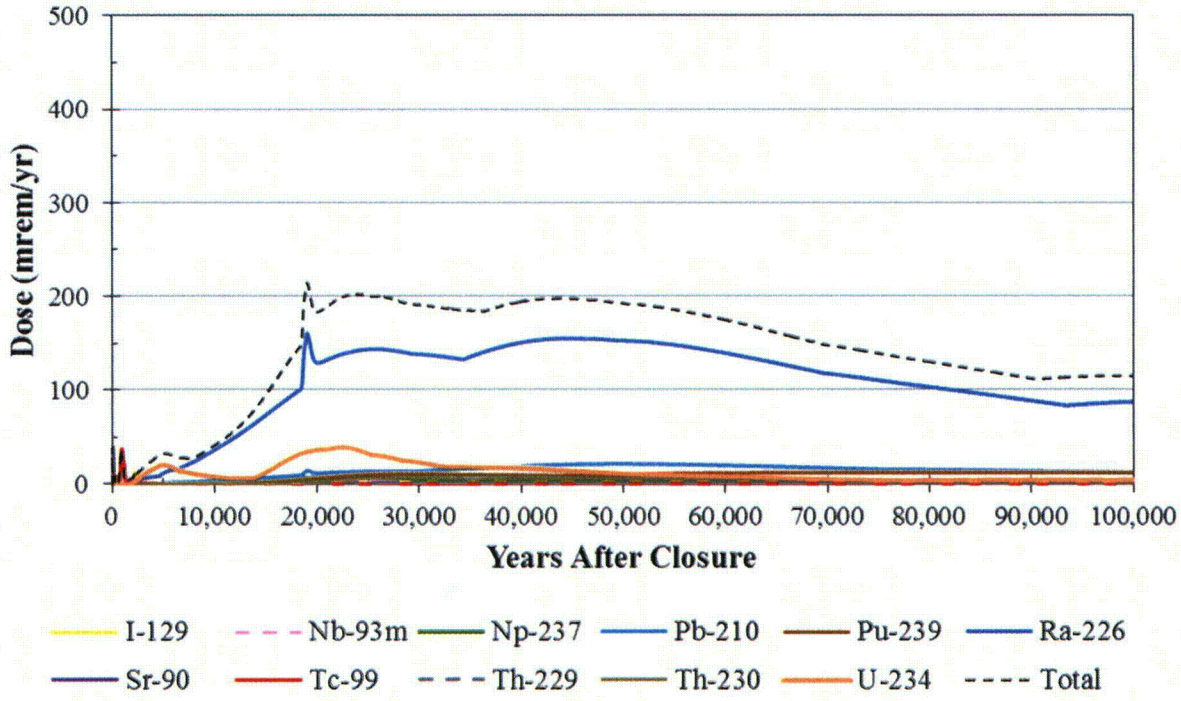

Figure CC-INT-1.3: Case C Chronic IHI Dose

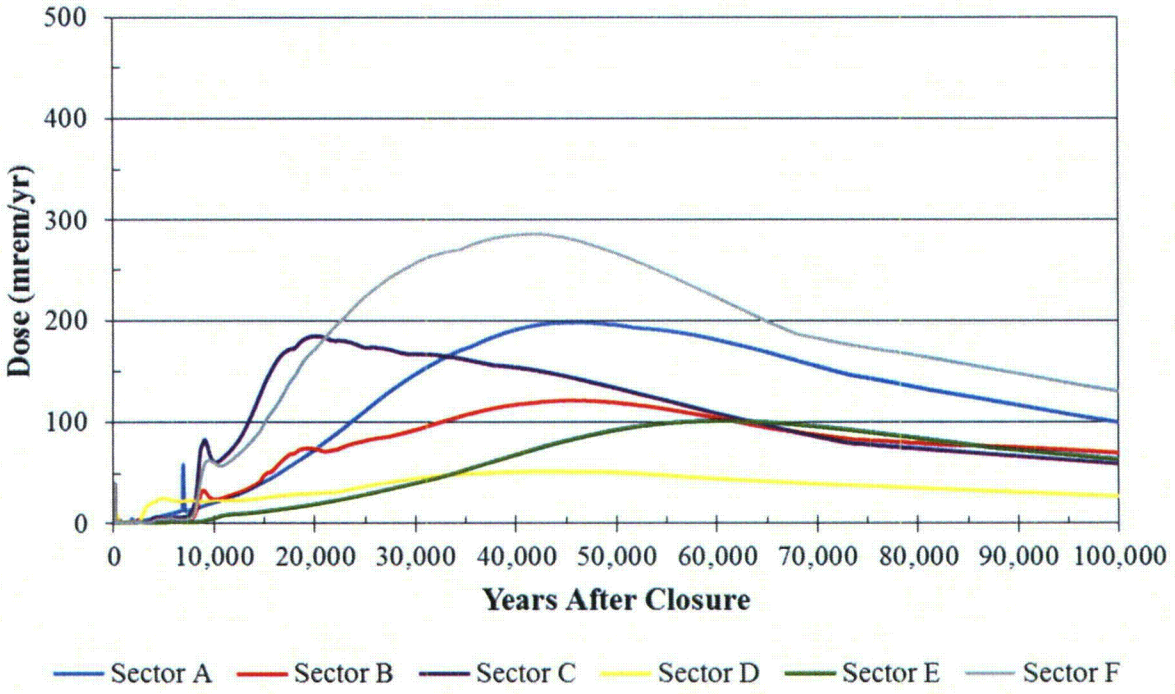

Figure CC-INT-1.4: Case C Individual Radionuclide Contributors to Chronic IHI Dose

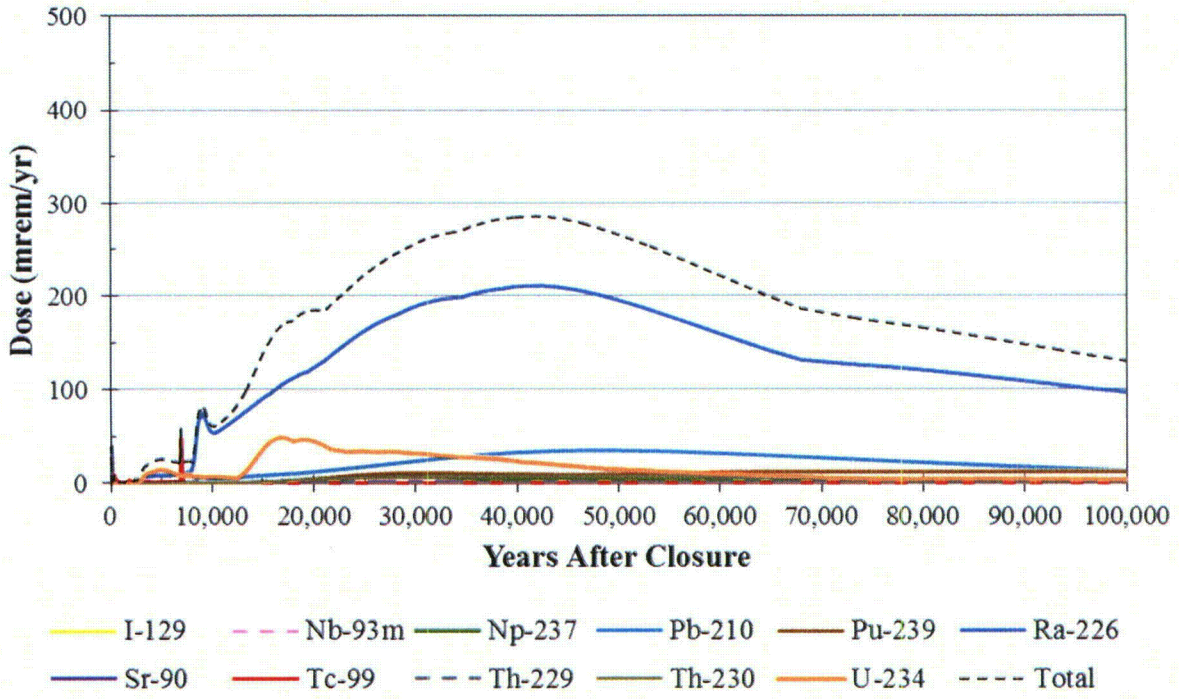

Figure CC-INT-1.5: Case D Chronic IHI Dose

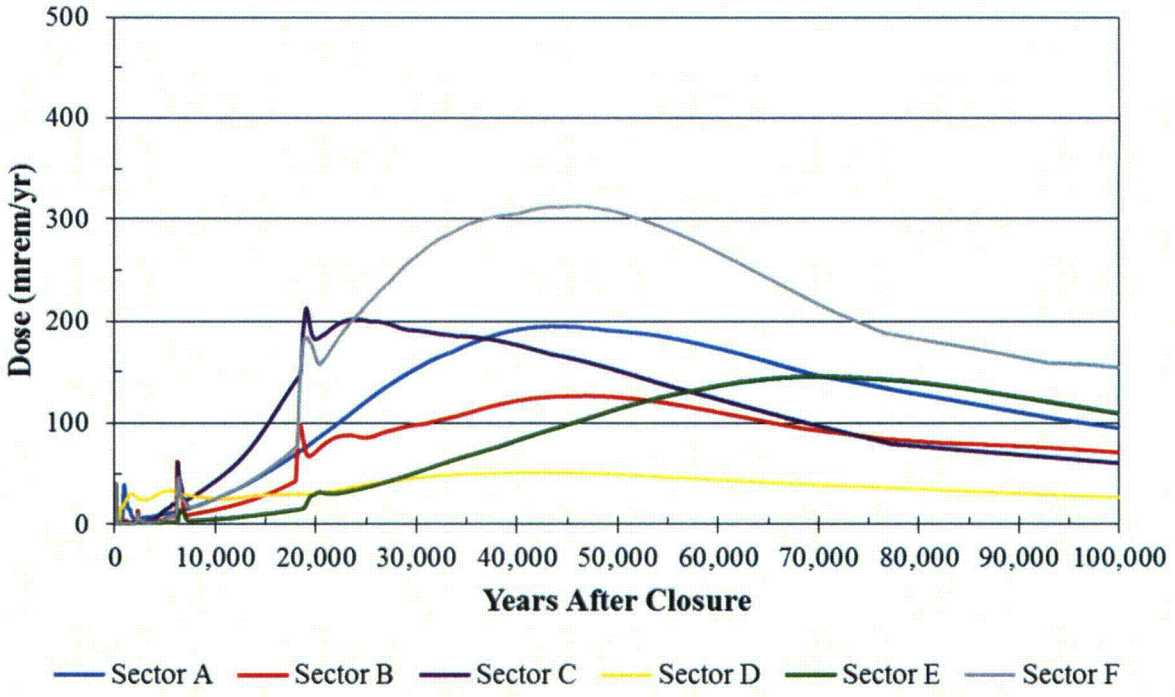

Figure CC-INT-1.6: Case D Individual Radionuclide Contributors to Chronic IHI Dose

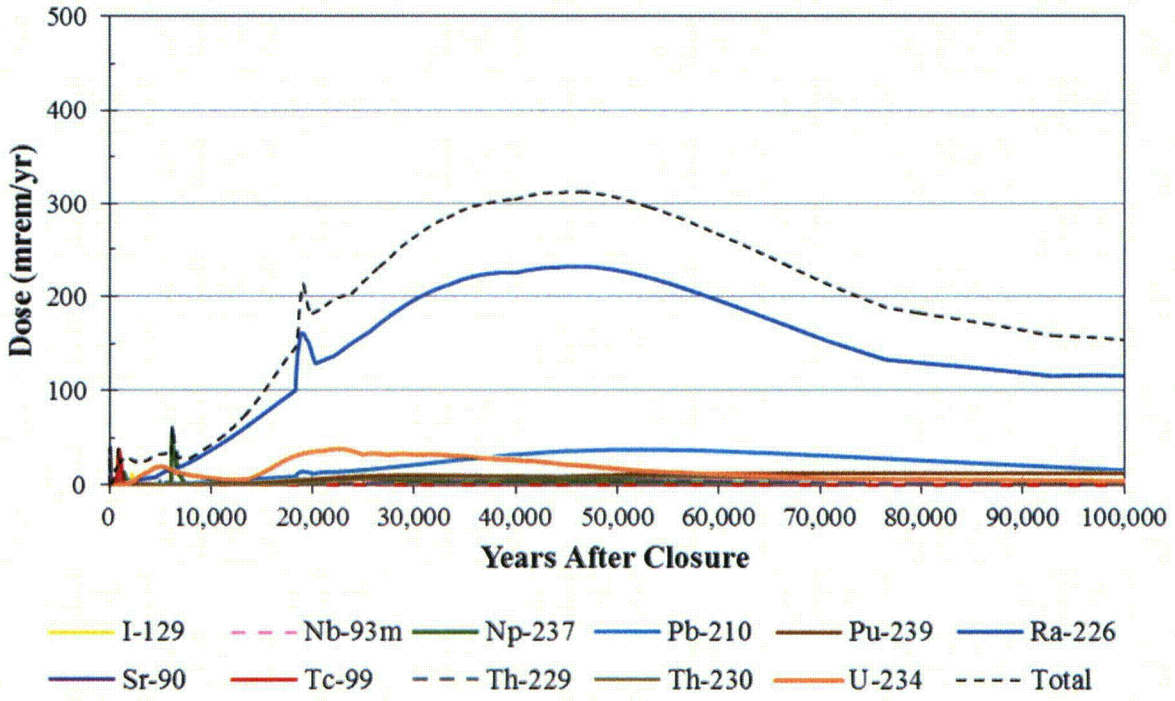

Figure CC-INT-1.7: Case E Chronic IHI Dose

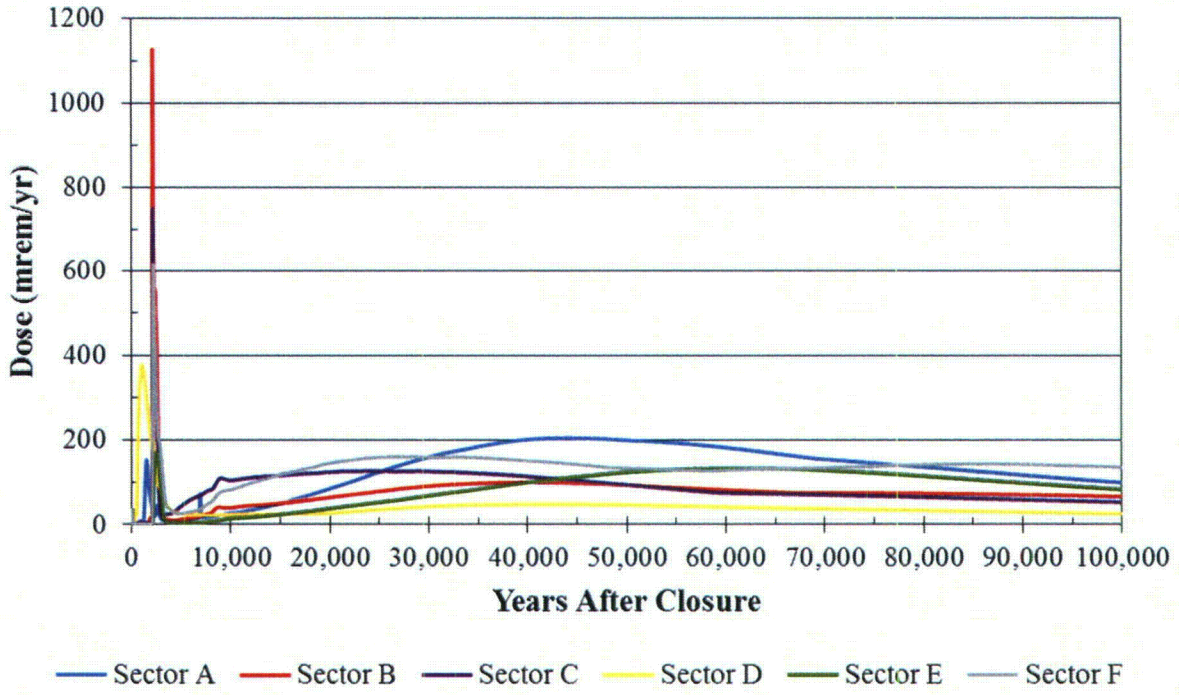

Figure CC-INT-1.8: Case E Individual Radionuclide Contributors to Chronic IHI Dose

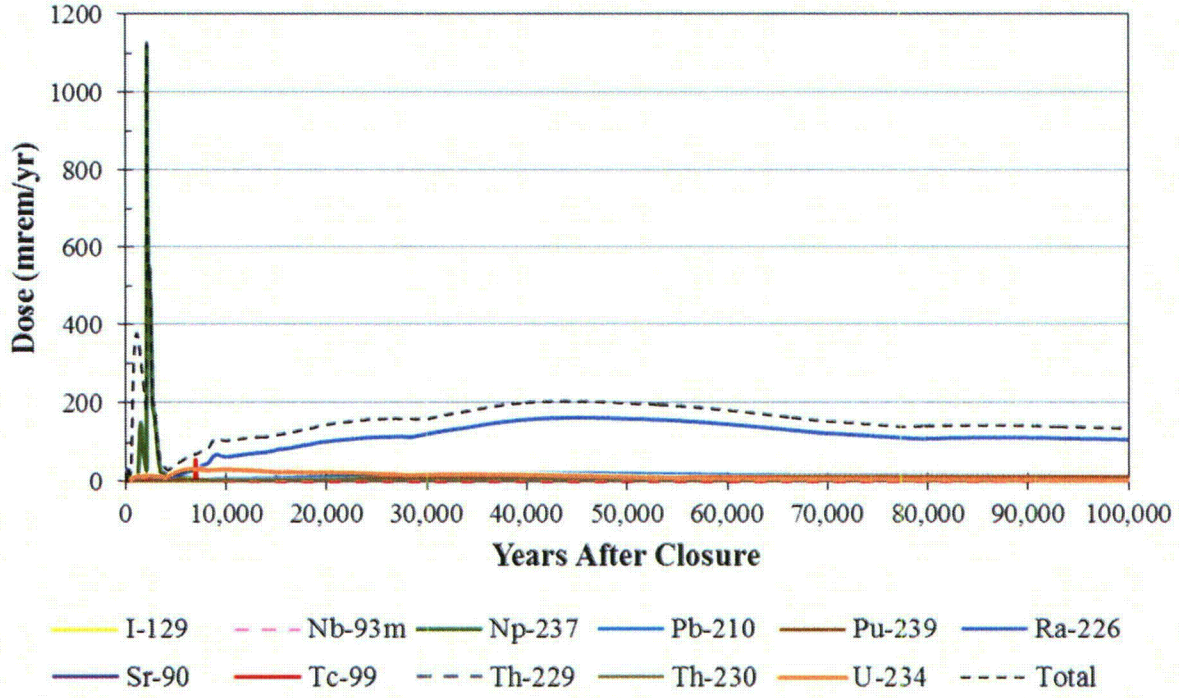

CC-INT-2

Provide detailed results for alternative case E.

Response CC-INT-2

The chronic IHI dose for Case E was estimated to peak at 1,127 mrem/yr (at 2,160 years after HTF final facility closure), as shown in Table CC-INT-1.1 and Figures CC-INT-1.7 and CC-INT-1.8 of the response to CC-INT-1. Case E is considered the least probable configuration out of the scenarios identified in Table CC-INT-1.1 (see Section 5.6.3.2 of the HTF PA and the response to RAI-NF-10).

Note that Case E modeling is a configuration used to represent an unanticipated, bounding scenario, and is presented as a thought exercise to understand the system better. As described in Section 4.4.2.5 of the HTF PA, the fast flow path in Case E is non-mechanistically assumed to bypass a number of barriers in this scenario. This fast flow path would be:

1. Liquid passing through the roof of the waste tank;
2. Down the full height of the grouted waste tank through an assumed gap between the grout and the primary liner;
3. Along the entirety of floor of the waste tank contacting all of the residual waste (i.e., a gap would exist between the residuals at the waste tank bottom and the 100's of thousands of gallons of grout above the residuals;
4. Out through the center of the primary liner floor;
5. Through the grout layer between the primary tank and the secondary liner;
6. Through the annular pan; and
7. Completely through the basemat.

The fast flow occurs in Case E without the grout's reducing properties being imparted onto the associated liquid.

More than 99 % of the peak dose from Case E is attributed to a single radionuclide, Np-237, and the timing of this peak strongly indicates that the peak dose is driven by the simultaneous failure (at year 2,077) of all 17 of the Type III and Type IIIA tank liners. In other words, the fast flow path scenario outlined in items 1 through 7 above would occur for all 17 of the Type III and IIIA tanks simultaneously.

Case E is considered an unlikely scenario for the following reasons:

1. Fast flow paths are not expected to simultaneously bypass every barrier within every waste tank;
2. The concrete in the basemat is expected to retard the transport of Np-237;
3. The primary liner for each of the Type III and Type IIIA tanks are expected to fail at varying times;
4. Except for the type IV tanks, all waste tanks have cooling coils such that it is unlikely that fast flow paths, if they did occur, would develop only along primary tank walls and not along cooling coils. If fast flows occurred along the cooling coils the reducing capacity of the grout would be expected to be imparted onto tank pore water; and
5. Fast flows through the waste tank would not be expected to mobilize 100% of the contamination zone.

As such, it is expected that the peak doses associated with Np-237 in Case E would be significantly mitigated if these conservatisms were tempered in the modeling.

REFERENCES FOR RESPONSES

0008-8846(88)90042-7, (Copyright), Luke, K. and Glasser, F.P., *Internal Chemical Evolution of the Constitution of Blended Cements*, Cement and Concrete Research, Vol. 18(4), pp. 495–502, July 1988.

0016-2361(84)90337-5, (Copyright), Valković, V., et al., *Analysis of Fly Ash by X-Ray Emission Spectroscopy and Proton Microbeam Analysis*, Fuel, Vol. 63, pp. 1357-1362, October 1984.

0304-3894(96)01805-5, (Copyright), Glasser, F.P., *Fundamental Aspects of Cement Solidification and Stabilisation*, Journal of Hazardous Materials, Vol. 52, pp. 151-170, April 1997.

0956-053X(92)90044-J, (Copyright), Atkins, M. and Glasser, F.P., *Application of Portland Cement-Based Materials to Radioactive Waste Immobilization*, Waste Management, Vol. 12, pp. 105-131, 1992.

0956-053X(92)90051-J, (Copyright), Ewart, R., et al., *The Solubility of Actinides in a Cementitious Near-Field Environment*, Waste Management, Vol. 12, Issues 2-3, pp. 241-252, 1992.

BNL-82395-2009, Furhmann, M. and Gillow, J., *Fate of Contaminants in Contact with West Valley Grouts*, Brookhaven National Laboratory, Upton, NY, July 22, 2009.

CBU-PIT-2005-00131, *Response To Additional Information Request on Draft Section 3116 Determination For Salt Waste Disposal at Savannah River Site*, Savannah River Site, Aiken, SC, Rev. 1, July 14, 2005.

DHEC_04-11-2013, *Request for Concurrence to Proceed to Sampling and Analysis Phase of the Tank Closure Process for Tank 16H dated April 4, 2013*, Letter from Van Keisler (SCDHEC) to B. Hennessey (DOE-SR), South Carolina Department of Health and Environmental Control, Columbia, SC, April 11, 2013.

DOE G 435.1-1, *Implementation Guide for use with DOE M 435.1-1,* U.S. Department of Energy, Washington, DC, July 9, 1999.

DOE M 435.1-1, Chg. 1, *Radioactive Waste Management Manual,* U.S. Department of Energy, Washington, DC, June 19, 2001.

DOE/SRS-WD-2013-001, *Draft Basis for 3116 Determination for Closure of H-Tank Farm at the Savannah River Site*, Savannah River Site, Aiken, SC, Rev. 0, February 6, 2013.

DOI: 10.106/J, (Copyright), Lothenbach, B. and Winnefeld, F., *Thermodynamic Modeling of the Hydration of Portland Cement*, Elsevier Ltd., Cement and Concrete Research, Vol. 36, Issue 2, February 2006.

DPST-85-782, Fong, M.C.H., *Oxalic Acid Cleaning of Tank 24H*, Savannah River Site, Aiken, SC, September 9, 1985.

EPA_04-10-2013, *EPAs Concurrence to Preliminary Cease Waste Removal and Proceed to the Sample and Analysis Phase of the Tank Closure Process for Tank 16H*, Letter from R. Pope (EPA) to B. Hennessey (DOE-SR), U.S. Environmental Protection Agency, Atlanta, GA, April 10, 2013.

ISBN: 0-02-367412-1, (Copyright), Langmuir, D., *Aqueous Environmental Geochemistry*, Prentice Hall, Upper Saddle River, NJ, 1st ed., January 1997.

ISBN: 0-13-365312-9, (Copyright), Freeze, R.A. and Cherry, J.A., *Groundwater*, Prentice Hall, Englewood Cliffs, NJ, 1979.

ISBN: 3-527-30800-8, (Copyright), Bertolini, L., et al., *Corrosion of Steel in Concrete*, WILEY-VCH Verlag GmbH & Co, KGaA, Weinheim, 2004.

ISSN: 0950-0618, (Copyright), Raupach, M., *Chloride-Induced Macrocell Corrosion of Steel in Concrete – Theoretical Background and Practical Consequences*, Construction and Building Materials, Vol. 10, No. 5, pp. 329-338, 1996.

LWO-LWE-2007-00104, Clendenen, G.B., *Tank 5 & 6 Closure Sequence of Events*, Savannah River Site, Aiken, SC, Rev. 2, November 20, 2008.

LWO-LWE-2008-00283, Thaxton, G.D. and Vetsch, W.J., *Tank 5 Second Acid Strike Chemical Cleaning Report*, Savannah River Site, Aiken, SC, Rev. 0, October 20, 2008.

LWO-LWE-2008-00284, Thaxton, G.D. and Vetsch, W.J., *Tank 6 Second Acid Strike Chemical Cleaning Report*, Savannah River Site, Aiken, SC, Rev. 1, September 9, 2008.

ML100970781, *Savannah River Site H-Area Tank Farm Input Packages/References*, Memo to File from Lowman, D., U.S. Nuclear Regulatory Commission, Washington, DC, April 13, 2010.

ML13044A309, *Draft Basis for Section 3116 Determination for Closure of H-Tank Farm at the Savannah River Site, February 6, 2013 (DOE/SRS-WD-2013-001, Rev. 0)*, Memo to File from Shaffner, J., U.S. Nuclear Regulatory Commission, Washington, DC, February 13, 2013.

ML13086A080, *Summary of Webcast/Teleconference between U.S. Nuclear Regulatory Commission Staff and U.S Department of Energy Representatives Concerning Consultation, Per Section 3116 NDAA, on a Proposed Waste Determination Related to H Area Tank Farm at the Savannah River Site*, Note to File from Shaffner, J., U.S. Nuclear Regulatory Commission, Washington, DC, April 22, 2013.

ML13106A338, *Summary of Clarification Discussion Between the U.S. Nuclear Regulatory Commission Staff and the U.S. Department of Energy and Savannah River Remediation Staff Concerning Waste Release Potential Related to H Area Tank Farm at the Savannah River Site*, Note to File from Shaffner, J., U.S. Nuclear Regulatory Commission, Washington, DC, May 3, 2013.

ML13120A496, *Summary of Clarification Discussion Between the U.S. Nuclear Regulatory Commission Staff and the U.S. Department of Energy and Savannah River Remediation Staff Concerning Flow and Transport of Contaminants Related to H Area Tank Farm at the Savannah River Site*, Note to File from Shaffner, J., U.S. Nuclear Regulatory Commission, Washington, DC, May 10, 2013.

ML13154A327, *Summary of Clarification Discussion Between the U.S. Nuclear Regulatory Commission Staff and the U.S. Department of Energy and Savannah River Remediation Staff Concerning Flow Modeling and Calibration Related to H Area Tank Farm at the Savannah River Site*, Note to File from Shaffner, J., U.S. Nuclear Regulatory Commission, Washington, DC, July 5, 2013.

ML13183A410, *Summary of a Public Meeting between the U.S. Nuclear Regulatory Commission Staff and the U.S Department of Energy Staff and Contractors Concerning Requests for Additional Information Related to a Proposed Waste Determination for Closure of H-Area Tank Farm at the Savannah River Site; and a Consultation Site Visit by NRC Staff to H-Tank Farm*, Note to File from Shaffner, J., U.S. Nuclear Regulatory Commission, Washington, DC, August 1, 2013.

ML13193A072, *Summary of Clarification Discussion Between the U.S. Nuclear Regulatory Commission Staff and the U.S. Department of Energy and Savannah River Remediation Staff Concerning Flow Modeling and Calibration Related to H-Area Tank Farm at the Savannah River Site*, Note to File from Shaffner, J., U.S. Nuclear Regulatory Commission, Washington, DC, July 16, 2013.

ML13196A135, *U.S. Nuclear Regulatory Commission Staff Comments and Requests for Additional Information on the Draft Basis for Section 3116 Determination for Closure of H-Tank Farm at the Savannah River Site, DOE/SRS-WD-2013-001 Rev.0 and on Performance Assessment for the H-Area Tank Farm for the Savannah River Site, SRR-CWDA-2012-00128 Rev. 1*, Letter from Mohseni, A. (NRC) to Levitan, W. (DOE-HQ), U.S. Nuclear Regulatory Commission, Washington, DC, July 30, 2013.

ML13199A413, *Summary of Clarification Discussion between the U.S. Nuclear Regulatory Commission Staff and the U.S Department of Energy and Savannah River Remediation Staff Concerning Performance Assessment Modelling Uncertainty/Sensitivity Related to H Area Tank Farm at the Savannah River Site*, Note to File from Shaffner, J., U.S. Nuclear Regulatory Commission, Washington, DC, July 29, 2013.

ML13218A556, *Discussion and Clarification of U.S. Nuclear Regulatory Commission Request for Additional Information to Complete Preparation of a Technical Evaluation Report as Part of Consultation Regarding H-Area Tank Farm, Savannah River Site*, Memo to File from Shaffner, J. to Mohseni, A., U.S. Nuclear Regulatory Commission, Washington, DC, August 13, 2013.

ML13246A133, McKenney, C., et al., *Discussion of NRC Comments and Requests for Additional Information Needed to Complete Preparation of a Technical Evaluation Report for Consultation Regarding H-Area Tank Farm, Savannah River Site,* U.S. Nuclear Regulatory Commission, Washington, DC, August 29, 2013.

NDAA_3116, *Public Law 108-375, Ronald W. Reagan National Defense Authorization Act for Fiscal Year 2005, Section 3116, Defense Site Acceleration Completion*, October 28, 2004.

NUREG/CR-5542, Walton, J.C., et al., *Models for Estimation of Service Life Barriers in Low-Level Radioactive Waste Disposal,* Idaho National Engineering Laboratory, Idaho Falls, ID, September 1990.

NUREG/CR-6070, Seitz, R.R. and Walton, J.C., *Modeling Approaches for Concrete Barriers Used in Low-Level Waste Disposal,* Idaho National Engineering Laboratory, Idaho Falls, ID, November 1993.

PNNL-13421, Cantrell, K.J., et al., *Geochemical Processes Data Package for the Vadose Zone in the Single-Shell Tank Waste Management Areas at the Hanford Site*, Pacific Northwest Laboratory, Richland, WA, June 2007.

PNNL-21723, Cantrell, K.J. and Williams, B.D., *Equilibrium Solubility Model for Technetium Release from Saltstone Based on Anoxic Single-Pass Flow through Experiments*, Pacific Northwest National Laboratory, Richland, WA, September 2012.

PORTAGE-08-022, *H-Area Tank Farm Model Development for Tanks in the Water Table PORFLOW Version 6.20.0*, Savannah River Site, Aiken, SC, Rev. 0, November 2008.

S0016-2361(98)00132-X, (Copyright), Hower, J.C., et al., *Petrology, Mineralogy, and Chemistry of Magnetically-Separated Sized Fly Ash*, Fuel, Vol. 78, pp. 197-203, January 1999.

S4 Manual Procedure ADM.53, *Maximum Extent Practical (MEP) Documentation Process,* Savannah River Site, Aiken, SC, Rev. 0, November 13, 2012.

S4 Manual Procedure ENG.50, *LW Project and Closure Operating Plans*, Savannah River Site, Aiken, SC, Rev. 2, November 13, 2012.

SKB Report R-01-08, Höglund, L.O., et al., *Project SAFE: Modeling of Long-term Concrete Degradation Processes in the Swedish SFR Repository*, Swedish Nuclear Fuel and Waste Management Co. Stockholm, Sweden, April 2001.

SRNL-L3200-2011-00011, Millings, M.R., et al., *Summary Dissolved Oxygen in Water Table Wells at SRS*, Letter from J. Jordan, G. Flach, and D. Schep (SRNS) to K. Rosenberger and M. Layton (SRR), Savannah River Site, Aiken, SC, December 21, 2011.

SRNL-L6200-2010-00026, *PORFLOW Modeling Supporting the H-Tank Farm Performance Assessment*, Savannah River Site, Aiken, SC, Rev. 1, November 18, 2010.

SRNL-STI-2009-00473, Kaplan, D.I., *Geochemical Data Package for Performance Assessment Calculations Related to the Savannah River Site*, Savannah River Site, Aiken, SC, March 15, 2010.

SRNL-STI-2009-00492, Poirier, M.R. and Fink, S.D., *Analysis of Samples from Tank 5F Chemical Cleaning*, Savannah River Site, Aiken, SC, Rev. 0, December 9, 2009.

SRNL-STI-2009-00493, Poirier, M.R. and Fink, S.D., *Analysis of Samples from Tank 6F Chemical Cleaning*, Savannah River Site, Aiken, SC, Rev. 0, February 2, 2010.

SRNL-STI-2009-00636, Lilley, M.S., et al., *Iodine, Neptunium, Plutonium, and Technetium Sorption to Saltstone and Cement Formulations under Oxidizing and Reducing Conditions*, Savannah River Site, Aiken, SC, 2009.

SRNL-STI-2009-00821, Bannochie, C.J., et al., *Determination of Reportable Radionuclides for DWPF Sludge Batch 5 (Macrobatch 6),* Savannah River Site, Aiken, SC, Rev. 0, February 2010.

SRNL-STI-2010-00035, Langton, C.A., *Chemical Degradation Assessment for the H-Area Tank Farm Concrete Tanks and Fill Grouts*, Savannah River Site, Aiken, SC, Rev. 0, January 29, 2010.

SRNL-STI-2010-00047, Garcia-Diaz, B.L., *Life Estimation of High Level Waste Tank Steel for H-Tank Farm Closure Performance Assessment*, Savannah River Site, Aiken, SC, March 2010.

SRNL-STI-2010-00148, Jones, W.E., et al., *Hydrogeologic Data Summary in Support of the H-Area Tank Farm Performance Assessment*, Savannah River Site, Aiken, SC, Rev. 0, February 2010.

SRNL-STI-2010-00447, Jannik, G.T., et al., *Land and Water Use Characteristics and Human Health Input Parameters for Use in Environmental Dosimetry and Risk Assessments at the Savannah River Site*, Savannah River Site, Aiken, SC, Rev. 0, August 6, 2010.

SRNL-STI-2012-00087, Denham, M.E., *Evolution of Chemical Conditions and Estimated Plutonium Solubility in the Residual Waste Layer During Post-Closure Aging of Tank 18*, Savannah River Site, Aiken, SC, Rev. 0, February 28, 2012.

SRNL-STI-2012-00106, Hobbs, D.T., *Form and Aging of Plutonium in Savannah River Site Waste Tank 18*, Savannah River Site, Aiken, SC, Rev. 0, February 24, 2012.

SRNL-STI-2012-00178, Hay, M.S., et al., *Characterization of Tank 16H Annulus Samples*, Savannah River Site, Aiken, SC, Rev. 0, April 2012.

SRNL-STI-2012-00404, Denham, M.E. and Millings, M.R., *Evolution of Chemical Conditions and Estimated Solubility Controls on Radionuclides in the Residual Waste Layer During Post-Closure Aging of High-Level Waste Tanks*, Savannah River Site, Aiken, SC, Rev. 0, August 29, 2012.

SRNL-STI-2012-00479, Reboul, S.H., *Chemical Differences Between Sludge Solids at the F and H Area Tank Farms*, Savannah River Site, Aiken, SC, Rev. 0, August 2012.

SRR-CES-2009-00022, Clendenen, G.B., *Strategy for Tanks 5 and 6 Phase II Mechanical Sludge Removal,* Savannah River Site, Aiken, SC, Rev. 0, September 21, 2009.

SRR-CWDA-2010-00093, *H-Area Tank Farm Stochastic Fate and Transport Model,* Savannah River Site, Aiken, SC, Rev. 2, August 6, 2012.

SRR-CWDA-2010-00128, *Performance Assessment for the H-Area Tank Farm at the Savannah River Site*, Savannah River Site, Aiken, SC, Rev. 1, November 14, 2012.

SRR-CWDA-2011-00022, *Industrial Wastewater General Closure Plan for H-Area Waste Tank Systems*, Savannah River Site, Aiken, SC, Rev. 0, May 30, 2012.

SRR-CWDA-2011-00050, *Liquid Waste Tank Residuals Sampling and Analysis Program Plan*, Savannah River Site, Aiken, SC, Rev. 2, July 31, 2013.

SRR-CWDA-2011-00054, *Comment Response Matrix for United States Nuclear Regulatory Commission Staff Comments on the Draft Basis for Section 3116 Determination and Associated Performance Assessment for the F-Tank Farm at the Savannah River Site,* Savannah River Site, Aiken, SC, Rev. 1, October 25, 2011.

SRR-CWDA-2011-00117, *Liquid Waste Tank Residuals Sampling-Quality Assurance Program Plan*, Savannah River Site, Aiken, SC, Rev. 1, July 31, 2013.

SRR-CWDA-2011-00126, Marusich, C., *Tank 16 History of Waste Removal 1959 Through 2010*, Savannah River Site, Aiken, SC, Rev. 0, September 2011.

SRR-CWDA-2012-00011, *Features, Events, and Processes for Liquid Waste Performance Assessments*, Savannah River Site, Aiken, SC, Rev. 0, February 14, 2012.

SRR-CWDA-2012-00071, *Industrial Wastewater Closure Module for the Liquid Waste Tanks 5F and 6F F-Area Tank Farm*, Savannah River Site, Savannah River Site, Aiken, SC, Rev. 1, April 15, 2013.

SRR-CWDA-2012-00138, *Documentation of Removal of Highly Radioactive Radionuclides in Waste Tanks 5 and 6, F-Area Tank Farm Savannah River Site*, Savannah River Site, Aiken, SC, Rev. 0, May 13, 2013.

SRR-CWDA-2013-00041, *Proposal to Cease Waste Removal Activities in Tank 16 and Enter Sampling and Analysis Phase*, Savannah River Site, Aiken, SC, Rev. 1, April 1, 2013.

SRR-CWDA-2013-00049, *Savannah River Site Liquid Waste Facilities Performance Assessment Maintenance Program FY2013 Implementation Plan*, Savannah River Site, Aiken, SC, Rev. 1, May 9, 2013.

SRR-LWE-2010-00240, Clark, J., *Tank Mapping Methodology*, Savannah River Site, Aiken, SC, Rev. 1, November 28, 2012.

SRR-LWE-2011-00068, Sudduth, C.B., *The Viability of Oxalic Acid at SRS*, Savannah River Site, Aiken, SC, February 28, 2011.

SRR-LWE-2011-00201, Pasala, N.R., *Information on the Radiological and Chemical Characterization of the Savannah River Site Tank Waste As of July 5, 2011*, Savannah River Site, Aiken, SC, Rev. 0, September 2011.

SRR-LWE-2012-00082, Tisler, A., *CY 2011 Annual SCDHEC Technology Briefing*, Savannah River Site, Aiken, SC, April 30, 2012.

SRR-LWE-2013-00010, Clark, J.L., *Tank 16 Annulus Waste Volume Determination*, Savannah River Site, Aiken, SC, January 15, 2013.

SRR-LWE-2013-00057, *Tank 16 Sampling and Analysis Plan*, Savannah River Site, Aiken, SC, Rev. 0, May 2, 2013.

SRR-LWE-2013-00077, Tisler, A., *Annual SCDHEC Technology Briefing*, Savannah River Site, Aiken, SC, April 17, 2013.

SRR-STI-2013-00198, Subramanian, K.H. and Vitali, J.R., *Tank 12 Bulk Oxalic Acid Cleaning Flowsheet Strategy*, Savannah River Site, Aiken, SC, Rev. 0, April 2013.

SRR-WRC-2011-0004, Davis, N., *Revised Heel Removal Approach for Tanks 11 & 12*, Savannah River Site, Aiken, SC, May 11, 2011.

SRS_LW_FEPs_Rev0.xlsx, Data File Associated with FEPs Screening as Described in SRR-CWDA-2012-00011, *Features, Events, and Processes for Liquid Waste Performance Assessments,* Savannah River Site, Aiken, SC, Rev. 0, February 14, 2012.

SRS-REG-2007-00002, *Performance Assessment for the F-Tank Farm at the Savannah River Site*, Savannah River Site, Aiken, SC, Rev. 1, March 31, 2010.

U-ESR-H-00103, Clark, J. and Colleran, H., *Tank 12 Bulk Oxalic Acid Cleaning Operating Plan*, Savannah River Site, Aiken, SC, Rev. 2, May 2013.

U-ESR-H-00107, Clark, D.J., *Tank 16H: Preliminary Evaluation of Cessation of Annulus Waste Removal Activities*, Savannah River Site, Aiken, SC, Rev. 0, March 7, 2013.

V-ESR-G-00003, Caldwell, T., *Waste Removal Technology Baseline: Technology Development Description*, Aiken, SC, Rev. 1, June 15, 2011.

WSRC-RP-99-00436, Fellinger, T.L., et al., *Characterization of and Waste Acceptance Radionuclides to be Reported for DWPF Macro Batch 2 (ESP 215-ESP 221)*, Savannah River Site, Aiken, SC, Rev. 1, March 2004.

WSRC-STI-2007-00004, Lee, P.L., et al., *Baseline Parameter Update for Human Health Input and Transfer Factors for Radiological Performance Assessments at the Savannah River Site*, Savannah River Site, Aiken, SC, Rev. 4, June 13, 2008.

WSRC-STI-2007-00192, Hay, M.S., et al., *Characterization and Actual Waste Tests with Tank 5F Samples*, Savannah River Site, Aiken, SC, Rev. 1, August 30, 2007.

WSRC-STI-2008-00142, Bannochie, C.J., et al., *Determination of Reportable Radionuclides for DWPF Sludge Batch 4 (Macrobatch 5)*, Savannah River Site, Aiken, SC, Rev. 0, May 2008.

WSRC-STI-2008-00203, Hay, M.S., *Characterization of Samples from Tank 16H Annulus*, Savannah River Site, Aiken, SC, Rev. 0, May 2008.

WSRC-TR-2003-00250, Hiergesell, R.A., et al., *An Updated Regional Water Table of the Savannah River Site and Related Coverages*, Savannah River Site, Aiken, SC, Rev. 0, December 2003.

WSRC-TR-2004-00106, Flach, G.P., *Groundwater Flow Model of the General Separations Area Using PORFLOW*, Savannah River Site, Aiken, SC, Rev. 0, July 15, 2004.

WSRC-TR-2005-00157, Bannochie, C.J., et al., *Determination of Reportable Radionuclides for DWPF Sludge Batch 3 (Macrobatch 4)*, Savannah River Site, Aiken, SC, Rev. 0, May 2005.

WSRC-TR-99-00106, Flach, G.P., *Pre- And Post-Processing Software Associated with the GSA/FACT Groundwater Flow Model*, Savannah River Site, Aiken, SC, Rev. 0, April 1999.

X-CLC-H-00921, Sudduth, C.B., *Effects of Low Temperature Aluminum Dissolution (LTAD) on Tank 12 Sludge Heel*, Savannah River Site, Aiken, SC, Rev. 0, June 6, 2012.